UNIVERSITAT DE BARCELONA

Mitochondrial implication in intrauterine growth restriction and cardiovascular remodelling

Mariona Guitart Mampel

Mitochondrial implication in intrauterine growth restriction and cardiovascular remodelling

Thesis presented by

Mariona Guitart Mampel

For the degree of Doctor by the University of Barcelona

Thesis directed by

Glòria Garrabou and Francesc Cardellach

Medicine and Health Science Faculty, University of Barcelona

Barcelona, 2018

INDEX

1. ABBREVIATIONS

A

AceCS2: acetyl-CoA synthase 2

Acetyl-CoA: acetyl-coenzyme A

ADP: adenosine diphosphate

AGA: adequate for gestational age

ALDH2: aldehyde dehydrogenase, mitochondrial

ATP: adenosine triphosphate

ATP5A: ATP synthase subunit ATP5A

AU: arbitrary units

B

BNP: brain natriuretic peptide

BSA: bovine serum albumin

C

Cellox: endogen cell respiration

CBMC: cord blood mononuclear cells

CI: complex I

CII: complex II

CIV: complex IV

CI+III: complex I+III

CII+III: complex II+III

CO_2: carbon dioxide

CO: carbon monoxide

CoQ_9 and CoQ_{10}: coenzyme Q_9 and Q_{10}

COX5A: cytochrome c oxidase subunit 5a

CPR: cerebroplacental ratio

CS: citrate synthase

CytC: cytochrome C

Cyto: cytoplasm

D

DCPIP: 2,6-diclorophenolindophenol

DNA: deoxyribonucleic acid

DTNB: 5,5'-dithiobis-2-nitrobenzoic acid

E

EGTA: ethylene glycol tetra-acetic acid

ER: endoplasmic reticulum

ETC: electron transport chain

E/A ratio: early (E) to late (A) ventricular filling velocities ratio

F

FAD: flavine adenine dinucleotide

G

GDH: glutamate dehydrogenase

GM Oxidation: glutamate+malate oxidation

H

HAE: hydroxyalkenal

HCl: hydrochloric acid

HEPES: 4-(2-hydroxyethyl)-1-piperazineethanesulfonic acid

HMGCS2: 3-hydroxy-3-methylglutaryl-CoA synthase 2, mitochondrial

HSP-27: heat shock protein 27

I

IDH2: isocitrate dehydrogenase

IGF: insulin-like growth factor

IMM: inner mitochondrial membrane

IUGR: intrauterine growth restriction

K

KCN: potassium cyanide

kDa: kilodalton

L

LCAD (or ACADL): acyl-CoA dehydrogenase, long chain

M

MAM: mitochondrial-associated ER-membrane

MDA: malondialdehyde

MES: 2-(N-morpholino)ethanesulfonic acid

$MgCl_2$: magnesium chloride

Mit: mitochondria

mPTP: mitochondrial permeability transition pore

MRC: mitochondrial respiratory chain

mRNA: messenger ribonucleic acid

MRPL10: 39S ribosomal protein L10, mitochondrial

mtDNA: mitochondrial deoxyribonucleic acid

mt12SrRNA: mitochondrial 12S ribosomal RNA

Myof: myofilaments

N

N: sample size

NADH: reduced form of nicotidamide adenine dinucleotide

NAD^+: oxidized form of nicotidamide adenine dinucleotide

NADPH: nicotinamide adenine dinucleotide phosphate

NAPBQI: N-acetyl-p-benzoquinone imine

NDUFA9A: NADH dehydrogenase 1 alpha subcomplex subunit 9

NMN: Nicotinamide mononucleotide

nRNAseP: nuclear RNAseP gene

NS: not significant

O

OMM: outer mitochondrial membrane

OTC: ornithine transcarbamylase

OXPHOS: oxidative phosphorylation

P

PBMC: peripheral blood mononuclear cells

PBS: phosphate-buffered saline

PCR: polymerase chain reaction

PE: preeclampsia

PM Oxidation: pyruvate+malate oxidation

R

ROS: reactive oxygen species

S

SDHA: succinate dehydrogenase complex, subunit A

SDHB: succinate dehydrogenase complex, subunit B

SDS-PAGE: sodium dodecyl sulfate polyacrylamide gel electrophoresis

SEM: standard error of the mean

SERPINA1: alpha-1-antitrypsin

SGA: small for gestational age

SOD2: superoxide dismutase 2

T

TNB: 2-nitro-5-thiobenzoic acid

Tom20: mitochondrial import receptor subunit TOM20

tRNA: transference ribonucleic acid

U

UA Doppler: umbilical artery Doppler

UCP2: mitochondrial uncoupling protein 2

V

VDAC: voltage-dependant anion channel

VEGF: vascular endothelial growth factor

2. INTRODUCTION

2.1 INTRAUTERINE GROWTH RESTRICTION

Intrauterine growth restriction (IUGR), also known as foetal growth restriction, is a common obstetric complication that affects 5-10% of all pregnancies in Western countries, being 2-3 times more prevalent in undeveloped countries such as India or Africa (1–3).

Although its definition remains ambiguous due to its challenging clinical management for variability in clinical presentation, IUGR is defined as the failure of the foetus to achieve its full growth potential, with an estimated foetal weight below the 10th percentile for gestational age (4). These newborns recover a standard weight and size after delivery and during perinatal development but long-term effects remain unknown, becoming the most frequent cause of perinatal mortality and long-term morbidity (3,5).

In terms of physiopathology, a distinction should be made between those foetuses constitutionally small, denominated small for gestational age (SGA), and those foetuses which genetic potential weight is restricted, as IUGR (6). Thus, SGA only refers to a decreased foetal size and weight independent of the causes and symptoms, while IUGR is defined by pathological smallness and prompt to developmental problems. In general terms, IUGR is associated with hemodynamic redistribution as a reflection of foetal adaptation to undernutrition or hypoxia, histological and biochemical signs of placental disease and higher risk of preeclampsia (7). It is quite common to confuse these two terminologies leading to the necessity to identify SGA foetuses to distinguish those babies who are pathologically small and reduce false-positive cases. It is already demonstrated that prenatal identification of SGA and IUGR babies results in a reduction of adverse perinatal outcomes and stillbirth.

2.1.1 Causes of IUGR

Although it could be produced by a variety of causes, IUGR is frequently caused by placental insufficiency leading to foetal hypoxia.

However, there are some cases of IUGR which are not produced primarily by placental insufficiency, but indirectly resulting in placental insufficiency as a consequence of other alterations (8,9). Thus, within cases of IUGR not caused by placental insufficiency, IUGR can be classified depending on foetal and maternal aetiologies (summarized in Table 1).

Table 1. Causes or risk factors associated with IUGR independent of placental insufficiency

FOETAL
• **Genetic diseases/chromosomal defects (e.g., aneuploidy, uniparental disomy, etc.)**
• **Infections (e.g., cytomegalovirus, toxoplasmosis, malaria, etc.)**
• **Malformation**
• **Multiple gestation**
• **Placental or cord abnormalities (e.g., abruption, 2 vessel cord, etc.)**
MATERNAL
• **Constitutionally small mother or low pre-pregnancy weight**
• **Hypertension**
• **Pregestational diabetes**
• **Autoimmune disease**
• **Cardiac and renal disease**
• **Anaemia**
• **Toxic exposure (smoking, alcohol, illicit drugs)**
• **Malnutrition**
• **Live in high altitudes**
• **Live in developing countries**
• **Low socio-economic status**
• **Race (e.g., Afro-American)**
• **Family of prior history of pregnancy with IUGR or SGA**
• **Extremes of maternal age (<16 years and >35 years)**
• **Assisted reproductive technology**
• **Teratogens (e.g., anticonvulsants, warfarin, etc.)**

Adapted and modified from data contained in Hendrix N *et al.* and Lausman A *et al.* (8,9).

e.g.: stands for *exempli gratia* in Latin, which means "for example"; IUGR: intrauterine growth restriction; SGA: small for gestational age.

On the other hand, within cases of IUGR caused by placental insufficiency, IUGR could be classified depending on gestational age at diagnosis and umbilical artery Doppler (UA Doppler) (5), as summarized in Table 2:

- Early-onset: those IUGR diagnosed before 32-34 weeks of gestation, representing 20-30% of all IUGR cases. Early-onset IUGR is highly related to severe placental insufficiency and with chronic foetal hypoxia, explaining the existence of UA Doppler

abnormalities in a high proportion. In these cases, IUGR is frequently caused by infection, chromosomal anomalies or genetic abnormalities. They are associated to PE in 50% of the cases and its perinatal morbidity and mortality is high, due to associated prematurity.

- Late-onset: when IUGR appears after 34 weeks of gestation and especially in term pregnancies (37 weeks), representing 70-80% of all IUGR cases. Normally, these cases are caused by mild placental insufficiency, thus UA Doppler is normal. In this group, the diagnostic is challenging, considering that could explain at least up to 50% of perinatal deaths by its low tolerance to hypoxia. Only 10% are associated to PE.

Table 2. Summary of the principal differences between early- and late-onset IUGR caused by placental insufficiency.

Early-onset IUGR	Late-onset IUGR
CHALLENGE: MANAGEMENT	CHALLENGE: DIAGNOSIS
Prevalence: ≈ 1-2 %	Prevalence: ≈ 3-5 %
Severe placental insufficiency ➢ Abnormal UA Doppler ➢ High association with PE	Mild placental insufficiency ➢ Normal UA Doppler ➢ Low association with PE
Severe hypoxia: systemic cardiovascular adaptation	Mild hypoxia: central cardiovascular adaptation
High morbidity and mortality	Low mortality

Adapted and modified from data contained in Figueras F *et al.* (5).

IUGR: intrauterine growth restriction; UA Doppler: umbilical artery Doppler. It is a measure for the management of IUGR; PE: preeclampsia. It is another obstetric complication associated in some cases with IUGR.

2.1.2 Placental insufficiency

A normal placental development and function are essential for a successful foetal development. Placenta is a key organ between mother and foetus, providing nutrients and oxygen to the embryo (10). Concretely, the 'trophoblast' (from greek *trephein* 'to feed' and *blastos* 'germinator'), formed by cells from the outer layer of the blastocyst, is a substantial part responsible of supplying the nutrients (Figure 1) (11). The placenta

exerts a number of other pivotal functions that highlight the importance of normal and proper differentiation of the trophoblast for a prosperous pregnancy development.
This vital development depends on several factors of both the pregnant women and the foetus and different placental factors may be involved.

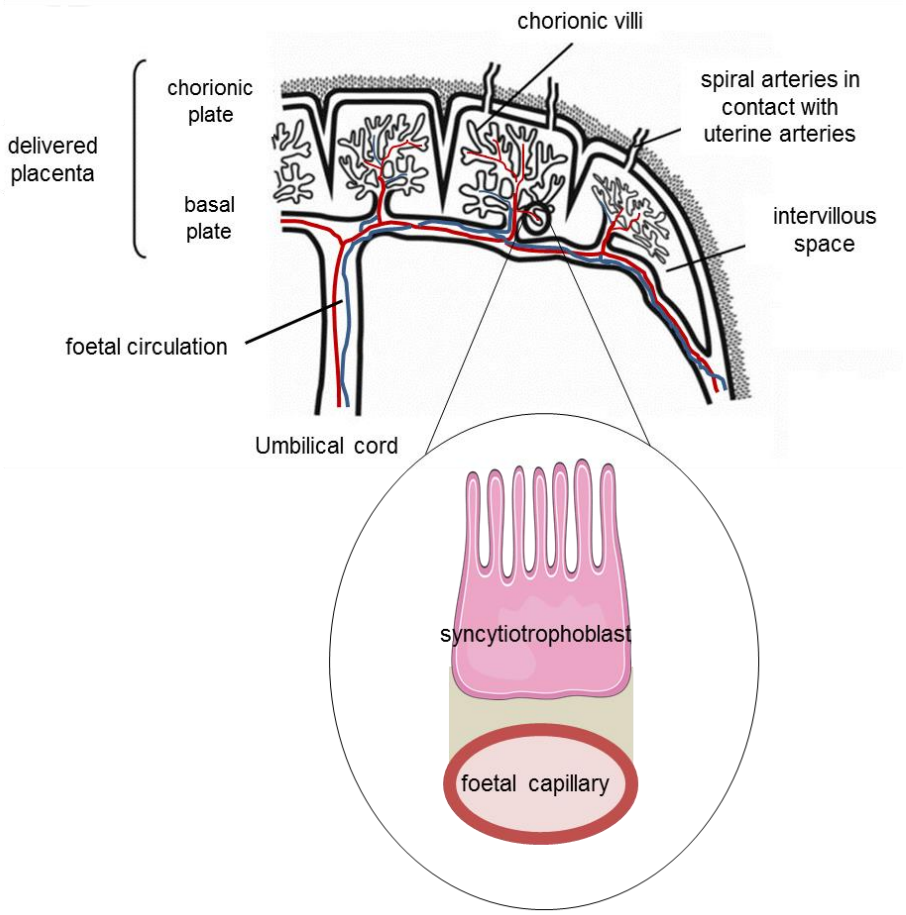

Figure 1. A cross-sectional microscopic representation of the basic morphology of human placenta with the foetal circulation in umbilical cord and chorionic villi. Maternal blood goes into the intervillous space in contact with the chorionic villi, which includes the syncytiotrophoblast layer and the foetal capillary endothelial cells.

Image adapted and modified from Sibley CP *et al.* (12) and Gaccioli *et al.* (13).

One side of the placenta is connected with the uterus (through spiral arteries) and the other side is attached to a liquid-filled sac that contains the foetus. Additionally, the foetoplacental circulation includes the umbilical cord and the blood vessels from the placenta that transport foetal blood (Figure 1).

Human placenta presents three main layers. The first layer of maternal-foetal exchange is the syncytiotrophoblast, which is a multinucleated epithelium that covers the

chorionic villi in contact with maternal blood of the intervillous space (Figure 1). Studies of placental morphology show the importance of villi, which contain papillary networks derived from foetal circulation, demonstrating distinct abnormalities of villi related with particular presentations of IUGR. An important general morphologic observation in IUGR that effect on diffusional permeability of the placenta is that the surface area of the syncytiotrophoblast is reduced whereas the thickness of the exchange barrier formed by the trophoblast and foetal capillary endothelium is increased (14). A second layer of mononucleate cytotrophoblast cells is the cytotrophoblast which are predominantly progenitor cells for the syncytiotrophoblast. And finally, a connective tissue placed on the villous tree where is located the foetal capillary endothelium (15).

Additionally, there are evidences demonstrating increased placental apoptosis in IUGR, reflecting altered turnover of the placental cells in association with changes in size and architecture of this organ.

All these alterations are denominated ‘placental insufficiency’ that lead to placental hypoxia and reduced nutrient supply, thus poor oxygen transportation compromising the foetus in development and causing a foetal remodelling with adulthood consequences. Indeed, one of the main organs of foetal adaptive response to placental insufficiency and hypoxia is the heart.

2.1.3 Management of IUGR

IUGR is still a concern among clinicians in terms of its diagnosis and management. It is important to be aware of the severity of growth restriction. So, careful monitoring of the foetus with IUGR and ongoing testing may be required. Nowadays, UA Doppler is considered the gold standard to provide successful diagnostic and prognostic information for IUGR management (16). UA Doppler is a technique that allows measuring the amount and speed of the blood flow through the blood vessels of the placenta. The usage of UA Doppler has a great value for the identification of IUGR, alone or combined with the cerebroplacental ratio (CPR). The CPR is essentially a diagnostic index that improves remarkably the sensitivity of UA Doppler alone (7).

The usage of UA Doppler in high-risk pregnancies has been correlated with a decrease in adverse outcomes and a 30% mortality reduction (17).

There is the need to use different parameters to make clinical decisions. Lately, it is

proposed to simplify the management of IUGR using succeeding approach based on three steps: a) identification of the “small foetus”; b) distinction between IUGR and SGA; and (c) time of delivery according to a protocol based on points of foetal decline (5).

By random convention, the placental insufficiency cases are usually defined as “true” IUGR, whereas the remaining cases are referred to as small for gestational age (SGA). As mentioned before, the distinction between IUGR and SGA is highly relevant and UA Doppler is critical to achieve this goal.

2.1.4 Prevention of IUGR

Although there is no treatment for IUGR, some conditions could help to minimize or retard its effects. These preventions will depend on both pregnant women and gynaecologist.
Treatments may include nutritional interventions in pregnant women, as optimal maternal nutrition could increase foetal weight. This evidence highlights the importance to understand how changing diet could improve foetal weight.

As previously mentioned it is important to monitor pregnancies with IUGR and perform an early delivery if the foetus wellbeing may be compromised. Early detection may also help with IUGR management and outcome.

IUGR may occur even if the mother is healthy. However, there are some factors that may increase the risk of IUGR, such as smoking (18) and poor maternal nutrition (for instance in developing countries such as Africa or India). Avoiding harmful lifestyles (such as drugs or tobacco), eating a healthy diet, and getting prenatal care may help to decrease the risks for IUGR.

Little is known about potential biomarkers or therapies to prevent IUGR. In fact, the modulation of diet could be one of the few targets to further investigate due to limitation of therapeutic approaches during pregnancy.

2.2 FOETAL CARDIAC FUNCTION

The heart is formed early in prenatal development being the first functional organ in vertebrate embryos. In human, the foetal heart and circulation is completed at the 8-9th week of gestation (19,20) thus, the heart beats spontaneously by week four of development. Foetal heart has four chambers, 2 atria connected via *foramen ovale* and two separated ventricles. In addition, there are two atroventricular valves (mitral and tricuspid) and two semilunar valves (aortic and pulmonary) that guarantee one-way flow through the heart. The main purpose of the heart is to create the required cardiac output to guarantee adequate blood perfusion to organs and to allow the adaptation to changing demands and working conditions.

The foetal circulatory system is different from that of a newborn baby, as pulmonary circulation is bypassed until birth. In the foetal heart, artery and aorta vessels are connected by the *ductus arteriosus*. The hemodynamic properties are crucial for the foetal heart development and circulation during the second and third trimester of pregnancy.

The foetal heart presents a limited capacity to increase its output as it normally manages at its high cardiac function curve. A modest increase in foetal heart rate could increase the cardiac output and bradycardia could compromise its function. The cardiac output is combined from left and right ventricles, being the right ventricle more contributive than the left one (65% versus 35%, approximately) (21). Foetal cardiac function is usually evaluated by the measurement of blood flow by conventional Doppler, cardiac morphometry in 2D or M-mode, tissue Doppler and 2D speckle tracking imaging (Figure 2) (22).

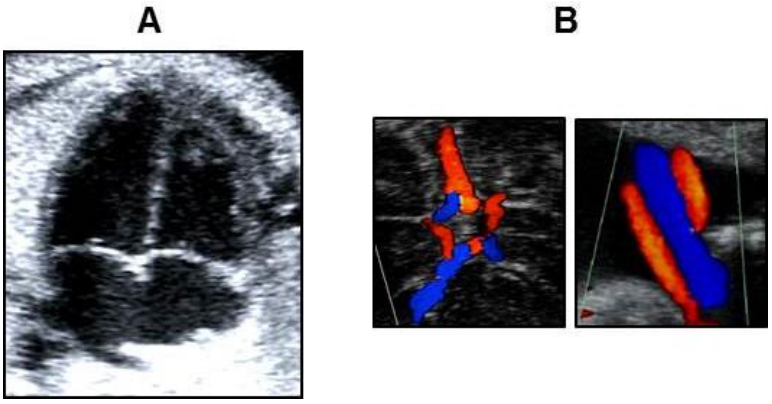

Figure 2. Foetal standard echocardiography of the heart (A) and Doppler imaging of vascular flux (B).

Image obtained and adapted from Rodriguez-Lopez *et al.* (23).

2.2.1 Cardiac remodelling associated to IUGR

As mentioned before, during placental insufficiency and hypoxia there is a foetal remodelling described first by Barker *et al.*, a phenomenon in which an *in utero* insult leads to functional changes in key organs remaining in postnatal life and leading to a greater risk of various diseases in adulthood (24). Under chronic hypoxia, the IUGR foetus is aimed to preferentially redirect its cardiac output to its vital organs (brain, heart, adrenal glands and liver). This consequence is called “brain sparing” effect that primarily origins an increase in the pulsatility of *ductus venosus*, which increases preload. As a result, IUGR newborns exhibit signs of cardiac remodelling and altered cardiovascular function.

Epidemiologic evidence has long confirmed a link between low birth weight and increased cardiovascular death in adulthood (25).

As heart is one of the most affected organs in response of foetal adaptive mechanisms to placental insufficiency and hypoxia, during embryonic development, the oxygen and nutrient limitation could lead to a cardiovascular remodelling at organ, tissue and subcellular levels. Different foetal cardiac phenotypes, elongated, globular and hypertrophic, may be observed (26). This cardiovascular remodelling associated to IUGR has been evidenced in animal models and in humans.

Multiple studies revealed that foetuses diagnosed with IUGR have cardiac systolic and diastolic dysfunction with increased E/A ratios (early (E) to late (A) ventricular filling velocities ratio) and myocardial performance index and reduced myocardial tissue velocities (24). Crispi *et al.* have demonstrated that these cardiac alterations remain present in pre-adolescence, adolescence and early-stage of adulthood, increasing the chance of suffering from some cardiomyopathy-like in adulthood (Figure 3) (27–29).

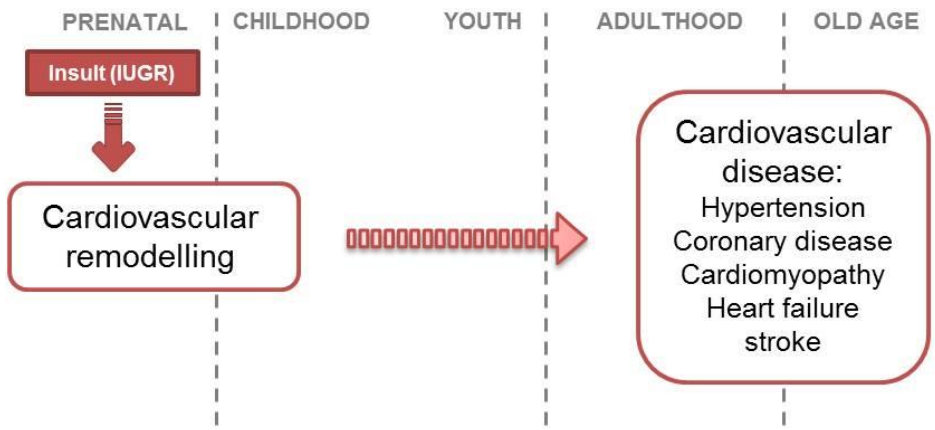

Figure 3. Cardiovascular remodelling associated to intrauterine growth restriction (IUGR) begins by an insult during prenatal stages, which can trigger functional changes in main organs persisting during postnatal life and leading to higher risk of different disease in adulthood.

Image obtained and adapted from Demicheva E *et al.* (24).

Cardiovascular disease is one of the major causes of mortality in developed countries (30,31). Thus, increased research in the field of IUGR and its cardiovascular remodelling is required to prevent potential cardiovascular disease.

Previous research of our group has established that neonatal heart from IUGR pregnancies present this cardiovascular dysfunction in terms of morphological changes and clinical biomarkers of cardiac adaptation (32). Actually, there are a few studies demonstrating that some markers of cardiac damage as brain natriuretic peptide (BNP) are elevated in neonatal blood from IUGR newborns and, additionally, levels of BNP are increased across foetoplacental Doppler stages of foetal compromise (33,34). Interestingly, another study demonstrated increased levels of BNP in preterm newborns with IUGR during postnatal life, which reinforces the tenacity of cardiac dysfunction during the first days of life (35).

However, the study of molecular mechanisms that lead to this cardiovascular remodelling in neonatal hearts is scare by the limitation of studying the target tissue of cardiovascular remodelling, the heart.

Both foetal and cardiac function needs high energy supply. As mitochondria are essential in foetal and cardiac development due to the strong dependence of cell bioenergetics in mitochondrial metabolism, the role of the mitochondria in foetal

programming is gaining attention. Mitochondrial are the powerhouse that furnished energy for cell function; therefore, a decrease in number or function activity are lately damaging for cells, particularly for those with high energy demand like cardiomyocytes. Consequently, different evidences support the involvement of mitochondria in IUGR and cardiovascular disorders.

2.3 MITOCHONDRIA

Mitochondrion is an organelle of 1-10 μm of size present in the cytoplasm of almost all eukaryote cells. Mitochondria are involved in a numerous and relevant cellular processes including metabolism and apoptosis. For that reason, mitochondria are being related to many diseases associated to growth abnormalities and cardiac damage.

Its origin is not yet well understood but according to endosymbiotic theory, mitochondria are descendants of ancient bacteria that were phagocyted for ancestral eukaryotic cells more than millions of years ago (36,37). This fact leads to a symbiotic relationship between both entities, one of them providing the energy, and the other one the essential nutrients needed to supply energy.

The number of mitochondria per cell varies depending on organisms and tissue. Although all DNA is enrolled within the nucleus, mitochondria have their independent genetic material, called mitochondrial DNA (mtDNA). It is a double-stranded circular and covalently closed molecule, found in the mitochondrial matrix in a multiple number of copies. The mtDNA encodes for 13 proteins becoming part of the structure and function of some complexes of the mitochondrial respiratory chain (MRC). The levels of mtDNA are frequently used as a mitochondrial content indicator (38). Thus, mtDNA is replicated, transcribed and translated in the mitochondrial matrix using their own machinery but also in coordination with proteins encoded in the nuclear DNA imported to the mitochondria. This reinforced the idea of an essential intergenomic communication between the mitochondria and the nucleus for a proper mitochondrial function and bioenergetic cell supply.

2.3.1 Structure

Mitochondria contain an outer membrane and an inner membrane that play a pivotal role in its activities, containing a unique collection of proteins that defined two internal compartments: the internal matrix space and a much narrower intermembrane space (Figure 4).

- The **outer mitochondrial membrane** (OMM) harmonized numerous interactions between the mitochondrial metabolic and genetic systems and the rest of the cell. It comprises nuclear-encoded proteins synthesized as precursor

proteins in the cytosol, targeted to the mitochondria and inserted into their target membrane via various pathways, e.g translocases such as TOM20, in charge of the recognition and translocation of cytosolic synthesized mitochondrial pre-proteins. The ubiquitous and conserved expression of TOM20 has been widely used to predict mitochondrial content. Additionally, the OMM contains large numbers of integral membrane proteins called porins forming channels that allow molecules up to 10.000 Daltons to freely diffuse from one side of the membrane to the other. OMM also contains specific proteins called porins or voltage-dependent anion channels (VDAC), responsible for transport of adenosine triphosphate (ATP) synthesized in mitochondria outside of the organelle to be available for cellular functions. Furthermore, VDAC has been implicated in prompting the apoptosis process mediated by the mitochondria. This OMM can be associated with the endoplasmic reticulum (ER) or late endosomes, forming a structure called MAM (mitochondrial-associated ER-membrane).

- The **inner mitochondrial membrane** (IMM) is highly specialized and is folded into numerous cristae, which greatly increase its total surface area. It is the membrane that separates the mitochondrial matrix from the intermembrane space.

  Importantly, the IMM is completely different in composition to the rest of cell membranes; it is highly impermeable and contains high levels of cardiolipin. The IMM locates the oxidative phosphorylation system (OXPHOS), the principal process in charge of energy production (39).

- The **intermembrane space** (determined by OMM and IMM) is where take place the accumulation of protons derived from the proton pumping through the different enzymatic complexes of the MRC.

  This space contains several enzymes that use the ATP circulation of the matrix to phosphorylate other nucleotides.

- The **mitochondrial matrix** (delimited by the IMM) contains hundreds of enzymes involved in a lot of metabolic pathways such as Krebs cycle and the β-oxidation of the fatty acids. It also contains several copies of mtDNA, mitochondrial ribosomes, tRNAs and various enzymes required for the expression of the mitochondrial genes.

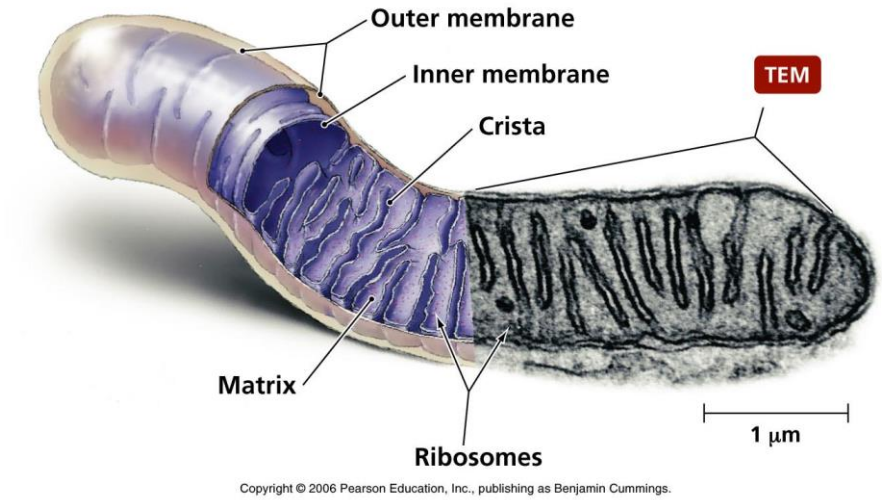

Figure 4. A scheme of the mitochondrial structure. In the right side there is a real image by Transmission Electron Microscopy (TEM). In the left side, there are depicted the different layers of the mitochondria.

Credits of the image to Person Education ©, Inc.

2.3.2 The oxidative phosphorylation system (OXPHOS)

Mitochondria synthesize (anabolic metabolism) and degredate (catabolic metabolism) the cellular substrates depending on the cell needs of a determined moment.

The catabolic pathways including the degradation of fatty acids, carbohydrates and amino acids provide energy in terms of ATP. These pathways converge at the formation of acetyl-coenzyme A (acetyl-CoA) that enters into the Krebs cycle to be degraded into carbonic dioxide (CO_2) and water (H_2O).These catabolic pathways and the Krebs cycle take place within the mitochondrial matrix.

The Krebs cycle begins when the acetyl-CoA (formed from fatty acids, carbohydrates or amino acid metabolism) reacts with the oxaloacetate to produce citrate by the activity of citrate synthase. This enzyme takes relevance due to its use as a mitochondrial content indicator for many researchers in the mitochondrial field (40). The whole Krebs cycle process generates reducing power in form of two intermediates: nicotinamide adenine dinucleotide (NADH) and flavin adenine dinucleotide ($FADH_2$). This reducing power is then used to generate a proton pumping through the MRC.

The MRC is composed by four complexes (I, II, III and IV) and two mobile electron carriers named coenzyme Q (CoQ) or ubiquinone (located between complex I, II and III) and cytochrome c (cyt c), positioned between complex III and IV. Together with the

ATP-proton synthase or complex V, they form the OXPHOS system (Figure 5).

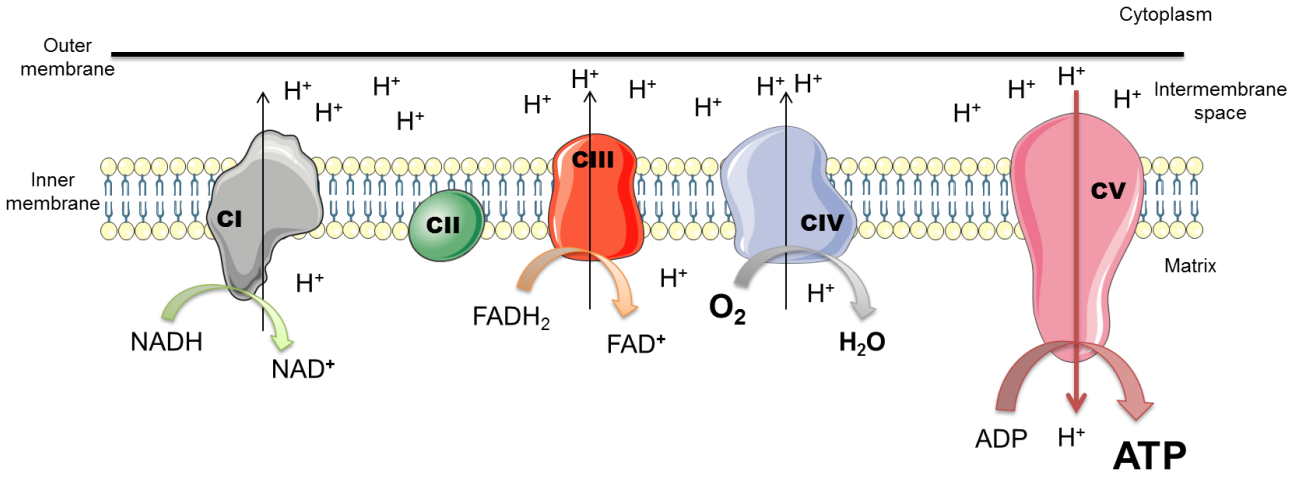

Figure 5. Representation of mitochondrial respiratory chain complexes (I-V). The reduction of NADH, $FADH_2$ and O_2 allows the accumulation of protons (H^+) in the intermembrane space creating a proton gradient used by the complex V to generate ATP.

ATP: adenosine triphosphate; CI: complex I; CII: complex II; CI+III: complex I+III; CII+III: complex II+III; CIV: complex IV; CV: complex V; FAD^+: oxidized form of flavin adenine dinucleotide; $FADH_2$: reduced form of flavin adenine dinucleotide; H_2O: water; NAD^+: oxidized form of nicotidamide adenine dinucleotide; NADH: reduced form of nicotidamide adenine dinucleotide; O_2: oxygen.

In more detail:

- **Complex I** or NADH dehydrogenase complex. It is the first and largest of the MRC complexes. It accepts electrons from NADH, helping to create an electrochemical potential gradient that pumps protons to the intermembrane space, and passes electrons through a flavin and at least five iron-sulphur centres, to finally lead these electrons to CoQ, that transfer them to complex III. Complex I is formed by approximately 46 subunits being seven of them encoded in the mtDNA.

- **Complex II** or succinate dehydrogenase. Its substrate is succinate which provides it with electrons. It is composed only by nuclear encoded subunits. Again, CoQ is responsible to transfer electrons, in this occasion from complex II to complex III.

- **Complex III** or ubiquinol-cytochrome C oxidoreductase. It transfers electrons from the reduced form of CoQ to cytochrome c (cyt c), the other mobile electron

carrier that transfer electrons from complex III to complex IV. This reaction pumps protons to the intermembrane space. Complex III is built with 11 subunits being only one encoded by mtDNA.

- **Complex IV** or cytochrome c oxidase. It is the complex that uses the oxygen to produce water molecules in a process denominated **mitochondrial or cellular respiration**. Oxygen is the terminal electron acceptor of the MRC, cyt c is reoxidized and protons transferred to the intermembrane space. It contains 11 subunits of nuclear origin and 3 subunits are synthesised in the mitochondria.

- **Complex V** or ATP-proton synthase. It plays a key role in energy production as being responsible for the synthesis of ATP from ADP and inorganic phosphate driven by the proton gradient force of returning protons back to the mitochondrial matrix.

2.3.3 Oxidative damage

Mitochondria are one of the principle centres of formation of reactive oxygen species (ROS) and the consequent presence of oxidative damage in the cells. In physiologic conditions, ROS is generated under control during the mitochondrial respiration through the MRC. However, under stress conditions of the cells or mitochondrial function alterations, ROS production can increase upon pathological threshold.

ROS are extremely reactive with lipids, proteins, carbohydrates or genetic material from mitochondria, generating a non-ending circle of mitochondrial damage that affect organelle structures to undergo lesion, thus causing more ROS production.

In order to regulate and control ROS production there are a variety of antioxidant enzymes such as the mitochondrial superoxide dismutase 2 (SOD2). In a physiologic situation, all the antioxidant mechanisms focus on attenuate high production of ROS acting as a protective system. However, usually in case of mitochondrial dysfunction, ROS levels increase beyond the threshold of detoxification and, even the level or activity of antioxidant defences in some cases.

2.3.4 Cellular pathways and mitochondria: mitochondrial deacetylase Sirtuin 3

Cellular pathways are highly regulated to quickly adapt to different environmental conditions. Concretely, acetylation of lysine residues of some enzymes represents a central process that regulates cellular metabolism and signalling. In mitochondria, the most common post-translational modification is the acetylation of proteins (41).

As mentioned before, mitochondria have crucial functions in the cell, mainly ATP generation, iron-sulphur cluster biogenesis, nucleotide biosynthesis, and amino acid metabolism. These functions feel the necessity for a secure regulation of mitochondrial activity and turnover. It is known that mitochondrial biogenesis is regulated by the nucleus and as before mentioned almost all mitochondrial proteins are encoded by nuclear genes, thus a tight communication network between the nucleus and mitochondria is fully needed which includes signalling cascades, dual-localized proteins to the two compartments and mitochondrial products sensed by nuclear proteins, among others (42).

This crosstalk between the nucleus and the mitochondria allows evaluation of the mitochondrial status, aligning cellular balance with the energetic needs. In case of increased needs of energy supply or mitochondrial dysfunction, the intergenomic communication is essential to adapt mitochondrial and bioenergetics activity to support organ function and proper organism growth. One of the main players for nuclear to mitochondrial communication are sirtuins.

Sirtuins are a conserved family of mammalian proteins that act predominantly as NAD-dependent deacetylases. They have different subcellular localization and widely participate in several biological functions like aging, transcription, apoptosis, inflammation, energy efficiency, among others (43). Sirtuins modulate cell adaptations directly deacetylating key protein targets. Concretely, the typical chemical reaction is the deacetylation of lysine coupled to the hydrolysis of NAD^+, by transferring the acetyl group to the ADP-ribose moiety to form O-acetyl-ADP-ribose, releasing free NAD^+, which is an inhibitor of sirtuin activity itself. The dependence of sirtuins on NAD^+ determine their activity directly linked to the energy situation of the cells, established through the ratio NAD^+/NADH, the absolute levels of NAD^+, NADH or nicotinamide or even a mix of these parameters (44).

In mammals exist seven sirtuin family members, including three of them (Sirtuin 3, Sirtuin 4 and Sirtuin 5) localized primarily in the mitochondria (45,46). For many years,

sirtuins have been linked to life-span regulation. However, more recent studies focused their attention in establishing alternative and diverse functions of sirtuins. One particular property of sirtuins that will be mentioned in this thesis is the regulation of mitochondrial number, turnover and activity. Emerging evidences suggest that sirtuins play a role as metabolic sensors by using intracellular metabolites, such as NAD^+, or short-chain carbon fragments like acetyl-CoA, in order to regulate mitochondrial function to overcome restriction of nutrient supply or in adaptation to hypoxic situations (47). In these settings, during years, the attention has been focused on Sirtuin 1 biology, which regulates inflammation, mitochondrial biogenesis and endothelial function, among other processes. Interestingly, its activity is reduced by oxidative damage. However, there is high interest in understanding the function of the others family members.

Concretely, Sirtuin 3 is a NAD^+-dependent protein deacetylase located in the mitochondrial matrix. It has been implicated in regulating metabolic processes by activating and deactivating mitochondrial target proteins by deacetylation of key lysine residues (Figure 6) (48,49).

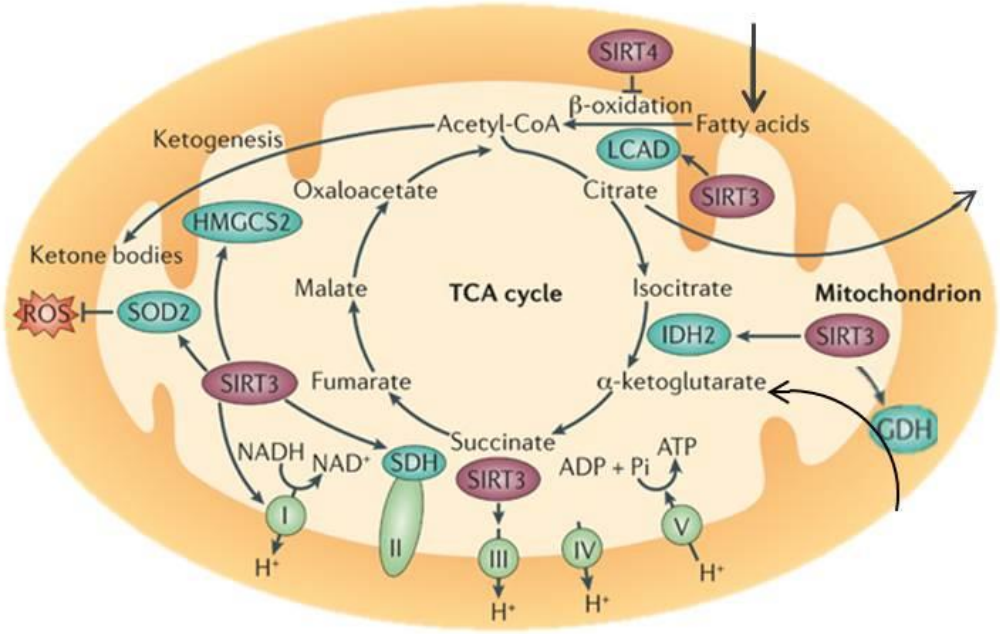

Figure 6. The implication of the Sirtuin 3 in mitochondrial function. Sirtuin 3 is directly regulating the activity of SOD2 to attenuate ROS levels. Additionally, Sirtuin 3 promotes fatty acid oxidation through LCAD, IDH2 and NDUFA9 subunit from MRC complex I and interacts with SDHA and SDHB subunits from MRC complex II, enhancing its activity and promoting cellular respiration.

Image adapted and modified from Riekelt H *et al.* (49).

Acetyl-CoA: acetyl-coenzyme A; GDH: glutamate dehydrogenase; H^+: protons; I: MRC complex I; IDH2: isocitrate dehydrogenase; II: MRC complex II; III: MRC complex III; IV: MRC complex IV; MRC: mitochondrial respiratory chain; LCAD (or ACADL): acyl-CoA dehydrogenase, long chain; NADH: reduced form of nicotidamide adenine dinucleotide; NAD^+: oxidized form of nicotidamide adenine dinucleotide; NDUFA9A: NADH dehydrogenase 1 alpha subcomplex subunit 9; ROS: reactive oxygen species; SDH: Succinate dehydrogenase subunit; SOD2: superoxide dismutase 2; SIRT3: sirtuin 3; SIRT4: sirtuin 4; TCA: tricarboxilic cycle or Krebs cycle; UCP2 Mitochondrial uncoupling protein 2.

There is evidence that Sirtuin 3 would enhance mitochondrial respiration and attenuate ROS production in cultured cells (50–52). Described targets in the MRC of Sirtuin 3 include subunit NDUFA9A of complex I, SDHA and SDHB subunits of complex II and ATP synthase subunit ATP5A. Additionally, the enzymes isocitrate dehydrogenase (IDH2) and glutamate dehydrogenase (GDH) are deacetylated by Sirtuin 3. The required mitochondrial enzyme acetyl-CoA synthase 2 (AceCS2) for generating acetyl-CoA is also a deacetylation target of Sirtuin 3. Moreover, Sirtuin 3 deacetyles and activates SOD2, a mitochondrial antioxidant enzyme, providing protection against oxidative damage, among others (summarized in Table 3) (53).

Table 3. List of described targets of sirtuin 3, their subcellular localization and the effect of deacetylation on protein function.

Targets	Localization	Sirtuin Action	Final Function
AceCS2	Mitochondria	Activates enzyme	Activate ketone metabolism
HMGCS2	Mitochondria	Activates enzyme	Activate ketone metabolism
OTC	Mitochondria	Activates enzyme	Reduces ammonia toxicity and ROS
GDH	Mitochondria	Activates enzyme	Oxidative deamination of glutamate
IDH2	Mitochondria	Activates enzyme	Reduces ROS
LCAD	Mitochondria	Activates enzyme	Promotes lipid processing
NDUFA9A	Mitochondria	Activates enzyme	Up-regulates ETC activity
SDHA and SDHB	Mitochondria	Activates enzyme	Up-regulates ETC activity
ATP5A	Mitochondria	Activates enzyme	Up-regulates ETC activity
SOD2	Mitochondria	Activates enzyme	Reduces ROS
ALDH2	Mitochondria	Deacetylation	Allows NAPQI binding to ALDH2, reducing its activity
MRPL10	Mitochondria	Inhibition of enzyme	Inhibition of mitochondrial ribosome
Cyclophilin D	Mitochondria	Deactivates enzyme	Prevents interaction with mPTP

Adapted and modified from data contained in Sack MN *et al.* (53).

AceCS2: acetyl-CoA synthase 2; ALDH2: aldehyde dehydrogenase, mitochondrial; ATP5A: ATP synthase subunit ATP5A; ETC: electron transport chain; GDH: glutamate dehydrogenase; HMGCS2: 3-hydroxy-3-methylglutaryl-CoA synthase 2, mitochondrial; IDH2: isocitrate dehydrogenase; LCAD (or ACADL): acyl-CoA dehydrogenase, long chain; mPTP: mitochondrial permeability transition pore; MRPL10: 39S ribosomal protein L10, mitochondrial; NDUFA9A: NADH dehydrogenase 1 alpha subcomplex subunit 9; NAPBQI: *N*-acetyl-*p*-benzoquinone imine; OTC: ornithine transcarbamylase; ROS: reactive oxygen species; SDHA: succinate dehydrogenase complex, subunit A; SDHB: succinate dehydrogenase complex, subunit B; SOD2: superoxide dismutase 2.

Despite the role of Sirtuin 3 in hypoxia is scarcely explored, the aforementioned emergent role of Sirtuin 3 in regulating diverse pathways in mitochondrial metabolism and stress response is shown in Figure 7 in a situation of nutrient restriction (43).

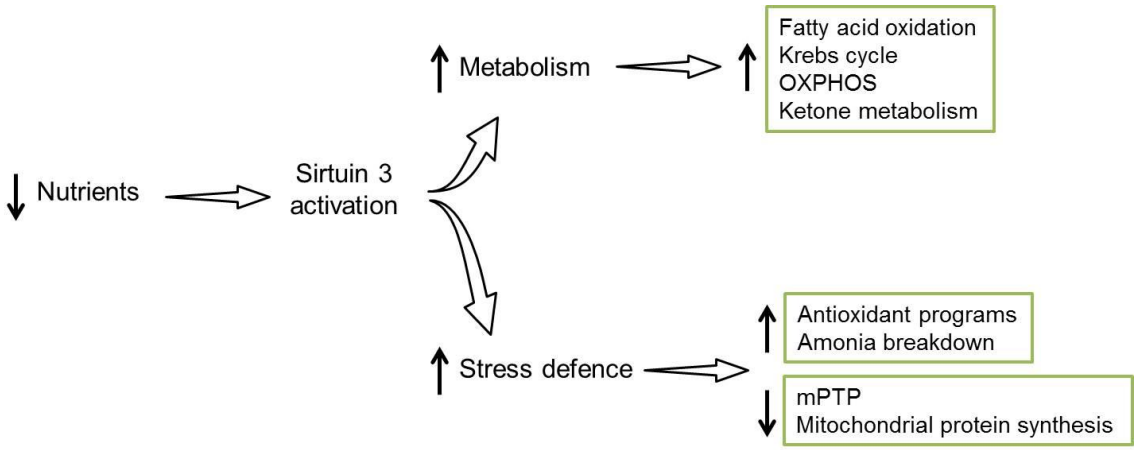

Figure 7. A scheme representing the role of Sirtuin 3 in a situation of metabolic adaptation and stress defence in the context of low nutrient supply.

Adapted and modified from data contained in Sack MN *et al.* (43).

mPTP: mitochondrial permeability transition pore; OXPHOS: oxidative phosphorylation.

2.4 CURRENT RESEARCH IN IUGR

Research in IUGR is fundamental in an attempt to understand its etiopathology and reduce its foetal and perinatal mortality and related-consequences after birth. One of the greatest challenges is based on developing potential biomarkers for the diagnosis of IUGR.

To date, the literature on IUGR has highlighted several molecular pathways involved in energy homeostasis, autophagy, methylation or metabolism, among others. Interestingly, a growing field of interest in IUGR is being focused on energy production to explain the attempted fail to achieve expected foetal and cardiac development.

2.4.1 Molecular mechanisms involved in human IUGR

Several studies based on proteomic analysis have been performed in serum, maternal and neonatal blood cells and placenta from pregnant women and infants with IUGR (54–57). These studies displayed significant proteome differences compared with normal pregnancies thus, indicating the existence of a variety of mechanisms and proteins that might be involved in the development of IUGR. However, further research is needed to elucidate the concrete roles of these proteins in IUGR. In summary, all this studies pointed out alterations in triglycerides levels and apolipoproteins being increased in maternal and neonatal blood from IUGR cases (55,56). These observations are linked to the fact of developing cardiovascular and metabolic disorders later in life supporting the 'Barker theory' of adverse conditions in intrauterine environment determine long-term effects after birth (58). Additionally, a proteomic study in human placenta presented dysfunction of several molecules indicating abnormal trophoblastic invasion and vascular development, such as nicotinamide adenine dinucleotide phosphate (NADPH) oxidase, alpha-1-antitrypsin (SERPINA1), insulin-like growth factor (IGF) and vascular endothelial growth factor (VEGF), and oxidative stress, all factors associated with apoptosis (57). Added to these proteomic studies there are a few data obtained from transcriptomic analysis in human placenta from IUGR pregnancies. Briefly, authors reported up regulation of inflammatory response as well as alterations in glucocorticoid metabolism with no difference in imprinted gene expression in human placental tissue (59). On the other hand, a transcriptomic analysis also in human placenta from IUGR subjects described that genes involved in mitochondrial function and OXPHOS were decreased affecting three out of five

complexes of the MRC, and thus energy production and metabolism (60).

Additionally, other lines of investigation to better understand molecular pathways involved in IUGR have been explored (61). For instance, previous research has established an increase of autophagy and apoptosis in placental cells from IUGR pregnancies (62,63). Furthermore, it has been described that the heat shock proteins, which are the molecular chaperones involved in the protein folding in response to physiological and environmental factors, are involved in IUGR, in which context, reduced expression of phosphorylated heat shock protein 27 (HSP-27) activates the apoptosis of placenta via activation of caspase 3 (64).

All the research in the field of IUGR has been mainly performed in placenta (whole tissue or isolated cell types) and, although in a few studies, in maternal peripheral and neonatal cord blood cells (PBMC and CBMC, respectively). However, the study either in maternal or neonatal blood cells has been already used in literature to study mitochondrial function (65–69). However, some research has been focused on evaluating molecular mechanisms underlying associated consequences of IUGR in other tissues, such as lung, kidney, liver, adipose tissue, among others. For this purpose, several animal models have been developed, being fundamental to overcome target tissue limitation and to further study the long-term consequences of this obstetric complication.

2.4.2 Animal models to study IUGR

Different animal models of IUGR have been developed consisting of carunclectomy, uterine artery ligation, uterine space restriction, caloric restriction or hypoxic conditions, among other procedures, in different species of animals (mainly sheep, pigs or rats models).

For instance, several experimental approaches have been used in sheep to mimic human IUGR. Some researchers used non-pregnant ewes to perform a surgical removal of the majority of the endometrial caruncles (called carunclectomy) from the uterus that results in the experimental restriction of placental and foetal growth (70–72). Then, they implanted vascular catheters in different places to control the blood flow to organs such as brain or heart (70). So, this model also allows studying the consequences in heart, in brain or even insulin signalling in skeletal muscle.

Another model with non-pregnant ewe consists of a restriction of the uterine space, which allows examination of IUGR relative to placental adaptation and foetal growth during development. This surgical technique is based on completely disconnect a single uterine horn, including separation of all intercornual connections using an electroautery (73). A similar procedure but inducing bilateral uterine artery ligation (both the right and the left uterine arteries) is also performed in pregnant rats to induce IUGR (74,75).

Furthermore, a model to study the effects of hypoxia in foetal organs consists of using pregnant guinea pigs and placed them in a plexiglass chamber containing 10.5% of oxygen for 14 days (hypoxic conditions). These authors have found that chronic intrauterine hypoxia reduce foetal body weight (76). The same group study the prenatal hypoxia effects placing the pregnant guinea pigs in the chamber with hypoxia conditions and allow them to deliver in the chamber (77). Additionally, other models with pregnant guinea pigs consist of inducing chronic placental insufficiency by uterine artery ligation. It is a technique commonly used to impair intrauterine growth restriction in rodents, since it exhausts uterine capacity leading to discordant foetal growth within offspring and different foetal growth restriction. Uterine artery ligation is performed at the base of the arterial arcade at day 28-30 of gestation (the gestation in pig ends at 63-66 days). Some researchers have used this model to study cardiac remodelling of aortic development to link it to later cardiovascular disease (78).

Additionally, there is an animal model of IUGR developed by administering a low-sodium diet to pregnant rats during the last 7 days of gestation. This model creates a full expansion of maternal circulating volume and the increase in uterine artery diameter, leading to reduced placental weight (79). On the other hand, rat models of IUGR based on caloric restriction have been extensively used to study IUGR and impaired cardiac function. Concretely, Keenaghan *et al.* have exposed pregnant rats to caloric restriction and acute hypoxic stress to evaluate cardiac response to hypoxia in a context of IUGR, describing to be more sensitive to hypoxia, leading to dysfunctional cardiac response (80). Additionally, research with IUGR muscle of rats based on uteroplacental ligation exhibited decreased rates of oxygen consumption and ATP production accompanied by decreased activity of pyruvate dehydrogenase (81).

Moreover, models of pregnant sows and gilt pigs feed with a commercial diet (simulating caloric restriction) during their pregnancies have been also used to study IUGR (82). Interestingly, this approach with IUGR piglets demonstrated an impaired hepatic mitochondrial biogenesis and energy homeostasis together with less mtDNA

levels (82,83). On the other hand, alternative animal models have been used to study mitochondrial function in IUGR and subsequent consequences. For example, it has been described less mtDNA in the jejunum of IUGR piglets as well as less mRNA levels of some of the MRC complexes (84).

Finally, a rabbit model of IUGR and cardiovascular remodelling was developed by our collaborator group, which consists of a selective ligation of the uteroplacental vessels that reduce 40% to 50% of oxygen and nutrients supply to the foetus in development (85). Concretely, this model has been used in this thesis to study the consequences of IUGR in the heart.

2.4.3 Importance of mitochondria in IUGR and cardiovascular remodelling

Some research on cardiovascular remodelling associated to IUGR has been carried out in the rabbit model of IUGR developed by our group (85,86). Using this approach, researchers have been able to overcome the target tissue limitation (heart). Additionally, this model represents an approach to study placental insufficiency evidenced in pregnant women with IUGR.

Several lines of evidence suggest that IUGR offspring from the rabbit model present biometric changes, high rates of mortality and morbidity and the reported cardiovascular alteration characteristic of human IUGR (1,87,88). These common alterations in animal model and humans validate the rabbit model of IUGR and associated cardiovascular remodelling.

Cardiac gene expression data in this rabbit model of cardiovascular remodelling suggests that there are alterations in different cellular pathways, all of them converging to mitochondria, specially: OXPHOS, oxygen homeostasis, complex I of the MRC and NADH dehydrogenase. Additionally, hearts of IUGR offspring show a looser packing of mitochondria and a higher cytosolic space between mitochondria and myofilaments (Figure 8). The relative volume occupied by mitochondria among the IUGR myocardium is reduced while the relative cytoplasm volume is increased (89). These findings are accompanied with no changes in size and number of mitochondria indicating that changes in the relative volume occupied by mitochondria are not due to changes in mitochondrial size or number. All these transcriptomic and ulstrastructural evidences lead to hypothesise a potential altered mitochondrial function in this obstetric complication.

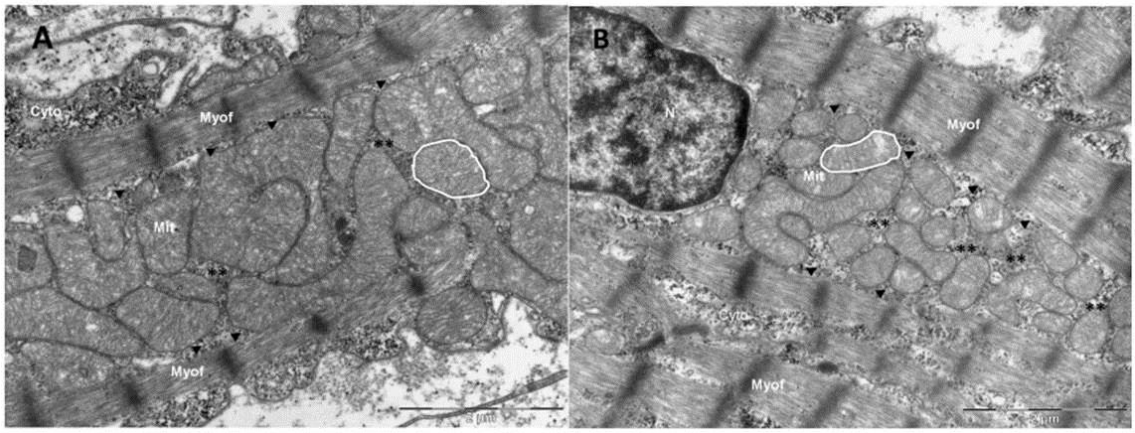

Figure 8. Cytoarchitectural organization of cardiomyocytes. Micrographs representing the typical organization of the intracellular space in foetal cardiomyocytes from control (A) and IUGR (B). While mitochondria are highly compacted and packed close to myofilaments in controls, they lose packaging and show an increased cytosolic space both within the mitochondrial network (indicated as ** in the image) and between mitochondria and myofilaments (indicated as ▼ in the image) in IUGR. Magnification: 20.000X. Scale bar: 2 µm.

Image obtained from Gonzalez-Tendero et al (89).

Cyto: cytoplasm; Mit: mitochondria; Myof: myofilaments; IUGR: intrauterine growth restriction.

Evidences of mitochondrial involvement in IUGR have also been obtained from studies in human pregnancies. For instance, it is already known that reduced birth weight is associated to *in utero* exposure of foetuses to tobacco, which has previously described to damage mitochondria in non-pregnant adult smokers (18). Carbon monoxide (CO) is one of the most potent harmful compounds of tobacco because its capacity to replace oxygen bound to organic molecules such as complex IV of the MRC. The specific inhibition of complex IV by CO has negative consequences on mitochondrial respiration and OXPHOS leading to an energetic deficit and increased ROS production lately promoting apoptosis. Furthermore, CO crosses the placental barrier and reaches the foetus in development. In this line, one study of our group reported mitochondrial dysfunction in smoking pregnant women complicated with IUGR, where the placental mitochondrial toxicity positively correlated with diary tobacco consumption and prompt mitochondrial toxicology of CO as the cause of this “toxic” IUGR. Additionally, mitochondrial dysfunction is present and correlated at maternal-foetal level between maternal PBMC and neonatal CBMC, highlighting that mitochondrial damage characteristic of chronic smokers is transferred to foetal mitochondria, becoming the likely etiopathogenesis of associated ‘toxic’ IUGR.

Additionally to all this evidence, other authors have focused efforts in studying the

mitochondrial function in human IUGR. For example, Novielli C *et al.* demonstrated increased levels and higher methylation of mtDNA in cord blood from IUGR newborns (68). Also, another study evaluated cord blood biomarkers of cardiac dysfunction and damage in IUGR newborns, highlighting the increased levels of cord blood BNP levels in IUGR newborns (69). Furthermore, there are data available describing decreased MRC CI, CI+III and CIV in IUGR cases and also other obstetric complications such as PE (90). Following the same line of investigation, Mando *et al.* found lower mRNA levels of MRC CII, CIII, and CIV in IUGR cytotrophoblast cells but no differences at the protein level, suggesting a posttranscriptional compensatory regulation. They suggested different mitochondrial content and activity depending on the placental cell lineage (91). Also interestingly, other authors have been studied the placenta from SGA cases, demonstrating a lower mtDNA content and a higher SOD activity, which parameters maintained negative association (92). Nevertheless, other author's results do not argue in favour of a mitochondrial involvement in placental insufficiency, suggesting that the glycolytic pathway may represent a key energetic source in placental insufficiency diseases (93). Increasing but controversial data supports the need for exhaustive mitochondrial functional phenotyping of IUGR, assessing at the same time the implication of different tissues and, ideally, evaluating placental, maternal and foetal effects.

On the other hand and independently of IUGR, certain human cardiomyopathies are associated to mitochondrial alterations (94). Mitochondria seem to rely at the basis of inflammatory processes and cellular senescence characteristic of arteriosclerosis and several cardiomyopathies (95,96). For instance, in human dilated cardiomyopathy there is evidence of alterations in the enzymatic activity of complex III of the MRC (97). Furthermore, a number of mitochondrial diseases occur with some cardiomyopathy in both adults and children (94,98,99). Actually, cardiomyopathy is a common feature of paediatric patients with OXPHOS disorders (100).

As mentioned previously, mitochondrial dysfunction could lead to oxidative stress and, oxidative stress contributes to mitochondrial dysfunction. In the context of pregnancy, it is already known that ROS production seems to play a pivotal role during foetal programming and also in cardiovascular remodelling, both in response of the suboptimal intrauterine environment (101–103).

Currently, there is few data supporting mitochondrial dysfunction or oxidative stress in the idiopathic form of this obstetric complication and associated cardiovascular remodelling (60,90,91). However, all this background points out the relevant need to

widely characterise mitochondrial implication in IUGR in an attempt to search etiopathologic targets, novel biomarkers and potential therapeutic approaches for this obstetric complication.

In the following pages, the present thesis provides evidence of the mitochondrial implication in IUGR and cardiovascular remodelling through an exhaustive characterization of the mitochondrial function. We first attempt to evaluate mitochondrial function in the target tissue of cardiovascular remodelling (the heart) and in the tissue responsible for oxygen and nutrient supply into the foetus in development (the placenta) in a rabbit model of IUGR, to secondly validate results in human pregnancies at placental, maternal and neonatal level. The deeper understanding of mitochondrial implication in IUGR and foetal cardiovascular remodelling might help to develop new tools for the management of this obstetric complication and associated long-term effects.

3. HYPOTHESIS AND OBJECTIVES

We hypothesise a mitochondrial involvement in IUGR and associated cardiovascular remodelling in accordance to deregulation of metabolic sensors as Sirtuin 3. The association of molecular alterations with clinical manifestations may improve the knowledge for further research on potential novel biomarkers or therapeutic strategies for this obstetric complication.

The main objectives of this thesis are to:

1. Establish whether mitochondrial transcriptional and ultrastructural changes, previously evidenced in hearts of IUGR offspring from the rabbit model, are translated to mitochondrial alterations at functional level in the 'target tissue' of cardiovascular remodelling, the heart (study 1).

2. Evaluate this potential mitochondrial dysfunction in the tissue responsible for oxygen and nutrient supply to the foetus (the placenta) in the same rabbit model (study 1).

3. Determine whether mitochondrial imbalance is also present in the placenta from human pregnancies with IUGR (study 2).

4. Assess if similar mitochondrial disarrangements are evident in peripheral and cord blood cells from pregnant women and their newborns with IUGR (study 2).

5. Establish the involvement of potential regulator of mitochondrial dysfunction as Sirtuin 3 both in the rabbit model and human pregnancies with IUGR in association to mitochondrial dysfunction (studies 1 and 2).

6. Correlate the severity of IUGR and cardiovascular remodelling (biometric and clinical data) with experimental results in both the animal model (study 1) and human pregnancies (study 2) to contribute to deepen in the knowledge of potential biomarkers or therapeutic targets of this obstetric complication.

4. METHODS

4.1 STUDY DESIGN

This thesis contains two studies: the first performed in animals and the second performed in patients. Both are transversal and controlled studies that share common milestones and experimental methodological approaches.

4.1.1 Animal model

Six New Zealand white pregnant rabbits were used to obtain 16 IUGR and 14 control offspring by reproducing a model of IUGR previously reported (85,86). This model was based on the selective ligature of uteroplacental vessels to reduce 40 to 50% of oxygen and nutrient supply into the foetuses in development. The ligation was performed only in one of the two uterine horns in order to obtain, in the same pregnancy, the IUGR (from the manipulated horn) and control (from the non-manipulated horn) offspring (Figure 9).

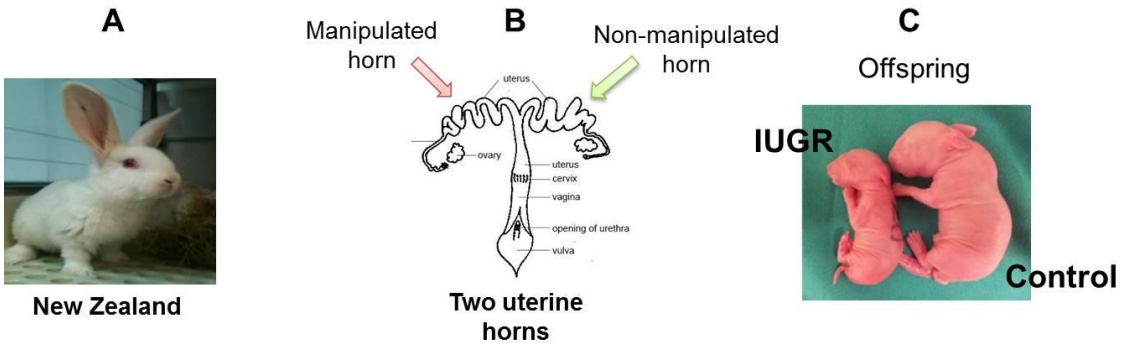

Figure 9. A) The **New Zealand** breed used to reproduce the rabbit model of intrauterine growth restriction (IUGR) and cardiovascular remodelling. **B)** The **two uterine horns** characteristic of rabbit that allow obtaining IUGR and control offspring in the same pregnancy by manipulating one of the two uterine horns. **C)** A representation in size of one **IUGR rabbit versus a control rabbit** after delivery.

Concretely, pregnant animals were fed with standard diet and water *ad libitum*, with 12h/12h of light cycle. At day 25 of gestation, in each pregnant rabbit, the selective ligature of uteroplacental vessels in only one of the two uterine horns was performed. Briefly, tocolysis (progesterone 0.9mg/kg intramuscular) and antibiotic prophylaxis (Penicillin G 300.000 UI intravenous) were administered before uteroplacental vessel surgery. Ketamine (35 mg/kg) and xylazine (5 mg/kg) were given intramuscularly for anaesthesia induction. Inhaled anaesthesia was maintained with a mixture of 1-5% isoflurane and 1-1.5 l/min oxygen. After a midline laparotomy, both uterine horns were

exteriorized but only one was ligated to reproduce IUGR. At day 30 (full-term pregnancy), a caesarean section was proceeded to obtain both IUGR and control offspring from the same pregnancy (all six pregnant rabbits with the same gestational age) (85,86). After the procedure, the abdomen was closed and animals received intramuscular meloxicam 0.4 mg·kg_1·24 h_1·48 h, as postoperative analgesia. Offspring weighting under the 10^{th} percentile of birth weight were considered IUGR if they accomplished two criteria: weighting less than 60 grams (maximum cut-off) and never weighting higher than any control offspring from the same nest (Table 4).

Table 4. Sample size included for each pregnant rabbit according to 10^{th} percentile of birth weight.

Pregnant rabbit	N Offspring	
	N Control	***N IUGR***
1	1	1
2	4	4
3	4	4
4	2	2
5	1	1
6	2	4
N total	**14**	**16**

N: number of sample; IUGR: intrauterine growth restriction

All newborn rabbits were sacrificed by decapitation after caesarean and the hearts of newborn rabbits were immediately removed from the chest cavity and were then weighed and preserved with Biops medium (2.77mM CaK_2EGTA, 7.23mM K_2EGTA, 5.77 mM Na_2ATP, 6.56 mM $MgCl_2 \cdot 6H_20$, 20mM Taurine, 15mM $Na_2Phosphocreatine$, 20mM Imidazole, 0.5mM Dithiothreitol and 50mM MES, pH 7.1) on ice. Likewise, the placentas of these newborn rabbits were identified, weighed and preserved with Biops medium (prepared as mentioned previously), on ice.

All biometric parameters were measured once, following standardized protocols (85,86).

Animal handling and all the procedures were performed in accordance to the prevailing regulations and guidelines (104–106) and with the approval of the Animal Experimental Ethics Committee of the University of Barcelona (Barcelona, Spain).

4.1.2 Pregnant women and their newborns

A single-site, cross-sectional and observational study at the Maternal-Foetal Medicine Department of the Hospital Clinic of Barcelona (Spain) was conducted for two years.

This study included 14 pregnancies complicated by IUGR which was defined as estimated birth weight below the 3th percentile or, alternatively, below the 10th percentile in case of abnormal UA Doppler or abnormal CPR (7,107). Birth weight percentile was calculated considering birth weight, weeks of gestation and neonatal gender. Despite final IUGR diagnostic is only confirmed at delivery, all potential pregnancies complicated by IUGR in views of trimestral echography follow up were monitored during the gestational period. In parallel, 22 uncomplicated pregnancies with appropriate for gestational age (AGA) newborns were considered as the control group (Table 5).

Additional information: maternal age at delivery, mode of delivery, placental weight, newborn sex, pH umbilical artery cord blood and preeclampsia incidence were collected and registered in a database. Also, the Apgar 5' score which reports the clinical status of the newborn immediately after birth (108). It is determined by evaluating five components of the newborn on a 0-2 scale (to a maxim score of 10 indicating the healthiest status): activity (muscle tone), pulse, grimace (reflex irritability), appearance (skin colour) and respiration. The score is reported at 1 minute and 5 minutes after birth for all infants, and at 5-minute intervals thereafter until 20 minutes for infants with a score less than 7. Following these criteria, in this study, we classified the newborns between normal (8-9/10) and abnormal Apgar (3-6/8-10).

As a reliable marker of foetal cardiac remodelling, Brain Natriuretic Peptide (BNP) levels were measured in neonatal plasma by the CORE laboratory of our Hospital using an Advia Centaur XP. (69,109).

Table 5. Sample size used to analyse each experimental parameter in human pregnancies.

Parameters	Placenta		Maternal PBMC		Neonatal CBMC	
	N Control	*N IUGR*	*N Control*	*N IUGR*	*N Control*	*N IUGR*
Clinical data	22	14	22	14	22	14
Enzymatic activities of the MRC	21	13	22	14	21	9
Oxygen consumption	15	11	18	11	18	7
Lipid peroxidation	21	13	20	14	21	9
Cellular ATP levels	21	13	22	13	22	10
mtDNA copy number	-	-	-	-	20	10
Sirtuin 3 levels	13	9	-	-	-	-

ATP: adenosine triphosphate; CBMC: cord blood mononuclear cells; IUGR: intrauterine growth restriction; MRC: mitochondrial respiratory chain; mtDNA: mitochondrial DNA; N: number of sample; PBMC: peripheral blood mononuclear cells;

The inclusion criteria were: >18 years of age, singleton pregnancies, delivery >22 weeks of gestation and no tobacco consumption in both IUGR and control pregnancies. Pregnant women taking potentially toxic drugs for mitochondria and with familial history of mitochondrial disease were excluded.

The study was approved by the Ethical Committee of our hospital and it was performed following the Declaration of Helsinki. All participants provided a written informed consent.

4.2 SAMPLE PROCESSING

4.2.1 Animal model

Left ventricle was used for mitochondrial studies because is the target tissue in which previous transcriptomic and ultrastructural alterations were observed. Additionally, is the tissue were cardiomyopathies are preferentially manifested.

Each left ventricle and placental tissue were processed as follows (Figure 10): a piece of each tissue was maintained in fresh conditions with Biops medium to assess mitochondrial oxygen consumption, and the remaining tissue was cryopreserved at -80ºC and further homogenized (Caframo technologies, Ontario, Canada) at 5% (w/v) in mannitol buffer for mitochondrial analysis.

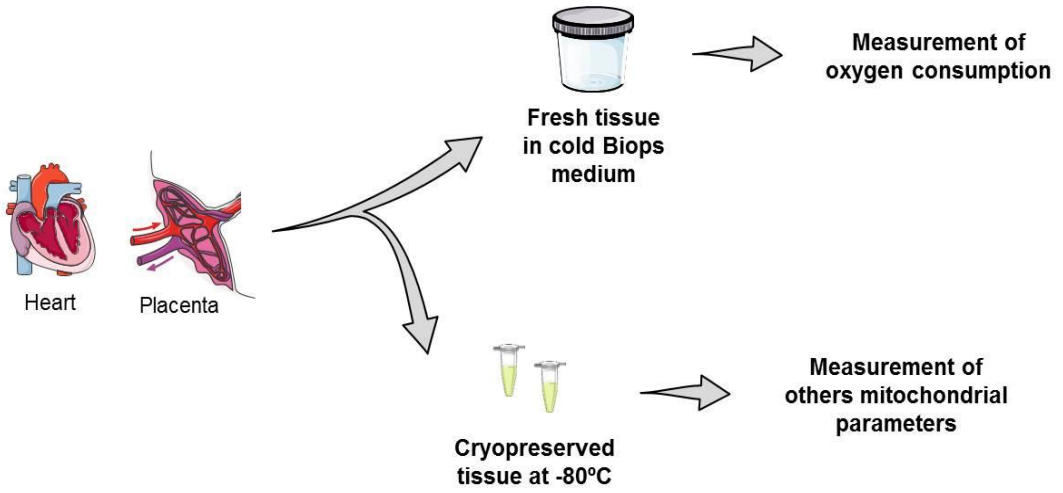

Figure 10. Two different types of **sample processing** depending on posterior analysis **of heart and placental tissue from the offspring of the rabbit model.**

The protein content was quantified in left ventricle heart and placental homogenates using the bicinchoninic acid colorimetric assay (Thermo Scientific assay kit Prod #23225, Waltham, MA, USA) to normalize experimental measures.

4.2.2 Pregnant women and their newborns

At delivery, **placental samples** were weighted and, after discarding blood residuals, a full thickness section (from both maternal and foetal side) was obtained and processed as follows (Figure 11): a piece of 500 mg of placenta was homogenized (Caframo technologies, Ontario, Canada) with 10% BSA-Solution A to further isolate fresh mitochondria and immediately perform *in vivo* oxygen consumption assay. The remaining placental tissue was immediately cryopreserved at -80ºC and further homogenized at 5% (w/v) in Mannitol buffer to perform the rest of mitochondrial analysis.

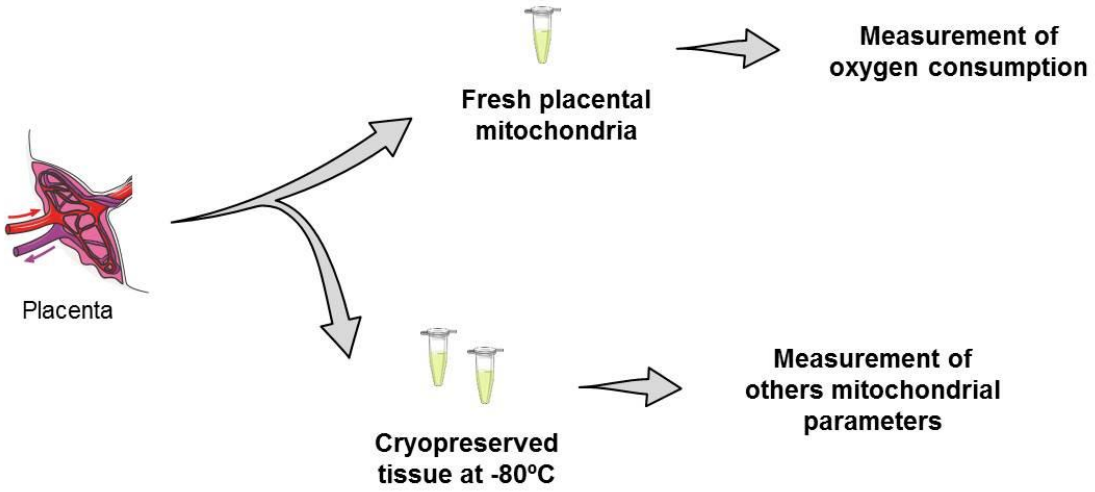

Figure 11. Two different types of **sample processing** depending on posterior analysis **of human placental tissue from pregnant women.**

Immediately after delivery, 10-20 ml of **maternal peripheral blood and neonatal cord blood** were collected to isolate mononuclear cells as it has been previously validated its usefulness for the study of mitochondrial dysfunction (65–67).

In detail, maternal and neonatal blood was collected in EDTA tubes to isolate **plasma** (1500 g, 15 minutes) and immediately frozen at -80ºC for posterior analysis. Afterwards, peripheral blood mononuclear cells (PBMC) and cord blood mononuclear cells (CBMC) were also isolated from blood by density gradient centrifugation using Ficoll-Lymphoprep (Histopaque®1077, Sigma Diagnostics, St. Louis, MO) in sterile conditions (Figure 12) (110). Briefly, fresh blood was diluted 1:1 with phosphate buffer saline (PBS) 1x and 20-30mL of diluted blood was deposited over 15mL of Ficoll® with caution, avoiding mixing, in a 50mL conical centrifuge tube. Tubes were centrifuged for

30 min at 660g at room temperature, without break. PBMC or CBMC stay in the interface within the Ficoll solution and blood plasma due to the density of these cells. Finally, PBMC or CBMC were recovered and washed with PBS 1x. One aliquot of each sample was maintained in fresh conditions with PBS buffer to assess *in vivo* mitochondrial oxygen consumption, and the remaining aliquots were stored at -80°C until further mitochondrial analysis. The protein content was quantified as mentioned before to normalize experimental measures.

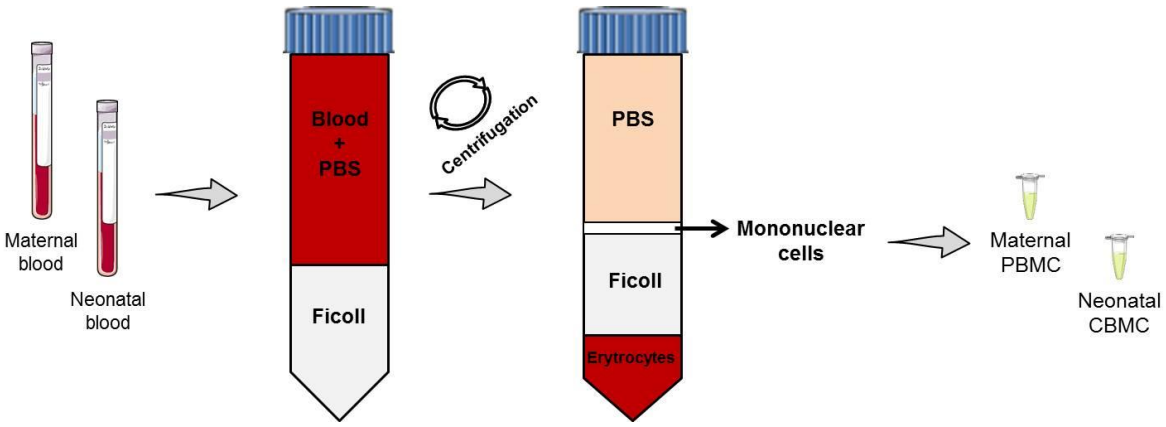

Figure 12. Scheme representing the isolation of human mononuclear cells from maternal peripheral blood and neonatal cord blood using a density gradient with Ficoll®
CBMC: cord blood mononuclear cells; PBMC: peripheral blood mononuclear cells; PBS: phosphate buffer saline

4.3 TISSUE HOMOGENIZATION

A 5 % (w/v) homogenate was performed from the cryopreserved tissue (heart and placental rabbit tissue or human placental tissue), following a procedure set up at 0-6ºC (Figure 13).

First of all, a mechanical disintegration with scissors was made in mannitol buffer from an amount of 30-50 mg of tissue. This disintegrated tissue was transferred into a potter and it was homogenized (from 3 to 10 strokes) at 850 rpm with a homogenizer. Once a homogenized solution was obtained, it was transferred to a microtube in order to centrifuge (650g for 20 minutes) and eliminate the cellular rests. After centrifugation, the supernatant was collected as the 5% (w/v) homogenate and, consequently, protein content was determined to set a 2 mg/ml homogenate.

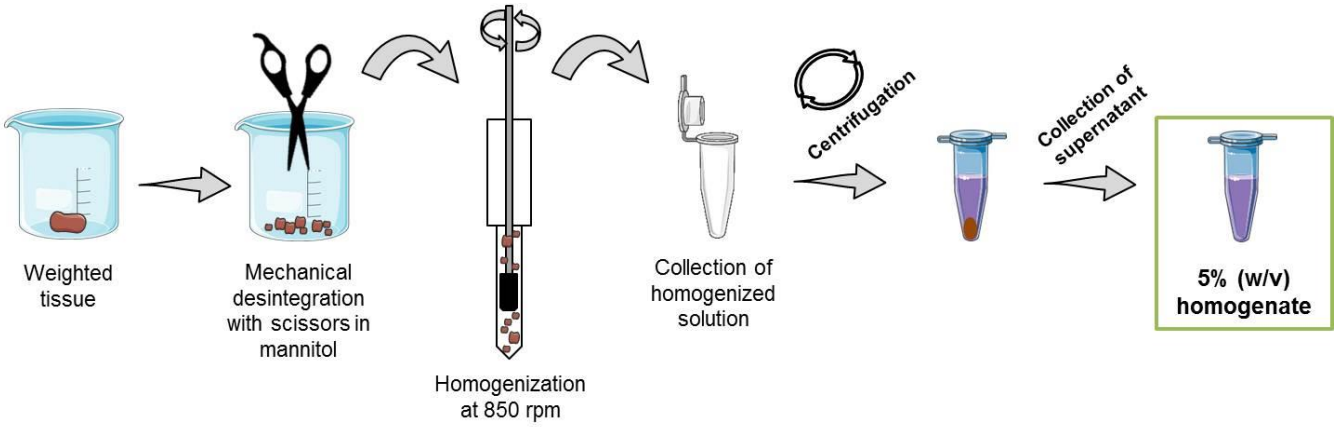

Figure 13. Preparation of a 5% (w/v) homogenate from tissue. A first step based on mechanical disintegration is required before the homogenization procedure. One centrifugation is needed to clean out and resuspend the remaining pellet to obtain the final 5% (w/v) homogenate.

4.4 MITOCHONDRIA ISOLATION

Placental mitochondria were isolated from human placenta through a density gradient centrifugation using Percoll® from 5 mg of fresh tissue, always set at 0-6ºC (Figure 14).

Tissue was placed into a beaker containing 1 mL of Solution A with BSA and a mechanical disintegration with scissors was performed. Immediately, the dispersed tissue was transferred into a potter and it was homogenized to break cell plasmatic membrane. Importantly, all this homogenized solution needs to be filtered and collected to a microtube. Then, the filtered homogenate was centrifuged at 2.000 rpm during 8 minutes to remove nucleus and cell debris. After centrifugation, the supernatant was collected in a tube as the homogenized tissue. To increase organelle extraction efficiency, the remaining pellet was resuspended with a calculated volume of Solution A + BSA. The process of homogenization with potter was repeated and also the centrifugation. After that, the supernatants were collected together and the whole homogenate was centrifuged at 10.000 rpm for 15 minutes to spin down organelles. Now, the supernatant (containing the remaining cytoplasm) was discarded and the resulted pellet (containing the mitochondrial-enriched fraction) was resuspended with 1mL of Percoll® + Solution A and centrifuged at 10.000 rpm for 8 minutes to wash isolated organelles. Again, the supernatant was discarded. Finally, the pellet containing a clean enriched-mitochondrial fraction was resuspended with 100 µL of Solution A + BSA.

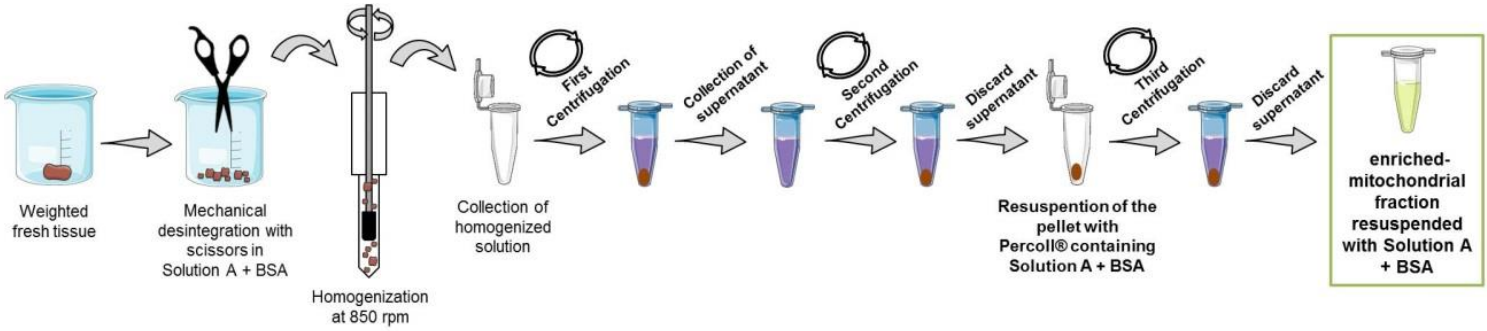

Figure 14. A schematic representation of isolation of mitochondria from tissue. A first step based on mechanical disintegration is required before the homogenization procedure. One centrifugation is necessary to eliminate cell debris and nucleus. The remained pellet should be resuspended with Percoll® containing solution A + BSA that together with the centrifugation prompt obtaining the enriched-mitochondrial fraction at the bottom of the microtube.
BSA: bovine serum albumin.

4.5 MITOCHONDRIAL STUDY

An exhaustive mitochondrial function study was performed through the assessment of enzymatic activities and protein subunit expression of some of the complexes of the MRC, oxygen consumption through endogen cell respiration (Cellox) and by adding exogenous substrates (glutamate and pyruvate) to stimulate Complex I (abbreviated as GMox and PMox, respectively, through the whole thesis). Also, the mitochondrial content, total ATP levels, oxidative damage and Sirtuin 3 protein expression was evaluated (Table 6).

Table 6. Summary of all mitochondrial function parameters analysed in each sample of both animal and human studies.

Mitochondrial parameter		Animal model		Human pregnancies		
		Heart	Placenta	Placenta	Maternal PBMC	Neonatal CBMC
Enzymatic activities of MRC	Complex I	x	x	x		
	Complex II	x	x	x	x	x
	Complex IV	x	x	x	x	x
	Complex I+II	x	x	x		
	Complex I+III	x	x	x		
Protein expression of MRC	SDHA	x	x			
	SDHB	x	x			
	COX5A	x	x			
	CoQ levels	x	x			
Oxygen consumption	Cellox				x	x
	GMox	x	x	x	x	x
	PMox	x	x	x	x	x
Mitochondrial content	Citrate synthase	x	x	x	x	x
	Tom20	x	x			
	mtDNA content					x
Total ATP levels		x	x	x	x	x
Oxidative damage	Lipid peroxidation	x	x	x	x	x
	SOD2 activity	x	x			
Sirtuin 3 expression		x	x	x		

ATP: adenosine triphosphate; CBMC: cord blood mononuclear cells; Cellox: cellular endogen oxidation (without substrates); CoQ: coenzyme Q; COX5A: cytochrome c oxidase subunit 5a; GMox: glutamate+malate oxidation; MRC: mitochondrial respiratory chain; mtDNA: mitochondrial DNA; PBMC: peripheral blood mononuclear cells; PMox: pyruvate+malate oxidation; SDHA: succinate dehydrogenase complex, subunit A; SDHB: succinate dehydrogenase complex, subunit B; SOD2: superoxid dismutase 2; Tom20: mitochondrial import receptor subunit TOM20.

4.5.1 Mitochondrial respiratory chain and citrate synthase activities

In order to study MRC function, the enzymatic activities of mitochondrial complex I, II, IV, I+III and II+III (CI, CII, CIV, CI+III and CII+III) were spectrophotometrically measured at 37ºC, as reported elsewhere (111).

The measurement of enzymatic activities of MRC in maternal PBMC and neonatal CBMC was restricted to CII and CIV based on previous results obtained from the animal model.

All enzymatic assays consisted of national standardized methods run in parallel with internal quality controls (111) and all the enzymatic assays, measured once per sample, simultaneously included both cases and controls.

Absorbance changes of the enzymatic activities along time were monitored in a HITACHI U2900 spectrophotometer using the UV-Solution software version 2.2 and were expressed as nanomoles of consumed substrate or generated product per minute and milligram of protein (nmol/minute·mg protein) (Table 7).

Table 7. Reagents, inhibitors and wavelength used to measure the enzymatic activities of each complex of the mitochondrial respiratory chain (MRC). The absorbance of the mix (Abs. variation) at the given wavelength (λ) is registered through changes of monitored reagent, due to electron passage from donor to acceptor. In some cases, a specific inhibitor for the same MRC complex allows the subtraction of unspecific activity or the blockade of the next electron transfer along the MRC.

	Monitored reagent	λ (nm)	Abs. variation	Electron donor	Electron acceptor	Inhibitors used
Complex I	NADH	340	Decrease	NADH	Decylubiquinone	Rotenone
Complex II	DCPIP	600	Decrease	Succinate	Decylubiquinone	KCN
Complex IV	Reduced cyt c	550	Decrease	Reduced cyt c	Oxygen	None
Complex I+III	Oxidized cyt c	550	Increase	NADH	Oxidized cyt c	Rotenone/ KCN
Complex II+III	Oxidized cyt c	550	Increase	Succinate	Oxidized cyt c	KCN

cyt c: cytochrome c; DCPIP: 2,6-diclorophenolindophenol; NADH: nicotinamide adenine dinucleotide, reduced form; KCN: potassium cyanide; λ: wavelength.

In more detail:

Complex I

Since this complex transfers electrons from NADH to ubiquinone, its activity can be determined monitoring the decrease of the absorbance from NADH at 340 nm. The CoQ (a hydrophobic natural acceptor) is replaced for decylubiquinone (a more hydrophilic compound).

It is important to take into account that NADH cytochrome b_5 oxidoreductase also oxidises NADH. As this activity is no sensitive to rotenone, its activity can be determined in a parallel assay containing rotenone, a specific inhibitor of complex I. Thus, the specific complex I activity (sensitive to rotenone) is calculated subtracting the unspecific activity by adding rotenone from the total activity without rotenone.

Composition of the reaction mix	
NADH	100 µM
Decylubiquinone	100 µM
Potassic phosphate	50 µM
BSA	3.75 mg/ml

Complex II

Since this complex transfers electrons from succinate to ubiquinone, its activity can be assessed monitoring the 2,6-diclorofenolindofenol (DCPIP) reduction evaluating the absorbance decrease at 600 nm of oxidized DCPIP. Here again, the CoQ (a hydrophobic natural acceptor) is replaced for decylubiquinone (a more hydrophilic compound). The basal line is subtracted from the activity that begins for the addition of decylubiquinone to posterior deducts the unspecific transfer of electrons to DCPIP.

Composition of the reaction mix	
Potassic phosphate	25 mM
Succinate	20 mM
DCPIP	50 µM
KCN	1 mM
BSA	2 mg/ml
Decylubiquinone	100 µM

Complex IV

Since this complex transfers electrons from reduced cyt c to oxygen, its activity can be determined monitoring the decrease of the absorbance from reduced cyt c at 550 nm.

Composition of the reaction mix	
Potassic phosphate	50 mM
Reduced cyt c	100 µM

Complex I+III

Since the combination of the activity of complex I and III transfers electrons from NADH (that it is oxidized to NAD+) to cyt c, its activity can be evaluated following the increase of the absorbance from reduced cyt c at 550 nm. The cyt c oxidation by complex IV is inhibited by cyanide (KCN) added in the reaction mix.

It is important to know that NADH can also be consumed by unspecific enzymes. Thus, the specific combined activity of complex I and III is the sensitive activity to rotenone calculated subtracting the non-sensitive activity to rotenone from the total NADH cytochrome C oxidoreductase.

Composition of the reaction mix	
NADH	200 µM
Cyt c	100 µM
Potassic phosphate	50 mM
BSA	1 mg/ml
KCN	1 mM

Complex II+III

Since the combination of the activity of complex II and III transfer electrons from succinate to cyt c, its activity can be assessed monitoring the increase of absorbance from reduced cyt c at 550 nm. The posterior oxidation of cyt c by complex IV is inhibited by KCN added to the reaction mix.

Composition of the reaction mix	
Succinate	20 mM
Cyt c	100 µM
Potassic phosphate	20 mM
BSA	2 mg/ml
KCN	1 mM

Citrate synthase activity

Mitochondrial content was determined through the enzymatic activity of citrate synthase. It is an enzyme participating in the Krebs cycle and validated as a good marker of mitochondrial mass. Citrate synthase catalyses the formation of citrate from oxaloacetate and acetyl-CoA. The reduced form of CoA, the CoA-SH, that is produced in last reaction transforms the 5,5'-dithiobis-2-nitrobenzoic acid (DTNB) into 2-nitro-5-thiobenzoic acid (TNB), at 412 nm. Thus, the citrate synthase activity could be evaluated by the increase of TNB absorbance at 412 nm.

Composition of the reaction mix	
DTNB	100 µM
Tris HCl pH 8.1	100 mM
Acetyl-CoA	300 µM
Oxaloacetate	500 µM
Triton 100x	0.1 %

4.5.2 Mitochondrial oxygen consumption

Different procedures for the measurement of oxygen consumption were performed depending on animal or patient source of sample.

4.5.2.1Animal model

To determine oxygen consumption of heart and placental tissue from IUGR and control offspring, 3-5 milligrams of each tissue were permeabilized on ice with 5% (w/v) saponin for 30 minutes in Biops medium. This permeabilized tissue was washed with cold respiration medium (Mir05: 0.5 mM EGTA, 3 mM $MgCl_2$, 60 mM K-lactobionate, 20 mM taurine, 10 mM KH_2PO_4, 20 mM HEPES, 110 mM sucrose and 0.1% (w/v) bovine serum albumin, pH 7.1) (Figure 15). High-resolution respirometry was performed at 37°C by polarographic oxygen sensors in a two-chamber Oxygraph-2k system according to the manufacturer's instructions (OROBOROS Instruments, Innsbruck, Austria). Manual titration of substrates and inhibitors was performed using Hamilton syringes (Hamilton Company, Reno, NV, USA). Data was recorded using the DatLab software v5.1.1.9 (Oroboros Instruments, Innsbruck, Austria).

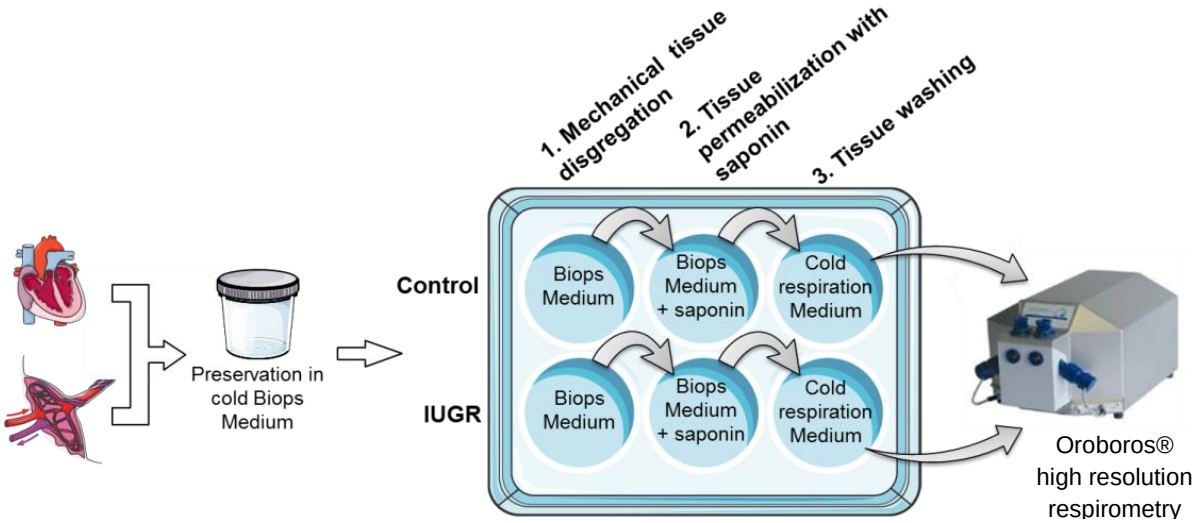

Figure 15. Permeabilization of fresh tissue with 5% saponin is required to perform mitochondrial oxygen consumption by Oroboros® high resolution respirometry.

Glutamate+malate oxidation (GM Oxidation), corresponding to electron donation of both substrates of MRC complex I, was quantified once in all samples. Specific oxygen uptake rates sensitive to antimycin a (which specifically inhibits mitochondrial oxygen consumption) were obtained following the manufacture's recommendations (112).

Oxygen consumption was normalized for the milligrams of dry tissue, thus, results were expressed as picomoles of oxygen consumed per second and milligram of tissue (pmol O_2/s·mg).

4.5.2.2 Pregnant women and their newborns

Isolated placental mitochondria, maternal PBMC and neonatal CBMC were used in fresh conditions to determine oxygen consumption at 37°C by polarography (oxygen electrode chambers from Hansatech Instruments) (Figure 16) (113).

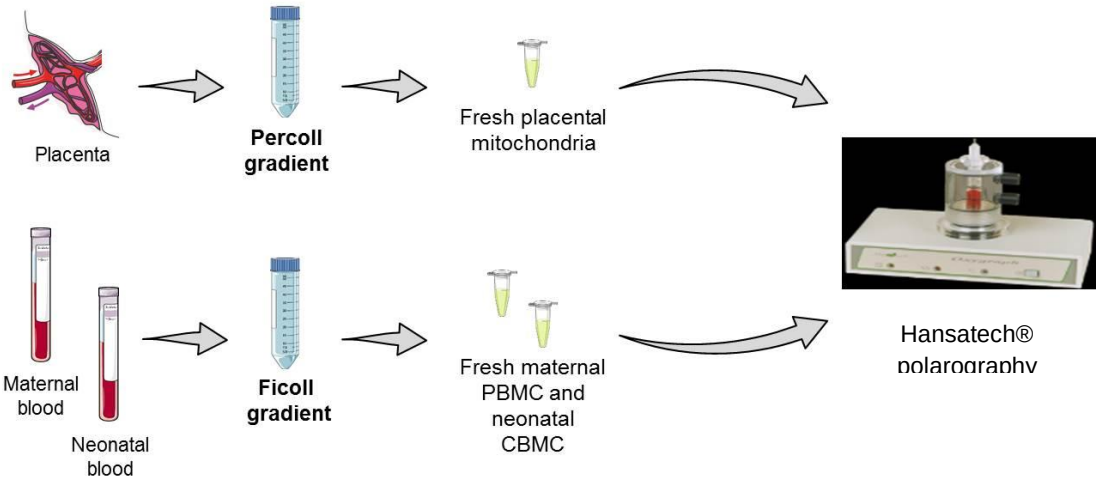

Figure 16. Mitochondrial oxygen consumption by Hansatech® polarography using fresh tissue.

Cellular oxygen consumption for endogen substrates (abbreviated as Cellox) was measured in intact maternal PBMC and neonatal CBMC. Digitonin was afterwards used to permeate blood cells. Manual titration of substrates for complex I stimulation (glutamate+malate or pyruvate+malate; throughout this paper, the terms GMox and PMox will refer to glutamate and pyruvate oxidation, respectively) was performed using Hamilton syringes (Hamilton Company, Reno, NV, USA). Data was recorded using O_2view Software.

Oxygen consumption was normalized by protein content, thus, results were expressed as picomols of consumed oxygen per second and milligram of protein (pmol O_2/s·mg prot.).

4.5.3 Mitochondrial coenzyme Q (CoQ) content

Tissue levels of CoQ_9 or CoQ_{10} (mobile electron transfer located within CI, CII and CIII in the MRC) were assessed in duplicates in the heart and placental homogenates from both cases and controls of the rabbit model by high pressure liquid chromatography (HPLC in reverse form) with electrochemical detection of the reduced and oxidized molecule, as described previously (114). Values were expressed as micromoles per liter (µmol/L).

4.5.4 Total cellular ATP levels

Cellular ATP levels were quantified in all samples in duplicates from both cases and controls using the Luminescent ATP Detection Assay Kit (Abcam, Cambridge, UK), according to the manufacturer's instructions. The results were normalized for protein content and expressed as picomolar of ATP per milligram of protein (pmol ATP/mg protein).

4.5.5 Lipid peroxidation (oxidative damage)

Lipid peroxidation was measured in duplicates as an indicator of oxidative damage into lipid membranes using the BIOXYTECH® LPO-586™ assay by spectrophotometric measurement of malondialdehyde (MDA) and 4-hydroxyalkenal (HAE) levels (both peroxides derived from fatty acid oxidation), according to the manufacturer's instructions (Oxis International Inc., CA, USA). The results were normalized for protein content and expressed as micromolar of MDA and HAE per milligram of protein (μM MDA+HAE/mg protein).

4.5.6 Mitochondrial DNA levels

Alternative measurement to determine mitochondrial content was performed by analyzing mitochondrial DNA (mtDNA) copy number. Thus, total DNA was phenol-chlorophorm-extracted, spectrophotometrically quantified and diluted at 5 ng/μl. Multiplex real-time PCR (PCR Applied Biosystems, Foster City, CA, USA, 7500 Real Time PCR System) was performed as previously reported by Moren el al. (115).

Briefly, determination of the mitochondrial 12S ribosomal RNA (mt12SrRNA) gene and the constitutive nuclear RNAseP gene (nRNAseP) was used. The former used mtF805 (5'-CCACGGGAAACAGCAGTGAT-3') and mtR927 (5'-CTATTGACTTGGGTTAATCGTGTGA-3') with the TaqMan Probe 6FAM-5'-TGCCAGCCACCGCG-3'-MGB (Sigma-Aldrich, St. Louis, MO, USA). The latter used a commercial kit (4304437; Applied Biosystems). Each well included 25 ng of total genomic DNA diluted in 20 μl total reaction mixture containing: 1x TaqMan Universal PCR Master Mix (ABI P/N 4304437), 1 μl RNAseP commercial kit and 125 nM of each mtDNA primer and 125 nM of mtDNA probe. The PCR was set for 2 minutes at 50°C, 10 minutes at 95°C, followed by 40 cycles each of 15 seconds of denaturalization at

95°C and 60 seconds of annealing/extension at 60°C. The mt12SrRNA gene was normalized by determining the nRNAseP nuclear gene and expressed as mt12SrRNA/nRNAseP ratio.

4.5.7 Western blot analysis

Twenty to forty µg of total protein were separated using 7/13% SDS-PAGE and transferred to nitrocellulose membranes (iBlot Gel Transfer Stacks, Life Technologies, Waltham, MA, USA). The membranes were hybridized with specific antibodies overnight at 4ºC. The expression of all studied proteins was measured once and normalized to β-actin protein (47kDa; 1:30.000; Sigma-Aldrich, St.Louis, MO, USA) which was used as a loading control. Inter-blot control samples were used to evaluate membrane variability. The ImageQuantLD program was used to quantify chemiluminiscence and expressed in arbitrary units reflecting intensity of band signal (in pixels) per surface.

Subunits of the MRC complexes

To determine the levels of protein expression of the subunits of the MRC complexes, the cleared lysates were subjected to SDS-PAGE and electroblotted. Proteins were visualized by immunostaining with anti-SDHA and anti-SDHB (both for CII; 70kDa and 30kDa respectively; 1:1000; Invitrogen, Paisley, UK) and also with anti-COX5A (for CIV; 16kDa; 1:1000; MitoSciences, Oregon, USA). Results were expressed as SDHA/β-actin, SDHB/β-actin and COX5A /β-actin ratios.

Mitochondrial import receptor subunit TOM20 (Tom20)

As a mitochondrial content marker, anti-Tom20 (20kDa; 1:1000; Santa Cruz Biotechnology, Dallas, USA) was hybridized with membranes. Results were expressed as the Tom20/β-actin ratio.

Superoxid dismutase 2 (SOD2)

SOD2 is a mitochondrial anti-oxidant enzyme pivotal in ROS release during oxidative stress. Membranes were hybridized with anti-SOD2 (24kDa; 1:1000; ThermoFisher Scientific, Waltham, MA, USA). Results were expressed as the SOD2/β-actin ratio.

Acetylated form of SOD2

To determine the activity of SOD2 enzyme, we evaluate its acetylated form (indicating less activity) by hybridizing the membranes with anti-SOD2/MnSOD (24kDa; 1:1000; Abcam, Cambridge, UK). Results were expressed as the acetylated SOD2/β-actin or acetylated/total SOD2 ratio.

Sirtuin 3

The protein content of Sirtuin 3, which is a sensor of mitochondrial and metabolic balance, was determined by hybridizing the membrane with anti-Sirtuin 3 (29 KDa; 1:500; Abcam, Cambridge, UK) in heart tissue from the rabbit model. Due to specificities of antigen detection, when evaluating Sirtuin 3 in placenta from human samples, another antibody was used, so the membranes were hybridized with anti-Sirtuin 3 (44 KDa; 1:250; Merck Millipore). In both cases, results were expressed as the Sirtuin 3/β-actin ratio.

Table 8. Summary with all tested proteins and their optimal conditions by Western blot.

Protein	Primary antibody reference	Band size (kDa)	Dilution used	SDS-PAGE	Secondary antibody used
SDHA	Invitrogen, Paisley, UK	70	1:1000	7 / 13 %	Anti-mouse
SDHB	Invitrogen, Paisley, UK	30	1:1000	7 / 13 %	Anti-mouse
COX5A	MitoSciences, Oregon, USA	16	1:1000	7 / 13 %	Anti-mouse
Tom20	Santa Cruz Biotechnology, Dallas, USA	20	1:1000	7 / 13 %	Anti-rabbit
SOD2	ThermoFisher Scientific, Waltham, MA, USA	24	1:1000	7 / 13 %	Anti-mouse
SOD2/MnSOD (acetylated SOD2)	Abcam, Cambridge, UK	24	1:1000	7 / 13 %	Anti-rabbit
Sirtuin 3	Abcam, Cambridge, UK	29	1:500	7 / 13 %	Anti-goat
β-actin	Sigma-Aldrich, St.Louis, MO, USA	46	1:30.000	7 / 13 %	Anti-mouse

SDHA: Succinate dehydrogenase complex, subunit A; SDHB: Succinate dehydrogenase complex, subunit B; COX5A: Cytochrome c oxidase subunit 5a; Tom20: Mitochondrial import receptor subunit TOM20; SOD2: Superoxid dismutase 2; SOD2/MnSOD; acetylated form of SOD2.

4.6 STATISTICAL ANALYSIS

All statistical analysis was performed with the 'IBM SPSS Statistics 20' software. Additionally, STATA software was used only to determine maternal influence in the animal model.

For the animal model, biometric data from the offspring (suggestive of IUGR and cardiovascular remodelling severity) as well as mitochondrial experimental results were expressed as means and standard error of the mean (SEM) or as a percentage of increase/decrease of IUGR-offspring compared to control offspring after filtering for outliers. Case-control differences were sought by non-parametric statistical analysis (Mann–Whitney independent sample test). Additionally, significance was adjusted by maternal influence (Random Effect regression model) in case of difference in some analysed parameter.

For human pregnancies, sociodemographic characteristics and perinatal outcomes were expressed as percentage of positive cases within the study cohort or means and SEM. Mitochondrial experimental results were expressed as means and SEM or as a percentage of increase/decrease of IUGR cases compared to control pregnancies after filtering for outliers. All results of IUGR pregnancies were compared to controls to assess the impact of IUGR and cardiovascular remodelling in our study cohort. So, mitochondrial experimental case-control differences were sought by non-parametric statistical analysis (Mann–Whitney independent sample test or odds ratio by Fisher's exact).

Finally, different correlations were obtained between biometric/clinical data and experimental results using the Spearman test to assess the dependence of this obstetric complication on mitochondrial function.

Differences were considered significant with a p value <0.05.

5. RESULTS

5.1 STUDY 1

Title:

Cardiac and placental mitochondrial characterization in a rabbit model of intrauterine growth restriction

Authors:

Mariona Guitart-Mampel, Anna Gonzalez-Tendero, Sergio Niñerola, Constanza Morén, Marc Catalán-Garcia, Ingrid González-Casacuberta, Diana L. Juárez-Flores, Olatz Ugarteburu, Leslie Matalonga, Maria Victoria Cascajo, Frederic Tort, Ana Cortés, Ester Tobias, Jose C. Milisenda, Josep M. Grau, Fàtima Crispi, Eduard Gratacós, Glòria Garrabou, Francesc Cardellach.

Reference:

Biochim Biophys Acta. 2018 May; 1862(5): 1157-1167.

Corresponding author: Glòria Garrabou and Francesc Cardellach

IF 2017: 3.68 (Q1); IF 2016: 4.70 (Q1)

See Annex section (page 143).

5.1.1 Biometric offspring data

The biometric results of both the IUGR and control offspring of the rabbit model are shown in Table 9 and Figure 17, in which, IUGR-offspring were presented as column bars demonstrating percentage of increase or decrease compared to controls (represented as the 0 baseline).

Birth weight, heart weight, left and right ventricle weight and placental weight were significantly decreased in IUGR-offspring compared to controls (−30.35 ± 2.99%, $p<0.001$; −29.73 ± 2.70%, $p<0.001$; −30.00 ± 0.00%, $p<0.005$; −36.36 ± 9.09%, $p<0.001$; −21.49 ± 4.85%, $p<0.001$, respectively), confirming the presence of IUGR and cardiac remodelling. When cardiac or placental weights were normalized to body weight, no significant differences were evidenced between IUGR and control offspring, suggesting global and proportioned organ and body mass reduction.

Table 9. Biometric data of experimental groups. Whole body, cardiac and placental weight are reduced in IUGR-offspring compared to control offspring.

Parameters	*Control*	*IUGR*	*% of increased (+) or decreased (-)*	*P value*
Birth weight (g)	52.26±1.32	36.40±1.56	-30.35±2.99	<0.001 [a]
Heart weight (g)	0.37±0.01	0.26±0.01	-29.73±2.70	<0.001 [a]
Left ventricle heart weight (g)	0.10±0.01	0.07±0.00	-30.00±0.00	<0.005 [a,] †
Heart/body weight x 100	0.71±0.02	0.73±0.05	+2.82±7.04	NS
Right Ventricle + Septum heart weight (g)	0.11±0.01	0.07±0.01	-36.36±9.09	<0.001 [a]
Placental weight (g)	7.63±0.48	5.99±0.37	-21.49±4.85	<0.001 [a,] †
Placenta/body weight x 100	0.15±0.01	0.17±0.01	+13.33±6.67	NS

Values were expressed as mean ± standard error of the mean. Case-control differences were sought by non-parametric statistical analysis and, in case of difference ([a]), significance was adjusted by maternal influence (†).

IUGR: Intrauterine Growth Restriction; NS: not significant.

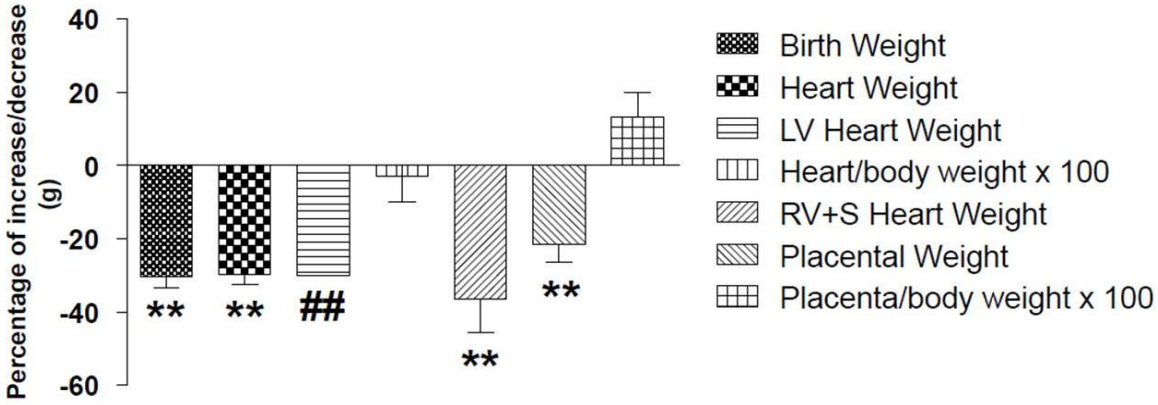

Figure 17. Biometric results of heart and placenta from rabbit offspring with intrauterine growth restriction (IUGR). IUGR-offspring were presented as column bars demonstrating percentage of increase or decrease compared to controls (represented as the 0 baseline). There was a significant decrease in birth weight in IUGR-offspring (control N=14 and IUGR N=16), accompanied by a reduction in heart (control N=13 and IUGR N=15), left (control N=11 and IUGR N=14) and right ventricle (control N=10 and IUGR N=13) and placental weight (control N=14 and IUGR N=16). Heart body weight relative to body weight (control N=13 and IUGR N=15) and also placental weight corrected by body weight (control N=14 and IUGR N=16) did not show significant differences between cases and controls.

Case-control differences were sought by non-parametric statistical analysis and, in case of difference; significance was adjusted by maternal influence (LV heart weight and placental weight).

LV: left ventricle; RV+S: right ventricle and septum; **: p<0.001; ##: p<0.005.

5.1.2 MRC activity, MRC expression and mitochondrial content

In order to explore mitochondrial function, the enzymatic activities of the complexes of the MRC were analysed in the homogenate of heart and placental tissue. In addition, the expression of some subunits of the complexes of the MRC was also measured in the same samples. And finally, mitochondrial content was evaluated through the activity of citrate synthase and the expression of protein Tom20. All of the raw data are presented in Supplementary Table 1 (S1).

A significant decrease of CII, CIV and CII+III enzymatic activities (−11.96 ± 3.16%, −15.58 ± 5.32% and −14.73 ± 4.37%, respectively; $p<0.05$ in all cases) was found in heart of IUGR-offspring compared to controls, while other complexes (CI and CI+III) also showed a decrease, although not significant (Figure 18). The same pattern was observed in placenta, although the decrease in CIV did not reach statistical significance in IUGR-offspring (CII: −17.22 ± 3.46%, $p<0.005$; CIV: -24.03 ± 8.26%, p=NS; CII+III: −29.64 ± 4.43%, $p<0.001$; Figure 18).

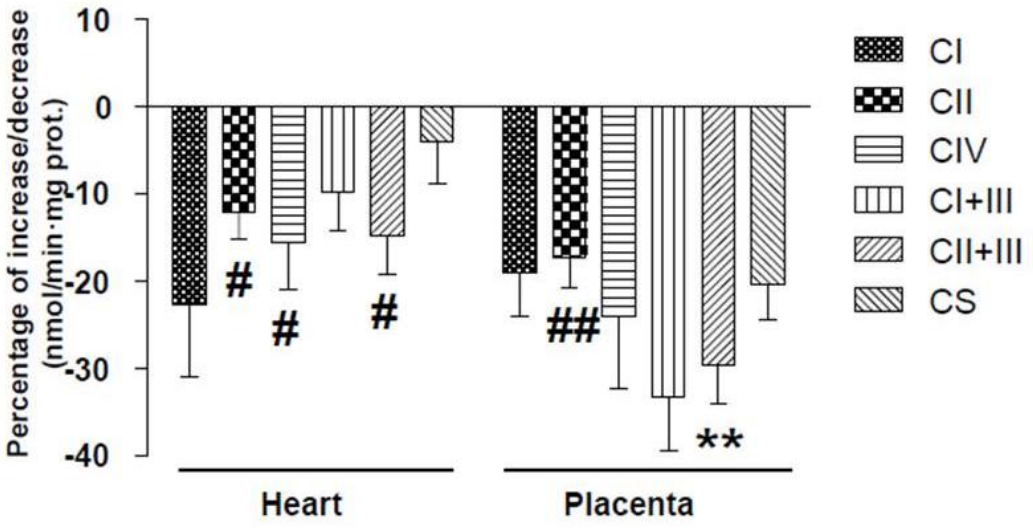

Figure 18. Enzymatic activities of the complexes of the mitochondrial respiratory chain (MRC) of heart (left) **and placenta** (right) **from IUGR-offspring compared to controls**. IUGR-offspring were presented as column bars demonstrating percentage of increase or decrease compared to controls (represented as the 0 baseline. A significant decrease of CII, CIV and CII+III enzymatic activities was observed in heart of IUGR-offspring, while CI and CI+III showed a not significant decrease (control N=10 and IUGR N=14 for all). The same pattern was observed in placenta, although the CIV decrease did not reach statistical significance in IUGR-offspring (CI: control N=14 and IUGR N=14; CII and CIV: control N=14 and IUGR N=16; CI+III: control N=13 and IUGR N=15; CII+III: control N=13 and IUGR N=16). Citrate synthase (CS) activity (mitochondrial content) was conserved in both heart (control N=10 and IUGR N=14) and placental (control N=14 and IUGR N=16) tissues from IUGR-offspring.

Case-control differences were sought by non-parametric statistical analysis and, in case of difference; significance was adjusted by maternal influence.

#: $p<0.05$; ##: $p<0.005$; **: $p<0.001$; CI, CII, CIV, CI+III, CII+III: MRC complex I, II, IV, I+III, II+III; CS: citrate synthase.

CII subunits SDHA and SDHB and CIV subunit COX5A were analysed by Western blot as were the complexes showing statistical significant differences in terms of enzymatic activities. Thus, studied subunits were conserved in cardiac tissue of IUGR-offspring compared to controls. Interestingly, regardless maintained expression of CII SDHA and CIV COX5A subunits in placental tissue, MRC CII SDHB subunit was significantly decreased (−44.12 ± 5.88%; $p<0.001$) in IUGR-offspring compared to controls (Figure 19 and Table S1).

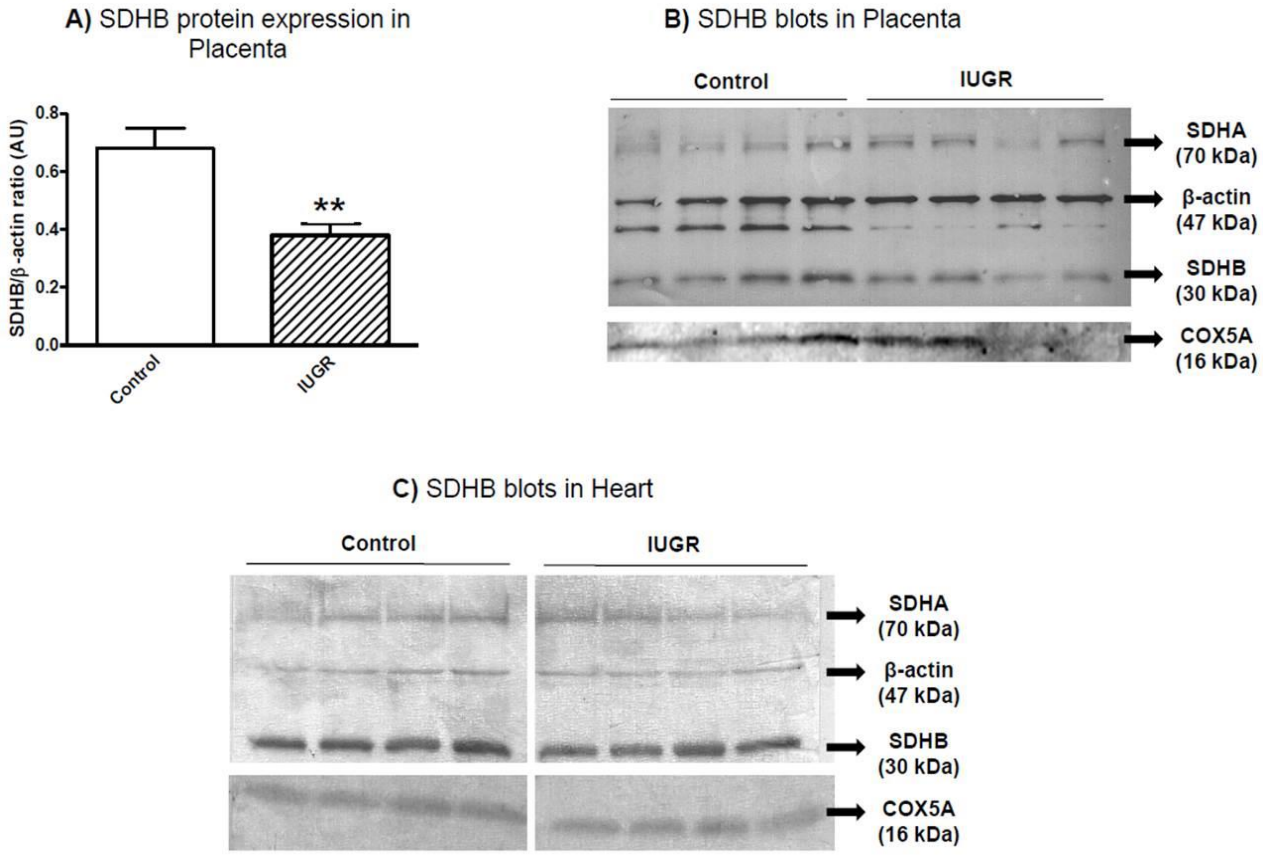

Figure 19. Expression of the mitochondrial respiratory chain (MRC) subunits SDHA and SDHB (from complex II) and COX5A (from complex IV) in IUGR-offspring and controls. A) This column bar graph represents **protein expression of SHDB subunit in placenta** from IUGR-offspring (striped bars; N=16) compared to placenta from controls (empty bars; N=14). SHDB/β-actin expression is significantly decreased in placenta from IUGR-offspring. The results were expressed as mean and standard error of the mean (SEM) compared to controls. Case-control differences were sought by non-parametric statistical analysis and, in this case; significance was adjusted by maternal influence (SDHB protein expression in placenta). **B)** A **representative Western Blot of SDHA, SDHB and COX5A protein expression in placenta** is shown in which β-actin was used as the loading control. **C)** A **representative Western Blot of SDHA, SDHB and COX5A protein expression in heart** is shown in which β-actin was used as the loading control.

IUGR: intrauterine growth restriction; SDHA: succinate dehydrogenase complex, subunit A; SDHB: succinate dehydrogenase complex, subunit B; COX5A: cytochrome c oxidase subunit 5a; **: p<0.001.

Finally, mitochondrial content was evaluated using two mitochondrial parameters. First, citrate synthase activity in both heart and placental tissues showed preserved mitochondrial content in IUGR-offspring compared to controls (Figure 18 and Table S1). Second, these results were confirmed by conserved Tom20 expression in the same samples (Figure 20 and Table S1).

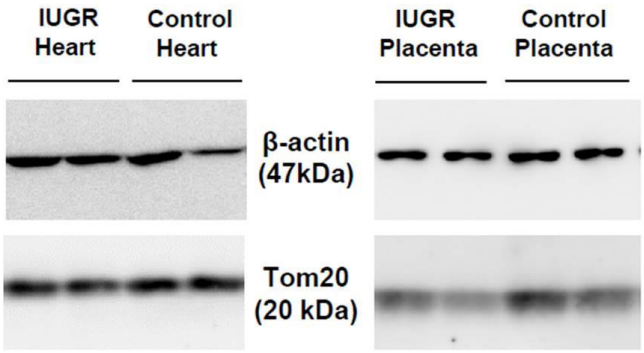

Figure 20. Representative Blot for the expression of mitochondrial import receptor subunit TOM20 (Tom20) in heart and placental tissue from IUGR-offspring and controls. No remarkable differences were observed in heart (control N=4 and IUGR N=8) and placenta (control N=15 and IUGR N=15) between cases and controls. β-actin was used as loading control.

IUGR: Intrauterine growth restriction

Relative MRC enzymatic activities to citrate synthase activity were in line with absolute MRC enzymatic activities, suggesting that MRC deficiencies were focused on a defect of mitochondrial enzymatic activity and protein expression rather than a decrease of the mitochondrial content.

5.1.3 Mitochondrial oxygen consumption

Heart and placental fresh tissue was permeabilized to further explore MRC function by terms of mitochondrial oxygen consumption. It is a measure to evaluate a global operation of the MRC. Thus, oxygen consumption through CI stimulation by glutamate+malate was quantified (GM oxidation).

We found a not significant decrease of CI-stimulated oxygen consumption in heart and placenta from IUGR-offspring compared to controls (−5.56 ± 6.46% and −25.64 ± 18.97%, respectively, both p=NS, Figure 21 and Table S1).

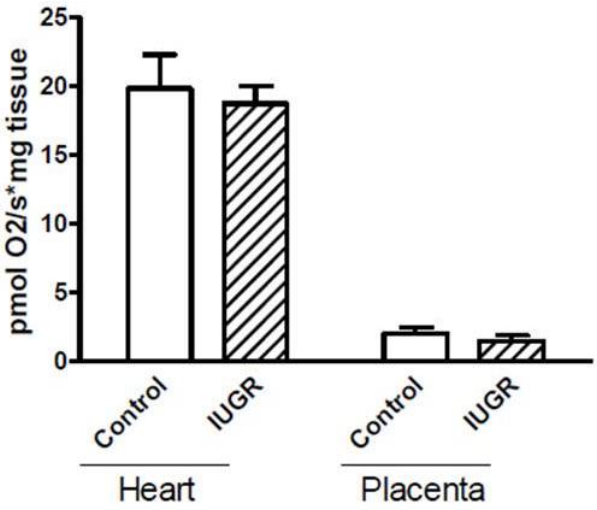

Figure 21. Mitochondrial oxygen consumption of heart and placenta from rabbit offspring with intrauterine growth restriction (IUGR). Mitochondrial oxygen consumption stimulated with substrate for complex I (glutamate+malate) in heart (left; control N=11 and IUGR N=14) and placenta (right; control N=13 and IUGR N=13) from IUGR-offspring (striped bars) compared to controls (empty bars). Oxygen consumption showed a not significant decrease on CI stimulation in heart and placenta from IUGR-offspring.

The results were expressed as means and standard error of the mean (SEM) compared to controls. Case-control differences were sought by non-parametric statistical analysis.

5.1.4 Mitochondrial CoQ content

Mobile electron transfer CoQ, responsible to transfer the electrons from CI and II to CIII, was analysed to better explore deficiencies in the enzymatic activities of the complexes of the MRC.

However, no differences were observed in CoQ_9 or CoQ_{10} content either in cardiac or placental tissue of IUGR-offspring with respect to control individuals (Table S1).

5.1.5 Total cellular ATP levels

Total ATP levels were measured to explore potential consequences of deficiencies in MRC enzymatic activities.

However, no remarkable differences were observed in total content of cellular ATP either in heart or placental tissues in IUGR and control offspring (Figure 22 and Table S1), suggesting no effects of MRC dysfunction in total ATP supply or the increase of alternative pathways of ATP production.

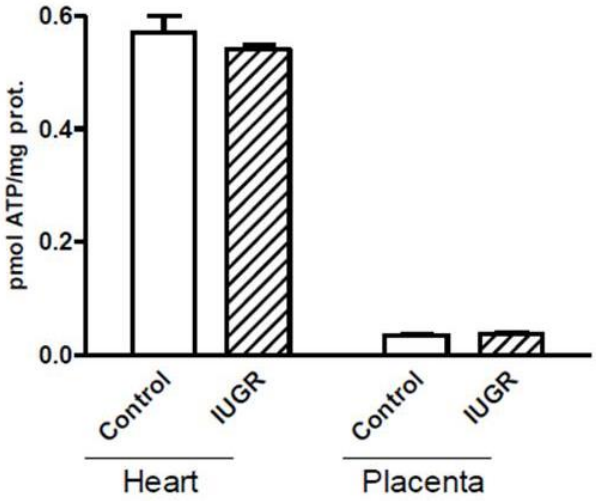

Figure 22. Total cellular ATP levels in heart and placenta from rabbit offspring with intrauterine growth restriction (IUGR). Total cellular ATP levels in heart (left; control N=10 and IUGR N=14) and placenta (right; control N=14 and IUGR N=16) from IUGR-offspring (striped bars) compared to controls (empty bars). No remarkable differences were observed in the total cellular ATP content either in heart or placental tissue.

The results were expressed as means and standard error of the mean (SEM) compared to controls. Case-control differences were sought by non-parametric statistical analysis.

ATP: adenosine triphosphate.

5.1.6 Lipid peroxidation (oxidative damage)

Oxidative damage, estimated by the rate of lipid peroxidation, was assessed in order to evaluate consequences of MRC impairment.

Lipid peroxidation showed a significant decrease of 39.02 ± 4.35% in hearts of IUGR-offspring compared to controls ($p<0.001$; Figure 23 and Table S1), probably reflecting the previous observed decrease in MRC enzymatic activities or the potential activation of antioxidant mechanisms. Contrarily, lipid peroxidation was considered to be preserved by showing a non-significant increase of 10.65 ± 7.33% in placenta from IUGR-offspring compared to the control group (p=NS; Figure 23 and Table S1), probably due to poor antioxidant defences characteristic of this tissue.

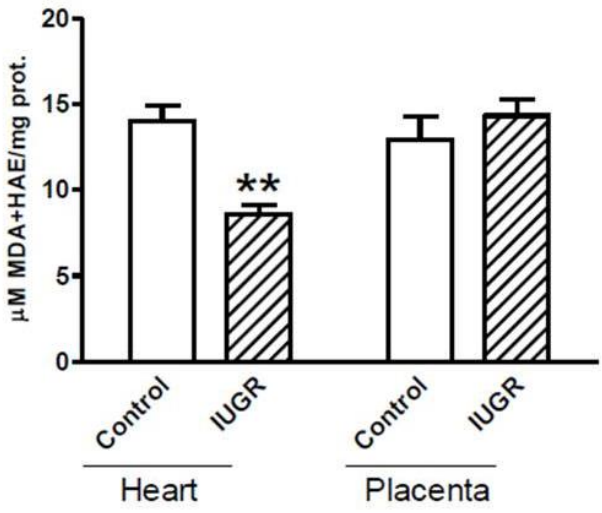

Figure 23. Lipid peroxidation in heart and placenta from rabbit offspring with intrauterine growth restriction (IUGR). Lipid peroxidation in heart (left; control N=10 and IUGR N=14) and placenta (right; control N=13 and IUGR N=16) from IUGR-offspring (stripped bars) compared to controls (empty bars). Lipid peroxidation showed a significant decrease in hearts while showing a not significant increase in placenta from IUGR-offspring.

The results were expressed as means and standard error of the mean (SEM) compared to controls. Case-control differences were sought by non-parametric statistical analysis and, in case of difference; significance was adjusted by maternal influence.

HAE: 4-hydroxyalkenal; MDA: malondialdehyde; **; p<0.001.

5.1.7 Expression and activity of SOD2

To better understand the altered and controversial patterns of oxidative damage, total SOD2 enzyme expression and activity was analysed as it is the main antioxidant enzyme within mitochondria.

However, no significant differences were observed in the protein content and activity of the antioxidant SOD2 enzyme between cases and controls in none of the studied tissues (Figures 24 and 25 and Table S1; either total SOD2/β-actin content or acetylated SOD2/β-actin).

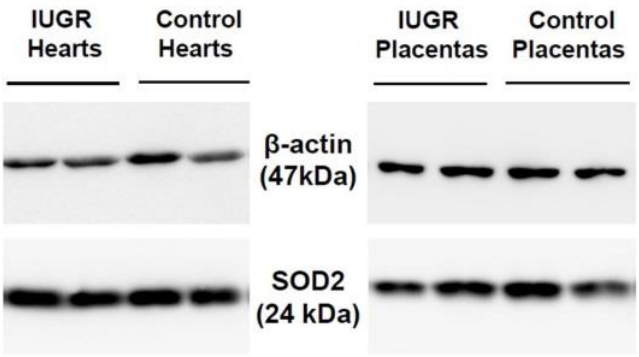

Figure 24. Representative Blot for the expression of superoxid dismutase 2 (SOD2) anti-oxidant enzyme in heart and placental tissue from IUGR-offspring and controls. No remarkable differences were observed in heart (control N=10 and IUGR N=14) and placenta (control N=15 and IUGR N=15) between cases and controls. β-actin was used as loading control.

IUGR: Intrauterine growth restriction.

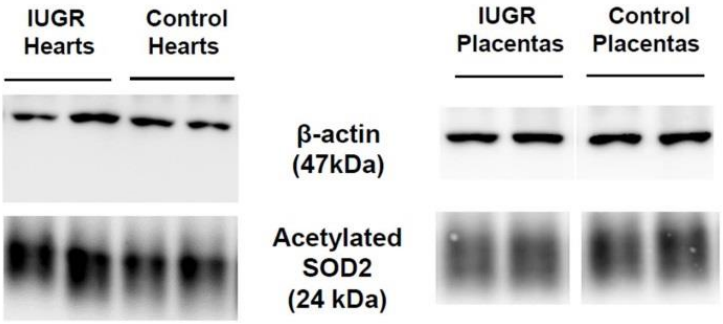

Figure 25. Representative Blot for the expression of the acetylated form of superoxid dismutase 2 (SOD2) anti-oxidant enzyme in heart and placental tissue from IUGR-offspring and controls. No remarkable differences were observed in heart (control N=8 and IUGR N=13) and placenta (control N=11 and IUGR N=14) between cases and controls. β-actin was used as loading control.

IUGR: Intrauterine growth restriction.

5.1.8 Sirtuin 3 protein expression

After the wide mitochondrial characterization, a potential factor responsible to regulate all these mitochondrial rearrangements such as Sirtuin 3 was evaluated.

Interestingly, Sirtuin 3/β-actin protein levels showed a significant increase of 84.21 ± 31.58% ($p<0.05$) in heart tissue of IUGR-offspring compared to controls (Figure 26 and Table S1), suggesting potential upregulation to compensate mitochondrial dysfunction.

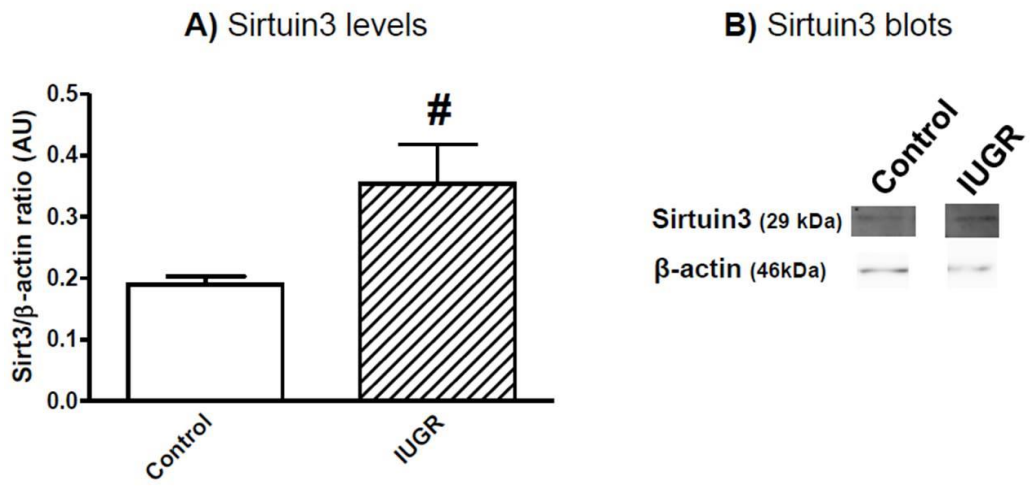

Figure 26. Mitochondrial levels of protein Sirtuin 3 (Sirt3/β-actin ratio) in heart of rabbit offspring with intrauterine growth restriction (IUGR). A) This column bar graph represents protein Sirtuin 3 levels in hearts from IUGR-offspring (striped bars; N=13) compared to hearts from controls (empty bars; N=10). Sirtuin 3/β-actin levels in heart tissue of IUGR-offspring showed a significant increase. The results were expressed as mean and standard error of the mean (SEM) compared to controls. Case-control differences were sought by non-parametric statistical analysis and, in this case; significance was adjusted by maternal influence. #: $p<0.05$. **B)** A representative Western Blot of Sirtuin 3 protein expression in hearts is shown in which β-actin is used as the loading control.

5.1.9 Associations between biometric features and experimental results

Supplementary Table S2 describes all the significant associations between the biometric data and experimental results of the IUGR and control offspring from the rabbit model. The most remarkable associations are described below and showed in Figure 27.

Firstly, birth weight was positively and significantly correlated with heart and left ventricle weight and also with placental weight (R^2=0.610, R^2=0.446 and R^2=0.557, respectively, $p<0.001$ in all cases; Figure 27A and B). Similarly, heart weight was correlated with left ventricle weight and placental weight (R^2=0.322, $p<0.005$; R^2=0.346, $p<0.001$), confirming the association of low birth weight characteristic of IUGR with cardiovascular remodelling.

Secondly, birth weight was positively and significantly correlated with enzymatic activities of CI, CII and CII+III in the heart of the both offspring (R^2=0.157, $p<0.05$; R^2=0.117, $p<0.05$; R^2=0.289, $p\leq0.005$; respectively; Figure 27C). The weight of the

other tissues was also positively and significantly correlated with the enzymatic activity of some MRC complexes (Table S2). Similarly, body, heart, left ventricle and placental weights were significantly and positively correlated with CII SDHB protein expression in placenta (R^2=0.304, p≤0.001; R^2=0.349, p<0.001; R^2=0.215, p<0.005; R^2=0.364, p<0.05, respectively; Figure 27D). These associations reinforced the dependence of proper organ and body weight on mitochondrial function. Interestingly, we found CII, CII+III and CIV enzymatic activity positively and significantly correlated with CII SDHB subunit expression in placenta (R^2=0.145, p<0.005; R^2=0.192, p<0.005; R^2=0.241, p<0.001, respectively), indicating the dependence of enzymatic activity on protein expression. On the other hand, birth weight and heart weight showed a significant positive correlation with lipid peroxidation in heart (R^2=0.325, p<0.005; R^2=0.498, p<0.001; respectively; Figure 27E). Moreover, oxidative damage in heart was positively and significantly correlated with the enzymatic activities of MRC CII and CII+III (R^2=0.136 and R^2=0.173, p< 0.05 in both cases), suggesting that low MRC function curses with low oxidative damage (through lipid peroxidation) at least in heart.

Finally, significant negative correlations were found between both birth and heart weight and Sirtuin 3/β-actin levels (R^2=0.153, p<0.05 and R^2=0.266, p<0.05, respectively; Figure 27F), pointing out the potential mechanism of modulation by Sirtuin 3 in front of mitochondrial imbalance.

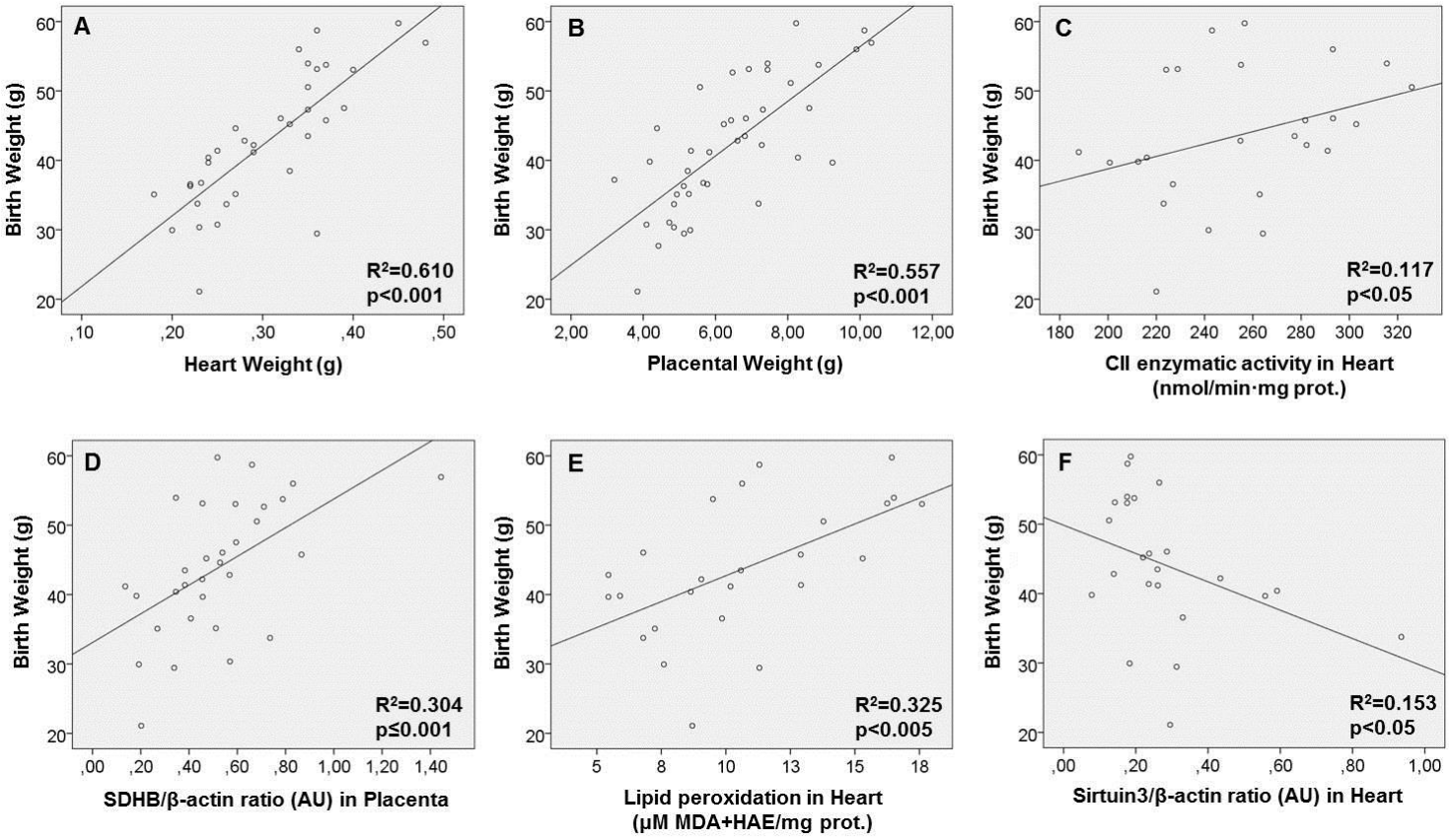

Figure 27. Associations between birth weight of intrauterine growth restriction (IUGR) and control offspring and some biometric data or experimental results. Herein, there are correlations demonstrating the positive association between birth weight and mitochondrial parameters and also the negative association with Sirtuin 3 expression, probably up-regulated as a homeostatic intent to revert mitochondrial lesion.

Spearman Rho tests were used to seek for statistical analysis.

AU: Arbitrary units; CII: MRC complex II; g: grams; HAE: hydroxyalkenal; MDA: malondialdehyde; MRC: Mitochondrial respiratory chain; R^2: coefficient of determination; SDHB: succinate dehydrogenase complex, subunit B.

5.2 STUDY 2

Title:

Mitochondrial implication in human pregnancies with intrauterine growth restriction and associated foetal cardiovascular remodelling

Authors:

Mariona Guitart-Mampel, Diana L. Juarez-Flores, Lina Yousseff, Constanza Moren, Laura Garcia-Otero, Vicente Roca-Agujetas, Marc Catalan-Garcia, Ingrid Gonxalez-Casacuberta, Ester Tobias, José C. Milisenda, Josep M. Grau, Fàtima Crispi, Eduard Gratacós, Glòria Garrabou, Francesc Cardellach.

Reference:

Under review to Clinical Science

Corresponding author: Glòria Garrabou and Francesc Cardellach

IF 2017: 5.2 (Q1)

See Annex section (page 143).

5.2.1 Clinical parameters

Table 10 shows sociodemographic characteristics and perinatal outcomes of study groups. No differences were found between IUGR cases and controls regarding maternal age, route of delivery, newborn sex or pH umbilical artery values.

Table 10. Sociodemographic characteristics and perinatal outcomes of the study groups.

Parameters	***Control*** ***N = 22***	***IUGR*** ***N = 14***	***P value***
Maternal age at delivery (years)	33.82±1.12	34.43±1.34	NS
Weeks of gestation	39.47±0.20	35.42±1.03	<0.001
Mode of delivery	20 caesarean (91%) 2 naturals (9%)	14 caesarean (100%) 0 naturals (0%)	NS OR [95% CI] = 0.28 [0.01-6.34]
Birth weight (g)	3440.27±87.59	1742.29±171.31	<0.001
Birth weight Percentile	58.32±5.94	0.64±0.23	<0.001
Placental weight (g)	566.67±118.93	329.64±24.26	<0.05
Newborn sex	45% female 55% male	54% female 46% male	NS OR [95% CI] = 0.70 [0.17-2.85]
pH Umbilical Artery cord blood	7.26±0.01	7.24±0.03	NS
Apgar 5'	21 normal (95%) 1 abnormal (5%)	9 normal (64%) 5 abnormal (36%)	<0.05 OR [95% CI] = 11.67 [1.19-114.65]
Preeclampsia	0 (0%)	4 (28.6%)	<0.05 OR [95% CI] = 0.05 [0.00-1.06]
Neonatal BNP levels (pg/ml)	26.84±3.03	85.68±26.28	<0.05

Values are presented as mean ± standard error of the mean. Case-control differences were sought by non-parametric statistical analysis.

BNP: brain natriuretic peptide; CI: confidence interval; g: grams; IUGR: intrauterine growth restriction; N: sample size; NS: not significant; OR: odds ratio.

As expected, pregnancies complicated by IUGR presented an earlier gestational age at delivery with respect to controls (p<0.001; Table 10) as our clinical protocol for IUGR indicates induction of labour about 37 weeks of gestation. Additionally, birth weight, birth weight percentile and placental weight were significantly decreased in IUGR

cases with respect to controls (all p<0.001; Figure 28 and Table 10). Moreover, IUGR group showed higher prevalence of preeclampsia (p<0.05; Table 10).

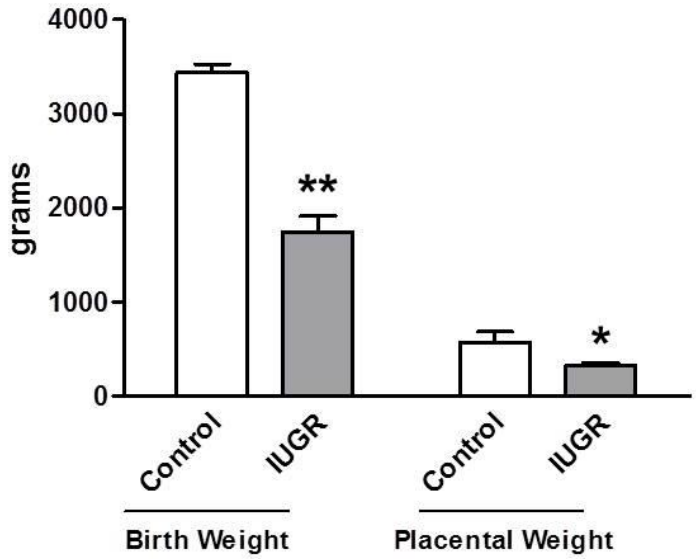

Figure 28. Anthropometric measures of the study groups. Birth weight was significantly reduced in newborns from IUGR pregnancies (grey bar; N=22) compared to controls (empty bar; N=14), as well as placental weight (grey bar; N=3; empty bar, N=14).

Results were expressed as mean ± standard error of the mean. Mann-Whitney tests were used to seek for statistical analysis between groups.

IUGR: intrauterine growth restriction; **: p<0.001; *: p<0.05.

IUGR newborns with abnormal Apgar presented significantly lower birth weight as compared to IUGR newborns with normal Apgar (p<0.05) and also to controls with normal Apgar (p<0.05), showing the association of birth weight and the health of the newborn.

BNP levels were significantly increased by 219.23 ± 97.91% in plasma from IUGR newborns compared to controls (p<0.05; Figure 29 and Table 10) indicating the presence of a cardiac remodelling.

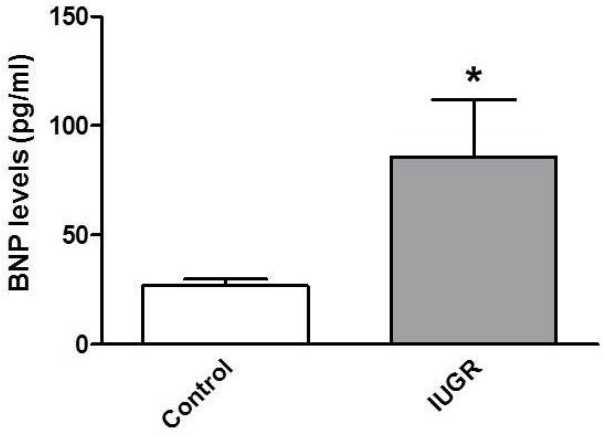

Figure 29. Cardiac remodelling in newborns from IUGR pregnancies. BNP levels were significantly increased in neonatal plasma from newborns of IUGR pregnancies (grey bars, N=21) with respect to controls (empty bars, N=9).

Results were expressed as mean ± standard error of the mean. Mann-Whitney tests were used to seek for statistical analysis between groups.

BNP: brain natriuretic peptide; IUGR: intrauterine growth restriction; *: $p<0.05$.

5.2.2 Mitochondrial study in placenta

5.2.2.1 MRC activity and mitochondrial content

To explore mitochondrial function, the enzymatic activities of the complexes of the MRC were analysed in placental tissue as well as the mitochondrial content (through the activity of citrate synthase).

MRC CI activity was significantly decreased in placental homogenate from IUGR pregnancies compared to controls (-32.95±10.36%; $p<0.05$; Figure 30 and Table S3), despite other MRC complexes (CII, CIV, CI+III and CII+III) were preserved (Figure 30 and Table S3).

Citrate synthase activity was preserved in placental homogenate from IUGR pregnancies with respect to controls (Figure 30 and Table S3), indicating no differences in mitochondrial content.

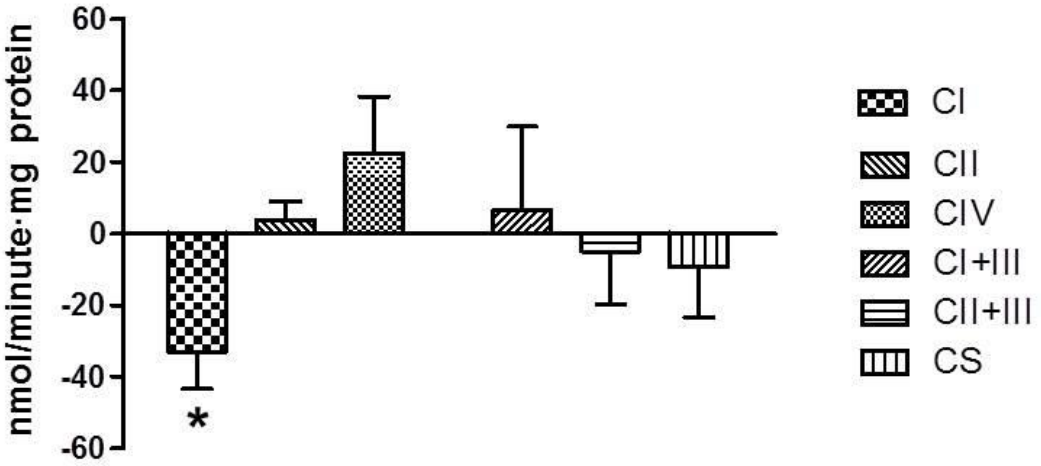

Figure 30. Enzymatic activities of the complexes of the mitochondrial respiratory chain (MRC) and citrate synthase (CS) in placental tissue. IUGR cohort was presented as column bars demonstrating percentage of increase or decrease compared to controls (represented as the 0 baseline). A significant decreased was observed in complex I activity (CI) while other complexes and also CS activity remained conserved (CI: control N=18 and IUGR N=11; CII and CIV: control N=20 and IUGR N=13; CI+III, CII+III and CS: control N=21 and IUGR N=13).

Results were expressed as a percentage of increase or decrease ± standard error of the mean. Mann-Whitney tests were used to seek for statistical analysis between groups.

CBMC: Cord blood mononuclear cells; CI: complex I activity; CII: complex II activity; CIV: complex IV activity; CI+III: complex I+III activity; CII+III: complex II+III activity; CS: Citrate synthase activity; IUGR: Intrauterine growth restriction; PBMC: Peripheral blood mononuclear cells; *: p<0.05.

MRC enzymatic activities relative to citrate synthase activity showed a similar pattern to absolute MRC enzymatic activities. All of the raw data are available in Supplementary Table 3 (S3). These results were in line with MRC enzymatic deficiencies in the animal model, suggesting that these reductions were focused on the decreased mitochondrial enzymatic activity rather than the decrease in mitochondrial content.

5.2.2.2 Mitochondrial oxygen consumption

Fresh placental mitochondria were used to evaluate mitochondrial oxygen consumption to further explore a global MRC function Thus, oxygen consumption through CI stimulation by pyruvate+malate and glutamate+malate was quantified (abbreviated as PM and GM oxidation).

Significant decreases of 46.12±5.79% and 49.71±19.54% in oxygen consumption stimulated for CI (PM and GM oxidation, respectively) were observed in placental

mitochondria from IUGR pregnancies compared to controls ($p<0.05$ in both cases; Figure 31 and Table S3), confirming previous results of decreased MRC CI enzymatic activity.

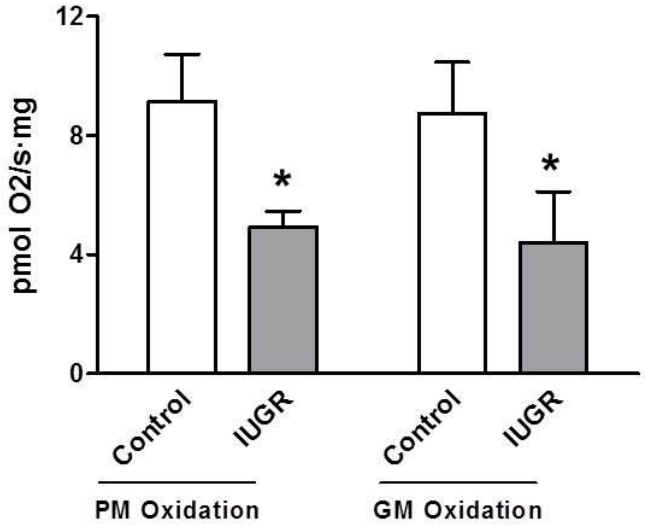

Figure 31. Oxygen consumption of the mitochondrial respiratory chain (MRC) in placental mitochondria. A significant decrease in MRC Complex I-stimulated oxygen consumption (both PM and GM Oxidation) was observed in the IUGR cohort (grey bars, PMox N=10 and GMox N=11) compared to controls (empty bars, PMox N=14 and GMox N=15).

Results were expressed as mean ± standard error of the mean. Mann-Whitney tests were used to seek for statistical analysis between groups.

GM Oxidation: glutamate+malate oxidation; IUGR: intrauterine growth restriction; PBMC: peripheral blood mononuclear cells; PM Oxidation: pyruvate+malate oxidation; *: $p<0.05$.

5.2.2.3 Total cellular ATP levels

To further explore potential consequences of MRC dysfunction, total ATP levels were measured.

No remarkable differences were observed in total content of cellular ATP in IUGR placental homogenates compared to controls (Figure 32 and Table S3), also indicating no consequences of MRC dysfunction in total ATP supply or the production of ATP by alternative metabolic pathways.

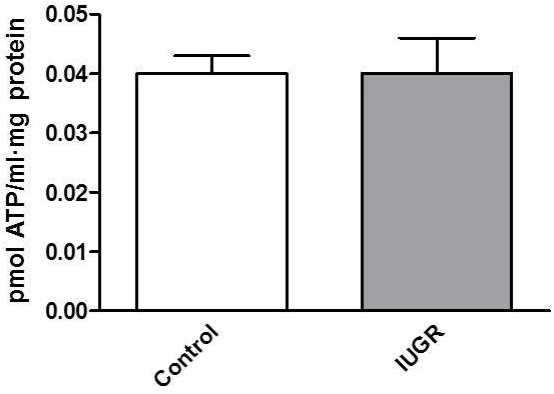

Figure 32. Total ATP levels in placental tissue. No significant differences were observed between IUGR pregnancies (grey bars, N=13) and controls (empty bars, N=21).

Results were expressed as mean ± standard error of the mean. Mann-Whitney tests were used to seek for statistical analysis between groups.

ATP: adenosine triphosphate; IUGR: intrauterine growth restriction.

5.2.2.4 Lipid peroxidation (oxidative damage)

Lipid peroxidation was analysed as an indicator of oxidative damage to found consequences of MRC impairment.

No relevant changes were observed in lipid peroxidation in IUGR placental homogenate compared to controls (Figure 33 and Table S3), probably as a result of decreased MRC function.

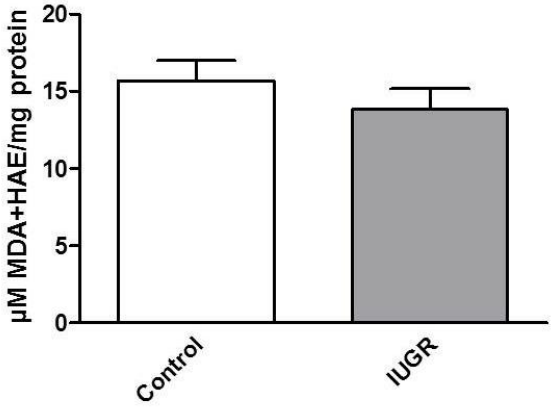

Figure 33. Lipid peroxidation as an indicator of oxidative damage in placental tissue. No significant differences were evidenced between IUGR pregnancies (grey bars, N=13) and controls (empty bars, N=21).

Results were expressed as mean ± standard error of the mean. Mann-Whitney tests were used to seek for statistical analysis between groups.

HAE: 4-hydroxyalkenal; IUGR: intrauterine growth restriction; MDA: malondialdehyde.

5.2.2.5 Sirtuin 3 protein expression

Sirtuin 3 may be a candidate to be involved in the regulation of mitochondrial rearrangements so it was evaluated in placenta.

A significant 117.78±51.11% increase of Sirtuin 3/β-actin protein expression was observed in placental homogenate from IUGR pregnancies with respect to controls ($p<0.05$; Figure 34A-B and Table S3), suggesting, as aforementioned in the rabbit model, a compensatory mechanism in an attempt to modulate mitochondrial dysfunction.

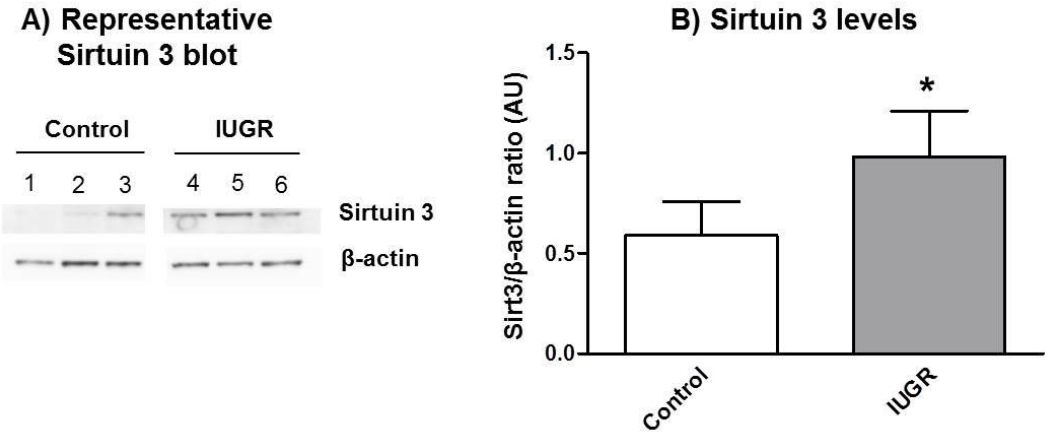

Figure 34. Sirtuin 3 protein levels in the placenta of the study groups. A) A representative Western Blot of Sirtuin 3 protein expression in human placenta is shown in both controls (1-3) and IUGR pregnancies (4-6). β-actin was used as the loading control. B) Graph showing the significant increase of Sirtuin 3 levels (Sirt3/β-actin ratio) in IUGR pregnancies (grey bars, N=12) compared with controls (empty bars, N=19).

Results were expressed as mean ± standard error of the mean. Mann-Whitney tests were used to seek for statistical analysis between groups.

AU: arbitrary units; IUGR: intrauterine growth restriction; Sirt3: Sirtuin 3.

5.2.3 Mitochondrial study in maternal and neonatal mononuclear cells

5.2.3.1 MRC activity and mitochondrial content

No differences in CII and CIV MRC enzymatic activities were observed in maternal PBMC or in neonatal CBMC (Figure 35 and Tables S4 and S5) from IUGR pregnancies compared to controls.

However, despite conserved citrate synthase activity in PBMC from IUGR pregnant women (Figure 35 and Table S4), there was a significant 39.19±12.61% decrease in neonatal CBMC from IUGR pregnancies compared to controls ($p<0.05$; Figure 35 and Table S5). Enzymatic activities of MRC complexes relative to citrate synthase activity showed no significant differences in maternal PBMC and neonatal CBMC. All of the raw data are presented in Supplementary Table 4 and 5 (S4 and S5).

In order to elucidate if the decrease of citrate synthase in CBMC from IUGR newborns was due to abnormalities in mitochondrial content or Krebs cycle, we measured alternative markers of mitochondrial mass such as levels of mtDNA that resulted unaltered (Table S5). This result suggests that Krebs cycle alteration may be concomitantly accompanying MRC dysfunction rather than the reduction in the mitochondrial number.

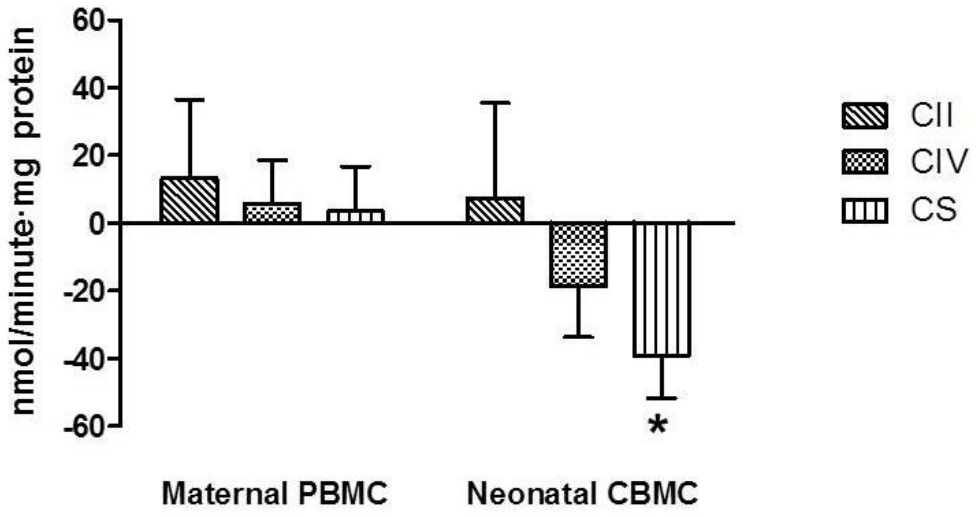

Figure 35. Enzymatic activities of the complexes of the mitochondrial respiratory chain (MRC) and citrate synthase (CS) activity in maternal and cord blood cells. IUGR cohort was presented as column bars demonstrating percentage of increase or decrease compared to controls (represented as the 0 baseline). No remarkable differences of MRC complexes were evidenced in both maternal PBMC (left; CII and CIV: control N= 22 and IUGR N=14) and neonatal CBMC (right; CII: control N=21 and IUGR N=9; CIV: control N=22 and IUGR N=9). Also, CS activity was maintained in maternal PBMC (control N=21 and IUGR N=13). However, a significant decrease of CS activity was found in neonatal CBMC (control N= 21 and IUGR N=8).

Results were expressed as a percentage of increase or decrease ± standard error of the mean. Mann-Whitney tests were used to seek for statistical analysis between groups.

CBMC: cord blood mononuclear cells; CII: complex II activity; CIV: complex IV activity; CS: citrate synthase activity; IUGR: intrauterine growth restriction; PBMC: peripheral blood mononuclear cells; *: $p<0.05$.

5.2.3.2 Mitochondrial oxygen consumption

Maternal PBMC from IUGR pregnant women presented conserved cellular oxygen consumption (p=NS; Figure 36 and Table S4) and trends to decrease of CI-stimulated oxygen consumption compared to controls (PMox: -31.55±11.36% and GMox: -25.00±10.45%; both p=NS; Figure 36 and Table S4).

Despite not reaching statistical significance, CBMC from IUGR newborns presented a tendency to decrease of both cellular and CI-stimulated oxygen consumption compared to controls (Cellox: -30.19±12.61%; PMox: -45.63±14.19%; GMox: -49.90±11.39; all p=NS; Figure 36 and Table S5). Noticeably, IUGR newborns presented higher mitochondrial deficits compared to mothers.

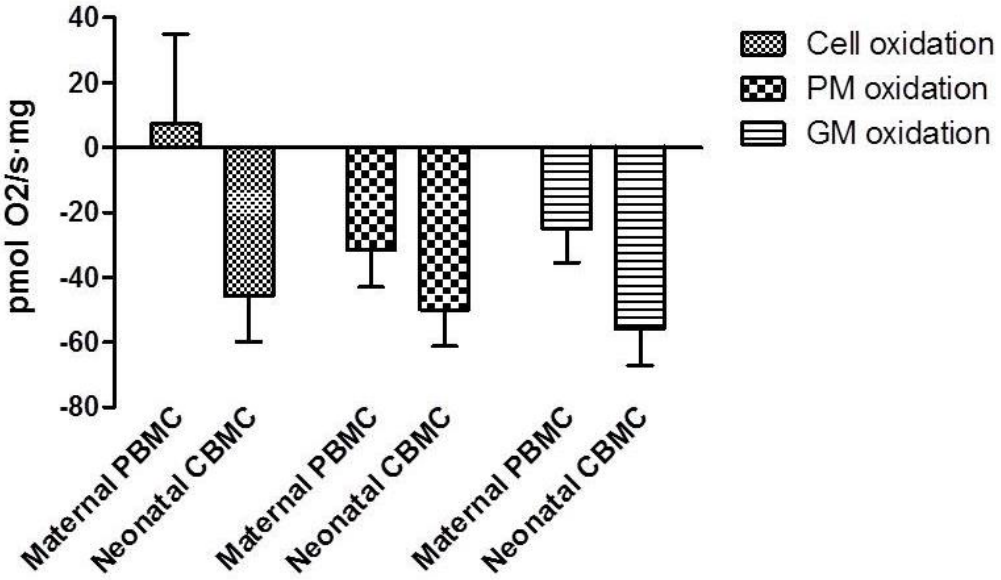

Figure 36. Oxygen consumption of the mitochondrial respiratory chain (MRC) in maternal and neonatal blood cells. IUGR cohort was presented as column bars demonstrating percentage of increase or decrease compared to controls (represented as the 0 baseline). Maternal PBMC from IUGR pregnancies presented conserved cellular oxygen consumption and trends to decrease of oxygen consumption stimulated for CI compared to controls (Cellox: control N=18 and IUGR N=11; PMox: control N=18 and IUGR N=9; GMox: control N=17 and IUGR N=9). Despite not reaching statistical significance, CBMC from IUGR newborns presented a tendency to decrease of both cellular and CI-stimulated oxygen consumption compared to controls (Cellox, PMox and GMox: control N=18 and IUGR N=7). Additionally, IUGR newborns presented higher oxygen consumption deficiencies compared to mothers.

Results were expressed as a percentage of increase or decrease ± standard error of the mean. Mann-Whitney tests were used to seek for statistical analysis between groups.

CBMC: cord blood mononuclear cells; Cellox or Cell oxidation: cellular endogen oxidation (without substrates); GM oxidation or GMox: glutamate+malate oxidation; IUGR: intrauterine growth restriction; PBMC: peripheral blood mononuclear cells; PMox or PM oxidation: pyruvate+malate oxidation.

5.2.3.3 Total cellular ATP levels

No changes of total ATP levels were observed in maternal PBMC or neonatal CBMC from pregnancies complicated by IUGR with respect to controls (-16.72±14.51% and 60.87±46.09%, respectively; p=NS; Figure 37 and Table S4-S5), suggesting no effects of MRC dysfunction in total ATP supply or the activation of alternative sources for ATP production.

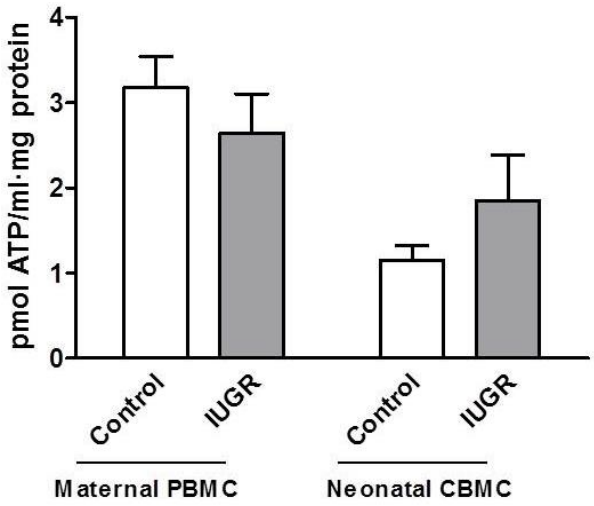

Figure 37. Total ATP levels in maternal and neonatal blood cells. No significant differences were observed in maternal PBMC and neonatal CBMC between IUGR pregnancies (grey bars; PBMC N=13 and CBMC N=10) and controls (empty bars; PBMC and CBMC N=22).

Results were expressed as mean ± standard error of the mean. Mann-Whitney tests were used to seek for statistical analysis between groups.

ATP: adenosine triphosphate; CBMC: cord blood mononuclear cells; IUGR: intrauterine growth restriction; PBMC: peripheral blood mononuclear cells.

5.2.3.4 Lipid peroxidation (oxidative damage)

No relevant changes were observed in lipid peroxidation in both maternal PBMC and neonatal CBMC from IUGR pregnancies with respect to controls (Figure 38 and Table S4-S5), once again reflecting decreased MRC activity.

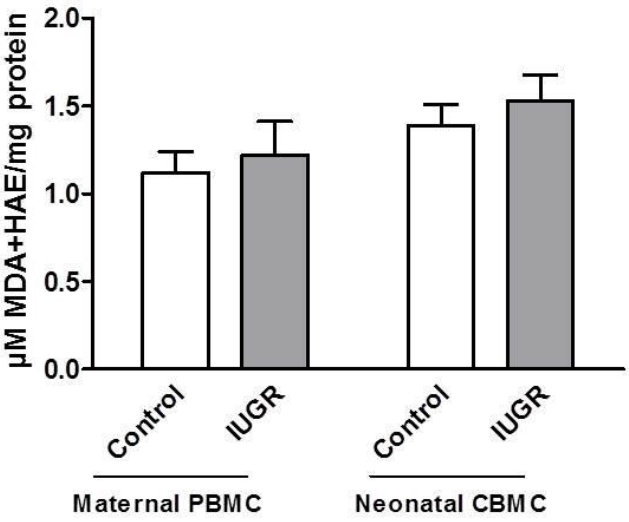

Figure 38. Lipid peroxidation as an indicator of oxidative damage in maternal and neonatal blood cells. No significant differences were evidenced in maternal PBMC and neonatal CBMC between IUGR pregnancies (grey bars; PBMC N=14 and CBMC N=9) and controls (empty bars; PBMC N=20 and CBMC N=21).

Results were expressed as mean ± standard error of the mean. Mann-Whitney tests were used to seek for statistical analysis between groups.

CBMC: cord blood mononuclear cells; IUGR: intrauterine growth restriction; MDA: malondialdehyde; HAE: 4-hydroxyalkenal; PBMC: peripheral blood mononuclear cells.

5.2.4 Associations between clinical data and experimental results

Supplementary Table S6 describes all the significant associations between the clinical data and experimental results in the cohorts of IUGR and control pregnancies. The most relevant associations are described below and showed in Figure 39.

Birth weight, as well as placental weight, were significantly and negatively correlated with cord blood BNP levels, confirming the association of IUGR with cardiovascular remodelling (R^2=0.526, p<0.001; Figure 39A; Table S6). Secondly, birth weight was also significantly and positively correlated with CI-stimulated oxygen consumption (PMox: R^2=0.197, p<0.05; GMox: R^2=0.279, p<0.01; Table S6) and MRC CI enzymatic activity (R^2=0.195, p<0.05; Figure 39B; Table S6) in placental tissue. These associations suggested that a proper weight of the newborn promotes a proper MRC CI function, or more likely, that efficient MRC CI function is required to reach a proper birth weight. Additionally, birth weight was significantly and negatively correlated with placental Sirtuin 3 levels (R^2=0.224, p<0.05; Figure 39C; Table S6), suggesting the adaptation mechanism that Sirtuin 3 is leading in response to IUGR.

Cord blood BNP levels also were significantly and negatively correlated with CI enzymatic activity in placenta (R^2=0.159, p<0.05; Figure 39D; Table S6) which additionally was significantly and negatively correlated with placental Sirtuin 3 levels (R^2=0.095, p<0.05; Figure 39E; Table S6). Those associations could demonstrate that cardiac adaptation defined by BNP levels is characterized by CI dysfunction and adaptive increase of Sirtuin 3 levels in the placenta.

Finally, maternal and neonatal CI-stimulated oxygen consumption were significantly and positively correlated (GMox; R^2=0.115, p<0.05; Table S6), demonstrating the strong dependence of foetal metabolism on maternal status. In addition, neonatal mitochondrial content significantly and positively correlated with neonatal and placental oxygen consumption (R^2=0.189, p<0.05; R^2=0.159, p<0.05; R^2=0.213, p≤0.001; Table S6), suggesting the dependence of foetal health on accurate placental function.

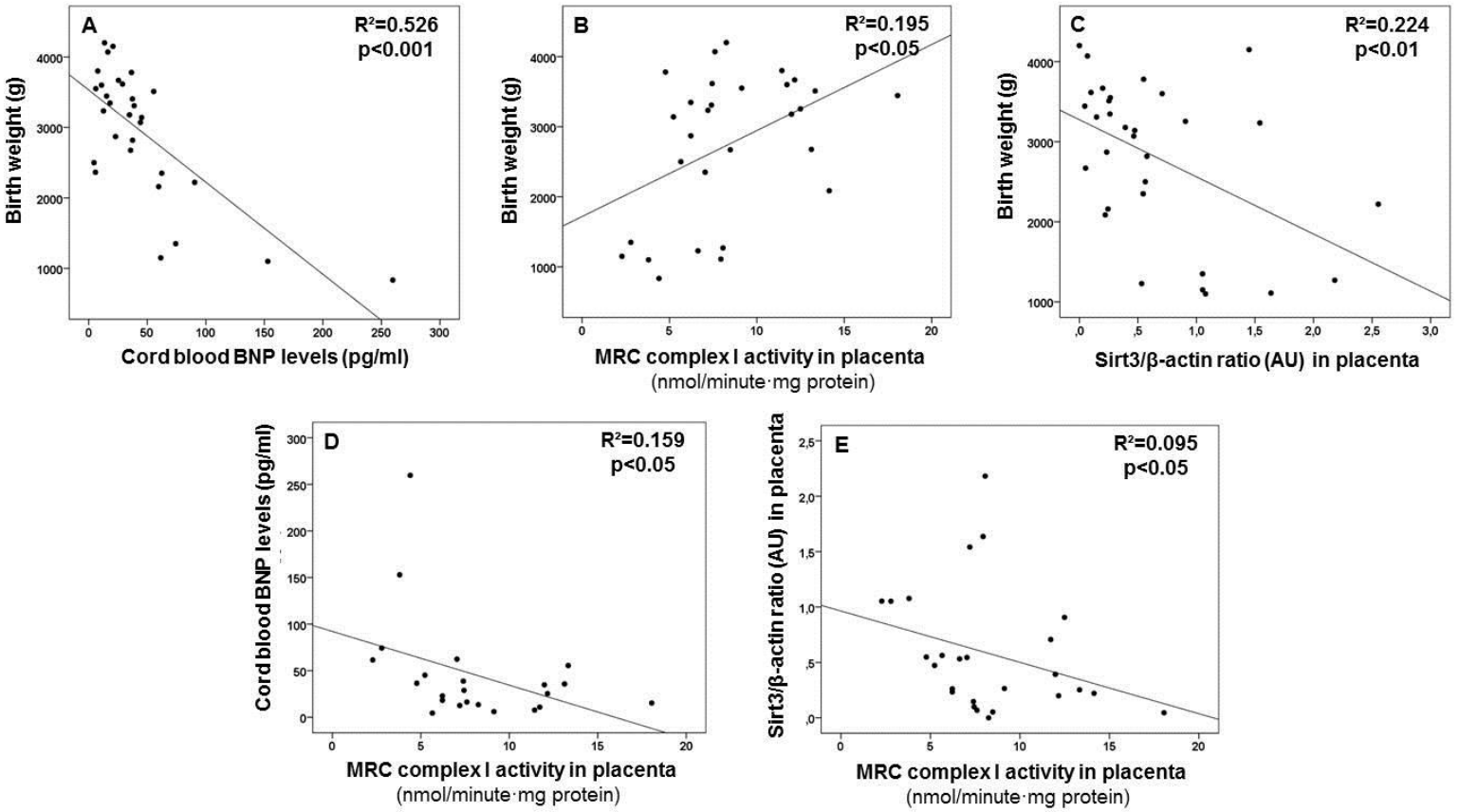

Figure 39. Association between clinical data and experimental results from pregnancies complicated by intrauterine growth restriction (IUGR) and controls. Decreased birth weight characteristic of IUGR is associated to increased BNP levels (as sign of cardiovascular remodelling) (**A**), decreased MRC CI in placenta (**B**) and enhanced Sirtuin 3 protein expression (**C**) (probably to compensate mitochondrial dysfunction). Additionally, dysfunctional MRC CI in placenta was directly associated to increased foetal BNP levels (**D**) and placental Sirtuin 3 protein expression (**E**), demonstrating the strong association among all these parameters.

Spearman Rho tests were used to seek for statistical analysis.

AU: arbitrary units; BNP: brain natriuretic peptide; CBMC: cord blood mononuclear cells; CI: MRC complex I; MRC: mitochondrial respiratory chain; R^2: coefficient of determination; Sirt3: Sirtuin 3.

6. DISCUSSION

There is the crucial need to elucidate the molecular basis of IUGR and cardiovascular remodelling despite relevant novel advances in the field (60,90,91). The main concern relies on the high prevalence of this obstetric complication (affecting 5-10% of all pregnancies) and its potential consequences in adulthood. A wide range of clinical manifestations have been associated with IUGR, including metabolic, neurological and cardiovascular disorders (24,116,117). These disorders are established during foetal development when the foetus has to strive against hypoxia, consequently leading to a foetal remodelling with eventual adverse outcomes later in adulthood (58,118). Among these long term consequences, this thesis is focused on the foetal cardiovascular remodelling that has been demonstrated in IUGR (1,69,87).

The need to overcome target tissue limitation to study the heart has been a major concern to advance in this field of research. To meet that aim, some animal models have been proposed (70,78,80,85). Those models based on the restriction of blood flow into the foetus in development have been proposed to recapitulate the placental insufficiency more accurately than others based on caloric restriction (78,85). Our group has developed a rabbit model of IUGR that consists of a selective ligature of the uteroplacental vessels in one of the two uterine horns to reduce 40-50% oxygen and nutrient supply to the foetus in development (85). This model allows to obtain, in the same pregnancy, IUGR offspring (from the manipulated horn) and controls (from the non-manipulated horn). The major advantage of this model is that reproduces the functional alterations in heart, reported in humans, and allows to investigate the consequent cardiovascular remodelling of IUGR by directly studying the heart. Additionally, as the model induces a combined restriction of oxygen and nutrients, also reproduces the role of the placenta in this obstetric complication, thus mimicking IUGR in human pregnancy.

Placenta is also the preferred tissue for the study of IUGR and other obstetric complications, especially those associated to placental insufficiency (68,90,91). Some research has also been performed using maternal and neonatal blood cells (18,55,56,68). Additionally, blood cells have been extensively used to evaluate mitochondrial function in other diseases (67,119). Those tissues offer a more accessible and non-invasive approach that, in case of maternal blood, might offer the major advantage of finding and monitoring potential novel prognostic and diagnostic biomarkers of this obstetric complication before birth.

Previous experimental studies pointed out mitochondrial deficits to play a relevant role in IUGR and associated cardiovascular remodelling (90,91,120). However, most of

them were limited on molecular findings in the case of the rabbit model of IUGR and cardiovascular remodelling (34,89,121), so functional studies were lacking in this field. Additionally, very little and controversial studies found in the literature investigate mitochondrial alterations in human pregnancies at molecular and functional level, highlighting the need for a more exhaustive study of mitochondrial involvement in this obstetric complication.

The present thesis aimed to evaluate the mitochondrial implication in IUGR and its associated cardiovascular remodelling by first assessing an exhaustive mitochondrial characterization in the animal model to finally validate obtained results in affected human pregnancies. Consequently, data provided in this thesis are presented in two separate studies. The first one evaluates the mitochondrial function in the target tissue of cardiovascular remodelling (the heart) and in the organ responsible for oxygen and nutrient supply into the foetus (the placenta) from a rabbit model of IUGR. The second study validates the findings from the rabbit model into human pregnancies complicated with IUGR.

The starting point of this thesis sought to confirm the expected phenotype of IUGR and associated cardiovascular remodelling both in the animal model and in the cohort of selected pregnant women.

Offspring with experimental induced IUGR showed altered biometric measures by a significant decrease in birth weight, accompanied by a reduction in heart and placenta, as previously reported by Gonzalez-Tendero *et al.* in the same animal model with equivalent percentage of reduction in birth, heart and placental weight (89), validating our animal model and the source of the samples. Thus, organ to body weight measures were preserved due to global and proportioned organ and body mass reduction. Cardiac hypertrophy and consequent increase in heart to body weight was not present in IUGR rabbits, resembling human conditions, in which globular and elongated hearts are usual, and hypertrophy occurs only in 17% of cases of IUGR (23,86,87,121–126).

The analysed cohort of pregnancies with IUGR reproduced the incidence of perinatal outcomes characteristic of IUGR (birth weight, placental weight, BNP levels, etc.) previously described in the bibliography (26), validating our IUGR cohort and also the source of the samples. We stratified the cohort in two groups: IUGR pregnancies (defined as bellow the 3th percentile or, alternatively, below the 10^{th} percentile in case of abnormal UA Doppler or abnormal CPR) and controls (with a percentile over the 10^{th}). As expected, IUGR pregnancies showed a reduced birth weight, birth weight percentile and placental weight as well as more incidence of abnormal Apgar in IUGR

newborns. Additionally, this cohort confirms the presence of a cardiovascular remodelling in newborns from IUGR pregnancies by an increase of BNP levels in cord blood, previously reported by our group and others (32,33,69). Interestingly, in our study, BNP levels were significantly and inversely associated with birth and placental weight confirming the strong association between IUGR and cardiovascular remodelling.

With respect to the mitochondrial characterization, both animal and human IUGR pregnancies presented clear signs of MRC dysfunction, showing findings consistent with that of Gonzalez-Tendero *et al.* who first reported MRC deficiency at transcriptomic level as well as ultrastructural mitochondrial alterations of cardiomyocytes from the offspring of the IUGR rabbit model (89). The first study in the animal model provided evidence of mitochondrial deficiency in the cardiac tissue of IUGR offspring, with a significant decrease of enzymatic activities of MRC CII, CIV and CII+III. The same pattern was observed in placenta from IUGR offspring, regarding CII and CII+III. Interestingly, birth weight, placental and left ventricle weight were significantly and positively correlated with the MRC enzymatic activities in heart (including CI, CII, CII+III and CIV), thereby strengthening the relevance of the need for adequate bioenergetic mitochondrial status to reach potential body, heart and placental weight. In line with the first study, the second study in human pregnancies also showed evidence of mitochondrial dysfunction in placenta from IUGR pregnant women focused on the enzymatic activity of MRC CI. Interestingly, birth weight was significantly correlated to placental MRC CI enzymatic activity, which is also significantly and inversely associated to BNP levels in newborns, thus reinforcing mitochondrial implication in this obstetric complication and cardiovascular remodelling. These findings of MRC CI enzymatic deficiency in human placenta were consistent with CI-stimulated oxygen consumption, also significantly decreased in this tissue. In agreement with this, the findings of oxygen consumption in cardiac and placental tissues from the rabbit model support mitochondrial dysfunction in IUGR, despite statistical difference was not reached. In neonatal and maternal blood cells, the CI-stimulated oxygen consumption decrease was also present, although not significantly, together with the decrease in endogenous oxygen consumption. Additionally, in the human cohort, materno-fetal correlations were observed regarding mitochondrial oxygen consumption parameters, confirming the dependence of neonatal bioenergetics in mitochondrial health status of the mother. Noticeably, IUGR newborns presented higher mitochondrial deficits in terms of oxygen consumption compared to mothers. This observation may support the hypothesis that the newborn is the most affected by

mitochondrial dysfunction together with the placenta. Actually, there was a significant positive correlation between CI-stimulated oxygen consumption in placenta and citrate synthase activity in neonatal blood cells, which activity was significantly decreased in IUGR newborns compared to controls. Furthermore, PBMC of pregnant women appeared not to be affected for such mitochondrial alterations reinforcing both the placenta and the foetus as the main pathological targets of this obstetric complication.

In some cases, specific discrepancies between oxidative and enzymatic MRC activities could be attributed to relevant alterations of independent enzymatic activities of MRC complexes, not detectable when analysing the whole MRC function in terms of impaired oxygen consumption. In any case, in our studies both data from animal and humans confirm decreased mitochondrial activity in the context of IUGR, in accordance to most of bibliography. The significant CI deficiency at enzymatic and oxidative level in human placenta was previously described by our group at transcriptional level in heart tissue of the IUGR animal model (89) and also by Beyramzadeh M *et al.* in placenta from high risk pregnancies (90). Previous research also demonstrated a decrease in OXPHOS in skeletal muscle from IUGR rats (81). Conversely to these findings, Mandó *et al.* observed higher oxygen consumption, both for CI+CII and CIV, in placenta from IUGR cases (91). Such contrarieties may be due to differential stimulation of specific MRC when measuring oxygen consumption, or more likely to the presence of different cell linages, for instance cytotrophoblasts and syncytiotrophoblasts from placenta that have multiple functions, different mitochondrial populations and also respond differently to exogenous stimulus (127).

Observed deficiencies of enzymatic activities of MRC complexes and oxygen consumption in IUGR cases from both animal and human studies may suggest malfunction of MRC or lack of oxygen delivery in IUGR hearts and newborns. The question if the mitochondrial alteration would be a primary cause or a secondary consequence remains elusive at present.

Mitochondrial decreased activity, as a consequence of hypoxia, may be supported by the maintenance and even decrease of oxidative stress in these pregnancies. Lipid peroxidation, as an indication of oxidative damage, did not show relevant differences between groups either in rabbit and human placental tissue, maternal PBMC or neonatal CBMC. Indeed, it was found to be significantly decreased in rabbit cardiomyocytes. Thus, diminished ROS production may be the consequence of decreased MRC function. In addition, lipid peroxidation levels in heart showed a significant positive correlation with MRC CII and CII+III enzymatic activities as well as

with birth and heart weight. These associations gave strengthen to the observed results, suggesting that the experimental hypoxia could limit not only the presence of oxygen but also the production of ROS as the whole MRC is less functional. We hypothesised that the decrease of mitochondrial function in IUGR without increase in oxidative stress would point out to placental insufficiency and hypoxia as the main causes for deficient mitochondrial function rather than a mitochondrial defect itself. Moreover, it seems that the antioxidant defence system was properly operating in IUGR cases as the antioxidant enzyme SOD2 in heart and placenta from offspring of the rabbit model was not altered. Previous studies in IUGR reported controversial results in oxidative damage (92,127,128) but in other pregnancy complications caused by placental insufficiency, such as preeclampsia, it is described an induction of oxidative stress in the placenta and maternal blood (93), as well as in certain risk pregnancies depending on the type of delivery (specially vaginal delivery because of intermittent perfusion of intervillous space of the placenta during uterine contractions) (101). In our cohort of IUGR pregnancies, we reduced preeclampsia comorbidity and vaginal delivery to avoid potential confounders. Whether these factors may explain controversies with literature should be deeper explored.

Previous research in foetal growth provided data about adaptive response to altered mitochondrial respiration deriving ATP production from aerobic metabolism to faster anaerobic metabolism (129). In a situation of placental hypoxia there is a metabolic reprogramming that leads to decreased oxygen consumption and increased anaerobic glucose consumption, which would, in turn, allow high availability of oxygen to the foetus in development at the expense of less accessible glucose (129). Our results showed no differences in total ATP levels in heart and placenta form the rabbit model and either in placental tissue or neonatal CBMC and maternal PBMC, suggesting this potential switch from aerobic to faster anaerobic metabolism to preserve ATP supply. Further studies in IUGR should be conducted to confirm our findings.

Consequently, mitochondrial decreased function may be not only restricted to MRC but also to an extensive metabolic adaptation to hypoxia.

As previously commented and with more detail, IUGR offspring from the rabbit model showed a common enzymatic alteration in MRC CII dysfunction in both heart and placenta. CII, also known as succinate dehydrogenase, is the molecular link between the Krebs cycle and the MRC. The Krebs cycle is a central pathway of the mitochondrial energetic metabolism, which is responsible for the oxidative degradation of the different dietetic supplies, feeding the MRC and, subsequently, activating ATP

synthesis. In order to further investigate the molecular basis of CII dysfunction in heart and placenta of IUGR offspring, the expression of CII SDHA and SDHB proteins was assessed, together with CoQ levels, the electron donor for CII. Interestingly, in front of preserved CoQ levels, SDHB subunit was found significantly decreased in placenta and positively and significantly correlated with CII, CII+III and CIV enzymatic activities. These findings suggested that MRC enzymatic dysfunction may be due, at least in placenta, to down-regulation of MRC subunit expression. Additionally, the significant and positive correlation between CII SDHB levels and all biometric parameters from IUGR and control offspring (body, placental and heart weights) highlighted the relevance of SDHB and CII in this obstetric complication. As CII is the only complex of the MRC exclusively encoded by the nuclear DNA (130), we hypothesised that its deficiency may be more likely associated with alterations in the oxidative metabolism events controlled by the nucleus, rather than a regulation associated with mitochondrial genome. The fact that protein expression of COX5A subunit from MRC CIV was preserved despite decreased activity from IUGR offspring, reinforced MRC CII implication and nuclear regulation of mitochondrial adaptations in the animal model of IUGR.

On the other hand, neonatal mitochondrial impairment was mainly characterized by the significant decrease of citrate synthase in CBMC, not described so far. Citrate synthase is a reliable marker of mitochondrial content (40), but it is also an enzyme participating in the Krebs cycle. As parallel measurement of citrate synthase activity in placental tissue and maternal PBMC as well as alternative markers of mitochondrial content (mtDNA) in neonatal CBMC yielded to preserved mitochondrial mass, we concluded that alterations in citrate synthase would be related to newborn metabolic imbalances rather than to mitochondrial content. Previous studies only performed at placental level showed controversial results for mitochondrial content in pregnancy complications associated with placental insufficiency such as IUGR or preeclampsia (91,131–133) as well as in alternative animal models of IUGR (81,82). In our study, results of citrate synthase activity in heart and placenta from the rabbit model demonstrated no changes in mitochondrial content. This was confirmed by Tom20 expression and also by previous results obtained by electron microscopy (89). The unique alteration in citrate synthase was restricted to neonatal CBMC from the human cohort that may therefore be more likely related to Krebs cycle function or nuclear regulation of mitochondrial disturbances. In accordance with these findings obtained in IUGR cases with placental hypoxia, environmental hypoxia has also been associated with alterations in the Krebs

cycle (134), which may also lead to neurological or cardiac clinical consequences (135).

One of the major nuclear pathways to modulate mitochondrial function (both MRC and Krebs cycle) in accordance to oxygen and nutrient supply are sirtuins. Following a potential line of investigation aiming to understand upstream molecular pathways regulating mitochondrial dysfunction and to attempt to find potential therapeutic targets easily influenced by diet (136), we explored Sirtuin 3 involvement in IUGR.

Concretely, Sirtuin 3 is the most important mitochondrial deacetylase encoded in the nucleus and plays a role in the regulation of mitochondrial function and OXPHOS (50,137,138). It has been associated to increased bioenergetic demands (139,140), often in the context of cardiovascular disease, acting as a protective mechanism in front of different stimulus (53,141,142). Interestingly, since mitochondrial CII is one of the targets of Sirtuin 3 (48,137), this protein is able to simultaneously interfere with MRC (Sirtuin 3 directly activates CII function by deacetylation of subunits SDHA and SDHB) and the Krebs cycle (where citrate synthase is also participating). In both studies, the significant increase of Sirtuin 3 observed in IUGR cases was associated with a significant decrease of CII enzymatic activity in both heart and placental tissues from rabbit and also with a significant decrease of citrate synthase activity in neonatal CBMC. We hypothesised that this up-regulation in Sirtuin 3 expression may be the compensatory response to imbalanced bioenergetics status.

Additionally, Sirtuin 3 has a role in anti-oxidation, promoting the maintenance of ATP levels, especially in hypoxia conditions (51,52). Interestingly, in heart from IUGR offspring, oxidative stress was found to be significantly decreased in the setting of conserved cellular ATP levels, suggesting that increased cardiac Sirtuin 3 levels may protect cardiomyocytes from oxidative stress insults and ATP deficiency in placental hypoxia. We hypothesised that Sirtuin 3 would exert a compensatory role in this phenotype by modulating mitochondrial lesion in cardiomyocytes. Moreover, the positively association between increased cardiac oxidative damage and body weight, heart weight and proper MRC activity suggested that the antioxidant protection of Sirtuin 3 may be more necessary in MRC dysfunction and abnormal foetal development. This hypothesis was also in line with significant negative correlation of body and heart weight with cardiac Sirtuin 3 levels.

In parallel, and as mentioned before, cellular ATP levels were also maintained in placental tissue, albeit with a not significant increased lipid peroxidation. This

juxtaposed phenotype in terms of ATP and oxidative damage between heart and placenta from the rabbit model may also be explained by the poor antioxidant defences characteristic of the placenta (101,143). Interestingly, as SOD2 expression and activity was preserved either in cardiac or placental tissue, we hypothesised that Sirtuin 3 would not be exerting its antioxidant action via SOD2 activity, despite being one of its targets.

In accordance to observed results in rabbit model, human placental Sirtuin 3 protein expression significantly increased, also probably as an adaptation mechanism to modulate the adverse mitochondrial phenotype. Interestingly, birth weight was inversely correlated with placental Sirtuin 3 expression, which also is inversely associated with MRC CI enzymatic activity in placenta, thus reinforcing involvement of Sirtuin 3 in this obstetric complication as a compensatory mechanism trying to enhance decreased mitochondrial activity. The human placental increase of Sirtuin 3 is also in front of conserved placental ATP levels and oxidative damage. Further work is required following this line of research to assess Sirtuin 3 involvement in IUGR and its potential role as a therapeutic target.

Both studies included in this thesis are encouraging because follow the same line of evidence and are consistent with literature, demonstrating a reduced mitochondrial activity especially in the newborn affected by IUGR and in placenta, which is widely affected in IUGR due to placental insufficiency. Cardiovascular remodelling is also a consequence of placental insufficiency leading to less oxygen availability to the heart. Consequently, there is a low MRC function, which consequently turns into less ROS production, and the activation of compensatory mechanisms to overcome mitochondrial imbalance, through Sirtuin 3 upregulation.

These features were evident in the animal model. Mitochondrial function alterations in IUGR offspring from rabbit model were not only confined to the target tissue of cardiovascular remodelling (heart), but rather were also present in placenta. Mitochondrial dysfunction in placenta (and probably also in heart and other tissues) might be caused by the *de novo* rearrangement adaptations imposed by the experimental hypoxia induced by the ligature of uteroplacental vessels in this animal model (128). Similar hypoxic conditions are also present in patients with IUGR due to placental insufficiency (16,144). These are undoubtedly examples of the foetal programing, first described by Barker (118), which establishes that physiologic adaptations to the foetal environment may condition organ development and consequent disease in adulthood. This fact was also evident in humans, where both

neonatal CBMC and placenta seemed to be more affected in terms of mitochondrial function.

The combination of findings from the two studies provides support for the conceptual premise that the placenta and the newborn are the most affected. Thus, further research should be undertaken to investigate placenta as a target to modulate mitochondrial function willing to prevent newborn injury and consequent cardiovascular remodelling. Additional research should be striven for investigating the cause of this placental insufficiency and the consequent hypoxia. It would be interesting to perform *in vitro* experiments in hypoxic-reperfusion conditions with cardiomyocyte or placental cells from IUGR cases and further evaluate mechanisms responsible for decreased mitochondrial function. Additionally, these approaches may provide a potential platform to test therapeutic strategies aimed to improve or even recover the mitochondrial function that it is known to work in suboptimal conditions. Given the evidences of hypoxia and the involvement of nuclear regulation in IUGR development through Sirtuin 3 implication, we support the design of future research, where it might be possible to use a diet intervention to modulate mitochondrial function, as reported in the case of resveratrol (a polyphenol that has antioxidant properties) in a IUGR animal model with piglets, that has been demonstrated to improve global MRC function along with mediating an increase of Sirtuin 1 (83). In line with this, one potential line of investigation could be the measurement of NADH/NAD^+ levels, which could give us information about Sirtuin 3, which activity depend on these metabolites. It would be possible that Sirtuin 3 was highly expressed as an adaptation mechanism in front of limited NAD+ substrate due to low MRC function and altered metabolism. In that case, Sirtuin 3 would not be as active as required to overcome mitochondrial imbalance due to substrate limitation. In that case, NAD^+ treatments providing intermediates (for example, NMN) would be of interest in IUGR (145,146). In a situation of inactive Sirtuin 3, a context of hyperacetylation of proteins could be possible which could, in turn, be the cause of some metabolic enzymatic inactivation, such as SDH from CII or citrate synthase. Since sirtuins can be modulated through dietary interventions (147), the potential use of such non-invasive approaches in human pregnancies is a strategy that should be further investigated to reduce the risk of obstetric complications and associated diseases in adulthood.

Finally, further research should be undertaken to investigate the long-term consequences of mitochondrial imbalance. Thus, follow-up studies of these newborns with IUGR are needed during the adolescence and investigate whether mitochondrial

alterations persist to clarify the impact of these findings in the population of adult subjects with IUGR, as it was previously demonstrated by Crispi *et al.* regarding the cardiovascular remodelling (1,148).

Some limitations and technical considerations should be acknowledged in this thesis.

First, IUGR is known to be a multifactorial obstetric condition where many pathways and aetiologies could finally lead to a unique phenotype. Second, more efforts are warranted to better clarify the functional consequences of the decrease of MRC CII, CIV and CII+III enzymatic activities in heart and placenta from the rabbit model as well as placental MRC CI function and neonatal citrate synthase activity in humans. It is important to keep in mind that the bioenergetic findings of the present approach may become more evident by the analysis under hypoxic conditions, other than the normoxic environment of experimental mitochondrial measures that could interfere in the results. Additionally, it is important to take into account the potential contribution of the different cell types of the affected tissues. However, avoiding the separation among different cell types of the studied tissues by including all placental and blood cell types offers a closer approach to the physiology.

Specifically, the animal model has some disadvantages or limitations. For instance, it is an acute model of hypoxia as the ligation is done by day 25 of gestation, which corresponds to third semester of pregnancy in humans, and the caesarean procedure is done by day 30. Thus, the selective ligation is performed when the rabbit heart is already formed (the complete organogenesis in rabbit is achieved by day 19.5 of gestation). In humans, the placental insufficiency leading to cardiovascular remodelling could be present since the first day of gestation heading different impacts on disease severity. Additionally, further studies with the rabbit model may ideally include additional measures to be collected (brain sparing, sex distribution, timing of development and maturation of the heart, cardiac severity markers, etc) to explore underlying mechanistic pathways.

On the other hand, we cannot exclude that the difference in gestational age at delivery between cases and controls in human pregnancies could have influenced the results. This limitation is difficult to overcome as most clinical protocols indicate finalization of gestation in IUGR with signs of placental insufficiency at 37-38 weeks. Additionally, several potential confounders such as maternal diet (influencing mitochondrial and metabolism regulation), socio-cultural environment or lifestyle, that were not controlled in this study may play a role in the observed results.

Interestingly, all rising evidences that support mitochondrial dysfunctional phenotype in other obstetric complications associated to placental insufficiency (for instance small for gestational age, preeclampsia, miscarriage or stillbirth) strengthen the relevance of mitochondrial role in proper foetal development. Actually, it is important to take into account the 28.6% of incidence of preeclampsia in our cohort of IUGR. Previous evidences demonstrate that, in cases of IUGR complicated by preeclampsia, there is mitochondrial implication (68,90). Therefore, comorbidity of IUGR with preeclampsia could be hampering our results and explaining controversy in the bibliography. However, we did not evidence high oxidative stress characteristic of preeclampsia (93), thus suggesting a minimal confounder in our study.

Despite these considerations, the consistency of our results, as well as the different associations found between clinical parameters and experimental findings in human pregnancies, or the similitude between human findings and experimental model results, strengthen the validity of the present findings.

The relevance of this thesis relies on the description of mitochondrial impairment in the offspring of a rabbit model of IUGR but also in newborns from pregnancies complicated by IUGR. This mitochondrial imbalance is widely present in the different studied tissues, including the heart and the placenta from the rabbit model and the placenta and neonatal blood cells from human pregnancies. The mitochondrial characterization of this obstetric complication could help to greater understand the pathophysiologic mechanisms underlying cardiac remodelling and IUGR. This thesis provides novel findings aimed to better comprehend the molecular mechanisms involved in this obstetric complication. An improved understanding of these molecular mechanisms could be crucial for exploring biomarkers and promoting potential therapeutic strategies for enhancing cardiovascular health in children suffering of IUGR. Given the high prevalence of IUGR and cardiomyopathy, the clinical significance and effects of improving strategies could have a solid impact in public health.

7. CONCLUSIONS

1) Mitochondrial dysfunction is present in the target tissue of cardiac remodelling (heart) in IUGR offspring of the rabbit model focused on MRC complex II, IV and II+III deficiency, confirming previous mitochondrial alterations described at transcriptional and ultrastructural level.

2) Such mitochondrial alteration is also present in the target tissue of placental insufficiency (placenta) from the same animal model in terms of MRC complex II and II+III deficiencies.

3) Human pregnancies with IUGR also manifest mitochondrial imbalance in the placenta, especially through the MRC CI dysfunction.

4) Mitochondrial disarrangements in IUGR patients are not confined to placenta; they are also present in cord blood cells from IUGR newborns in reference to Krebs cycle, and not further evidenced in maternal blood.

5) Sirtuin 3 expression is upregulated in both the animal model and human pregnancies with IUGR in accordance to dysfunctional mitochondrial phenotype.

6) The association of molecular alterations with clinical manifestations reinforce mitochondrial implication in IUGR and cardiovascular remodelling.

7) Taken together, these results confirm mitochondrial involvement in IUGR and associated cardiovascular remodelling in accordance to deregulation of the metabolic sensor Sirtuin 3, providing new insights for further research on potential novel biomarkers or therapeutic strategies for this obstetric complication.

8. REFERENCES

1. Crispi F, Bijnens B, Figueras F, Bartrons J, Eixarch E, Le Noble F, et al. Fetal growth restriction results in remodeled and less efficient hearts in children. Circulation. 2010;

2. Sharma D, Shastri S, Sharma P. Intrauterine Growth Restriction: Antenatal and Postnatal Aspects. Clin Med Insights Pediatr. 2016;

3. Alberry M, Soothill P. Management of fetal growth restriction. Archives of Disease in Childhood: Fetal and Neonatal Edition. 2007.

4. American College of O, Gynecologists. ACOG Practice bulletin No. 134: Fetal Growth Restriction. Obs Gynecol. 2013;

5. Figueras F, Gratacos E. An integrated approach to fetal growth restriction. Best Pract Res Clin Obstet Gynaecol. 2017;

6. Gardosi J. New definition of small for gestational age based on fetal growth potential. In: Hormone Research. 2006.

7. Figueras F, Gratacós E. Update on the diagnosis and classification of fetal growth restriction and proposal of a stage-based management protocol. Fetal Diagnosis and Therapy. 2014.

8. Hendrix N, Berghella V. Non-Placental Causes of Intrauterine Growth Restriction. Seminars in Perinatology. 2008.

9. Lausman A, McCarthy FP, Walker M, Kingdom J. Screening, diagnosis, and management of intrauterine growth restriction. J Obstet Gynaecol Can. 2012;

10. Cetin I, Alvino G. Intrauterine Growth Restriction: Implications for Placental Metabolism and Transport. A Review. Placenta. 2009.

11. John R, Hemberger M. A placenta for life. In: Reproductive BioMedicine Online. 2012.

12. Sibley CP, Turner MA, Cetin I, Ayuk P, Boyd CAR, D'Souza SW, et al. Placental phenotypes of intrauterine growth. Pediatric Research. 2005.

13. Gaccioli F, Lager S. Placental nutrient transport and intrauterine growth restriction. Frontiers in Physiology. 2016.

14. Zhang S, Regnault TRH, Barker PL, Botting KJ, McMillen IC, McMillan CM, et al. Placental adaptations in growth restriction. Nutrients. 2015.

15. Sibley CP, Brownbill P, Dilworth M, Glazier JD. Review: Adaptation in placental nutrient supply to meet fetal growth demand: Implications for programming. Placenta. 2010;

16. Cruz-Martinez R, Figueras F. The role of Doppler and placental screening. Best Practice and Research: Clinical Obstetrics and Gynaecology. 2009.

17. Westergaard HB, Langhoff-Roos J, Lingman G, Marsál K, Kreiner S. A critical appraisal of the use of umbilical artery Doppler ultrasound in high-risk pregnancies: Use of meta-analyses in evidence-based obstetrics. Ultrasound Obstet Gynecol. 2001;

18. Garrabou G, Hernàndez AS, Catalán García M, Morén C, Tobías E, Córdoba S, et al. Molecular basis of reduced birth weight in smoking pregnant women:

mitochondrial dysfunction and apoptosis. Addict Biol. 2016;

19. Phoon CKL. Circulatory physiology in the developing embryo. Current Opinion in Pediatrics. 2001.

20. Gerd Steding. The Anatomy of the Human Embryo. 2009.

21. Teitel DF, Klautz RJ, Cassidy SC, Steendijk P, van der Velde ET, van Bel F, et al. The end-systolic pressure-volume relationship in young animals using the conductance technique. Eur Hear J. 1992;

22. Crispi F, Gratacs E. Fetal cardiac function: Technical considerations and potential research and clinical applications. Fetal Diagnosis and Therapy. 2012.

23. Rodríguez-López M, Cruz-Lemini M, Valenzuela-Alcaraz B, Garcia-Otero L, Sitges M, Bijnens B, et al. Descriptive analysis of the different phenotypes of cardiac remodeling in fetal growth restriction. Ultrasound Obstet Gynecol. 2016;

24. Demicheva E, Crispi F. Long-term follow-up of intrauterine growth restriction: Cardiovascular disorders. Fetal Diagnosis and Therapy. 2014.

25. Barker DJ, Osmond C, Golding J, Kuh D, Wadsworth ME. Growth in utero, blood pressure in childhood and adult life, and mortality from cardiovascular disease. BMJ. 1989;

26. Crispi F, Miranda J, Gratacós E. Long-term cardiovascular consequences of fetal growth restriction: biology, clinical implications, and opportunities for prevention of adult disease. American Journal of Obstetrics and Gynecology. 2018.

27. Sarvari SI, Rodriguez-Lopez M, Nuñez-Garcia M, Sitges M, Sepulveda-Martinez A, Camara O, et al. Persistence of Cardiac Remodeling in Preadolescents with Fetal Growth Restriction. Circ Cardiovasc Imaging. 2017;

28. Rodriguez-Guerineau L, Perez-Cruz M, Gomez Roig MD, Cambra FJ, Carretero J, Prada F, et al. Cardiovascular adaptation to extrauterine life after intrauterine growth restriction. Cardiol Young. 2018;

29. Cruz-Lemini M, Crispi F, Valenzuela-Alcaraz B, Figueras F, Sitges M, Bijnens B, et al. Fetal cardiovascular remodeling persists at 6 months in infants with intrauterine growth restriction. Ultrasound Obstet Gynecol. 2016;

30. Celermajer DS, Chow CK, Marijon E, Anstey NM, Woo KS. Cardiovascular disease in the developing world: Prevalences, patterns, and the potential of early disease detection. J Am Coll Cardiol. 2012;

31. Gersh BJ, Sliwa K, Mayosi BM, Yusuf S. Novel therapeutic concepts: The epidemic of cardiovascular disease in the developing world: Global implications. European Heart Journal. 2010.

32. Crispi F, Hernandez-Andrade E, Pelsers MMAL, Plasencia W, Benavides-Serralde JA, Eixarch E, et al. Cardiac dysfunction and cell damage across clinical stages of severity in growth-restricted fetuses. Am J Obstet Gynecol. 2008;

33. Girsen A, Ala-Kopsala M, Mäkikallio K, Vuolteenaho O, Räsänen J. Cardiovascular hemodynamics and umbilical artery N-terminal peptide of proB-type natriuretic peptide in human fetuses with growth restriction. Ultrasound

Obstet Gynecol. 2007;

34. Iruretagoyena JI, Gonzalez-Tendero A, Garcia-Canadilla P, Amat-Roldan I, Torre I, Nadal A, et al. Cardiac dysfunction is associated with altered sarcomere ultrastructure in intrauterine growth restriction. In: American Journal of Obstetrics and Gynecology. 2014.

35. Leipälä JA, Boldt T, Turpeinen U, Vuolteenaho O, Fellman V. Cardiac hypertrophy and altered hemodynamic adaptation in growth-restricted preterm infants. Pediatr Res. 2003;

36. Lang BF, Gray MW, Burger G. Mitochondrial genome evolution and the origin of eukaryotes. Annu Rev Genet. 1999;

37. Margulis L. Symbiotic theory of the origin of eukaryotic organelles; criteria for proof. Symp Soc Exp Biol. 1975;

38. Côté HCF, Gerschenson M, Walker UA, Miro O, Garrabou G, Hammond E, et al. Quality assessment of human mitochondrial DNA quantification: MITONAUTS, an international multicentre survey. Mitochondrion. 2011;

39. Saraste M. Oxidative phosphorylation at the fin de siècle. Science (80-). 1999;

40. Barrientos A. In vivo and in organello assessment of OXPHOS activities. Methods. 2002;

41. Hosp F, Lassowskat I, Santoro V, De Vleesschauwer D, Fliegner D, Redestig H, et al. Lysine acetylation in mitochondria: From inventory to function. Mitochondrion. 2017;

42. Eisenberg-Bord M, Schuldiner M. Ground control to major TOM: mitochondria–nucleus communication. FEBS Journal. 2017.

43. Sack MN, Finkel T. Mitochondrial metabolism, sirtuins, and aging. Cold Spring Harb Perspect Biol. 2012;

44. Nogueiras R, Habegger KM, Chaudhary N, Finan B, Banks AS, Dietrich MO, et al. Sirtuin 1 and Sirtuin 3: Physiological Modulators of Metabolism. Physiol Rev. 2012;

45. Verdin E, Hirschey MD, Finley LWS, Haigis MC. Sirtuin regulation of mitochondria: Energy production, apoptosis, and signaling. Trends in Biochemical Sciences. 2010.

46. Lombard DB, Tishkoff DX, Bao J. Mitochondrial sirtuins in the regulation of mitochondrial activity and metabolic adaptation. Handb Exp Pharmacol. 2011;

47. Li XH, Liu SJ, Liu XY, Zhao HY, Yang MG, Xu DX, et al. Expression of SIRT3 in various glial cell types in the periventricular white matter in the neonatal rat brain after hypoxia. Tissue Cell. 2018;

48. Finley LWS, Haas W, Desquiret-Dumas V, Wallace DC, Procaccio V, Gygi SP, et al. Succinate dehydrogenase is a direct target of sirtuin 3 deacetylase activity. PLoS One. 2011;

49. Houtkooper RH, Pirinen E, Auwerx J. Sirtuins as regulators of metabolism and healthspan. Nature Reviews Molecular Cell Biology. 2012.

50. Lin L, Chen K, Khalek WA, Ward JL, Yang H, Chabi B, et al. Regulation of skeletal muscle oxidative capacity and muscle mass by SIRT3. PLoS One. 2014;

51. Ahn B-H, Kim H-S, Song S, Lee IH, Liu J, Vassilopoulos A, et al. A role for the mitochondrial deacetylase Sirt3 in regulating energy homeostasis. Proc Natl Acad Sci. 2008;

52. Wang Q, Li L, Li CY, Pei Z, Zhou M, Li N. SIRT3 protects cells from hypoxia via PGC-1α- and MnSOD-dependent pathways. Neuroscience. 2015;

53. Sack MN. Emerging characterization of the role of SIRT3-mediated mitochondrial protein deacetylation in the heart. AJP Hear Circ Physiol. 2011;

54. Ruiz MD, Cañete MD, Gómez-Chaparro JL, Abril N, Cañete R, López-Barea J. Alterations of protein expression in serum of infants with intrauterine growth restriction and different gestational ages. J Proteomics. 2015;

55. Wölter M, Röwer C, Koy C, Reimer T, Rath W, Pecks U, et al. A proteome signature for intrauterine growth restriction derived from multifactorial analysis of mass spectrometry-based cord blood serum profiling. Electrophoresis. 2012;

56. Wölter M, Röwer C, Koy C, Rath W, Pecks U, Glocker MO. Proteoform profiling of peripheral blood serum proteins from pregnant women provides a molecular IUGR signature. J Proteomics. 2016;

57. Miao Z, Chen M, Wu H, Ding H, Shi Z. Comparative proteomic profile of the human placenta in normal and fetal growth restriction subjects. Cell Physiol Biochem. 2014;

58. Barker D. The fetal and infant origins of adult disease. BMJ Br Med J. 1990;

59. Sitras V, Paulssen R, Leirvik J, Vårtun A, Acharya G. Placental gene expression profile in intrauterine growth restriction due to placental insufficiency. Reprod Sci. 2009;

60. Madeleneau D, Buffat C, Mondon F, Grimault H, Rigourd V, Tsatsaris V, et al. Transcriptomic analysis of human placenta in intrauterine growth restriction. Pediatr Res. 2015;

61. Gurugubelli Krishna R, Vishnu Bhat B. Molecular mechanisms of intrauterine growth restriction. J Matern Neonatal Med. 2017;

62. Hung TH, Chen SF, Lo LM, Li MJ, Yeh YL, Hsieh TT ang. Increased autophagy in placentas of intrauterine growth-restricted pregnancies. PLoS One. 2012;

63. Alejandre Alcázar MA, Morty RE, Lendzian L, Vohlen C, Oestreicher I, Plank C, et al. Inhibition of tgf-β signaling and decreased apoptosis in iugr-associated lung disease in rats. PLoS One. 2011;

64. Bahr B, Galan HL, Arroyo JA. Decreased expression of phosphorylated placental heat shock protein 27 in human and ovine intrauterine growth restriction (IUGR). Placenta. 2014;

65. Tyrrell DJ, Bharadwaj MS, Jorgensen MJ, Register TC, Molina AJA. Blood cell respirometry is associated with skeletal and cardiac muscle bioenergetics: Implications for a minimally invasive biomarker of mitochondrial health. Redox Biol. 2016;

66. Kramer PA, Ravi S, Chacko B, Johnson MS, Darley-Usmar VM. A review of the mitochondrial and glycolytic metabolism in human platelets and leukocytes: Implications for their use as bioenergetic biomarkers. Redox Biology. 2014.

67. Catalan-Garcia M, Garrabou G, Moren C, Guitart-Mampel M, Hernando A, Diaz-Ramos A, et al. Mitochondrial DNA disturbances and deregulated expression of oxidative phosphorylation and mitochondrial fusion proteins in sporadic inclusion body myositis. Clin Sci. 2016;

68. Novielli C, Mandò C, Tabano S, Anelli GM, Fontana L, Antonazzo P, et al. Mitochondrial DNA content and methylation in fetal cord blood of pregnancies with placental insufficiency. Placenta. 2017;

69. Perez-Cruz M, Crispi F, Fernández MT, Parra JA, Valls A, Gomez Roig MD, et al. Cord Blood Biomarkers of Cardiac Dysfunction and Damage in Term Growth-Restricted Fetuses Classified by Severity Criteria. Fetal Diagnosis and Therapy. 2017;

70. Poudel R, McMillen IC, Dunn SL, Zhang S, Morrison JL. Impact of chronic hypoxemia on blood flow to the brain, heart, and adrenal gland in the late-gestation IUGR sheep fetus. Am J Physiol - Regul Integr Comp Physiol. 2015;

71. Wang KC, Botting KJ, Padhee M, Zhang S, Mcmillen IC, Suter CM, et al. Early origins of heart disease: Low birth weight and the role of the insulin-like growth factor system in cardiac hypertrophy. Clin Exp Pharmacol Physiol. 2012;

72. Muhlhausler BS, Duffield JA, Ozanne SE, Pilgrim C, Turner N, Morrison JL, et al. The transition from fetal growth restriction to accelerated postnatal growth: a potential role for insulin signalling in skeletal muscle. J Physiol. 2009;

73. Meyer KM, Koch JM, Ramadoss J, Kling PJ, Magness RR. Ovine surgical model of uterine space restriction: interactive effects of uterine anomalies and multifetal gestations on fetal and placental growth. Biol Reprod. 2010;

74. Ogata ES, Bussey ME, Finley S. Altered gas exchange, limited glucose and branched chain amino acids, and hypoinsulinism retard fetal growth in the rat. Metabolism. 1986;

75. Lane RH, Flozak AS, Ogata ES, Bell GI, Simmons RA. Altered hepatic gene expression of enzymes involved in energy metabolism in the growth-retarded fetal rat. Pediatr Res. 1996;

76. Al-Hasan YM, Evans LC, Pinkas GA, Dabkowski ER, Stanley WC, Thompson LP. Chronic hypoxia impairs cytochrome oxidase activity via oxidative stress in selected fetal guinea pig organs. Reprod Sci. 2013;

77. Al-Hasan YM, Pinkas GA, Thompson LP. Prenatal hypoxia reduces mitochondrial protein levels and cytochrome c oxidase activity in offspring guinea pig hearts. Reprod Sci. 2014;

78. Thompson JA, Gros R, Richardson BS, Piorkowska K, Regnault TRH. Central stiffening in adulthood linked to aberrant aortic remodeling under suboptimal intrauterine conditions. Am J Physiol Regul Integr Comp Physiol. 2011;

79. Bibeau K, Sicotte B, Béland M, Bhat M, Gaboury L, Couture R, et al. Placental underperfusion in a rat model of intrauterine growth restriction induced by a reduced plasma volume expansion. PLoS One. 2016;

80. Keenaghan M, Sun L, Wang A, Hyodo E, Homma S, Ten VS. Intrauterine growth restriction impairs right ventricular response to hypoxia in adult male rats. Pediatr Res. 2016;

81. Selak MA, Storey BT, Peterside I, Simmons RA. Impaired oxidative phosphorylation in skeletal muscle of intrauterine growth-retarded rats. Am J Physiol - Endocrinol Metab. 2003;

82. Zhang H, Li Y, Hou X, Zhang L, Wang T. Medium-chain TAG improve energy metabolism and mitochondrial biogenesis in the liver of intra-uterine growth-retarded and normal-birth-weight weanling piglets. Br J Nutr. 2016;

83. Zhang H, Li Y, Su W, Ying Z, Zhou L, Zhang L, et al. Resveratrol attenuates mitochondrial dysfunction in the liver of intrauterine growth retarded suckling piglets by improving mitochondrial biogenesis and redox status. Mol Nutr Food Res. 2017;

84. Huang Q, Xu W, Bai KW, He JT, Ahmad H, Zhou L, et al. Protective effects of leucine on redox status and mitochondrial-related gene abundance in the jejunum of intrauterine growth-retarded piglets during early weaning period. Arch Anim Nutr. 2017;

85. Eixarch E, Figueras F, Hernández-Andrade E, Crispi F, Nadal A, Torre I, et al. An experimental model of fetal growth restriction based on selective ligature of uteroplacental vessels in the pregnant rabbit. Fetal Diagn Ther. 2009;

86. Eixarch E, Hernandez-Andrade E, Crispi F, Illa M, Torre I, Figueras F, et al. Impact on fetal mortality and cardiovascular Doppler of selective ligature of uteroplacental vessels compared with undernutrition in a rabbit model of intrauterine growth restriction. Placenta. 2011;

87. Gonzalez-Tendero A, Zhang C, Balicevic V, Cárdenes R, Loncaric S, Butakoff C, et al. Whole heart detailed and quantitative anatomy, myofibre structure and vasculature from X-ray phase-contrast synchrotron radiation-based micro computed tomography. Eur Hear J - Cardiovasc Imaging. 2017;

88. Ortigosa N, Crispi F, Bailón R, Rodriguez-Lopez M, Gratacós E, Savari S, et al. Heart morphology differences induced by intrauterine growth restriction and premature birth measured on the ECG in pre-adolescents. In: Computing in Cardiology. 2015.

89. Gonzalez-Tendero A, Torre I, Garcia-Canadilla P, Crispi F, García-García F, Dopazo J, et al. Intrauterine growth restriction is associated with cardiac ultrastructural and gene expression changes related to the energetic metabolism in a rabbit model. Am J Physiol Circ Physiol. 2013;

90. Beyramzadeh M, Dikmen ZG, Erturk NK, Tuncer ZS, Akbiyik F. Placental respiratory chain complex activities in high risk pregnancies. J Matern Neonatal Med. 2017;

91. Mando C, De Palma C, Stampalija T, Anelli GM, Figus M, Novielli C, et al. Placental mitochondrial content and function in intrauterine growth restriction and preeclampsia. AJP Endocrinol Metab. 2014;

92. D??az M, Aragon??s G, S??nchez-Infantes D, Bassols J, P??rez-Cruz M, De Zegher F, et al. Mitochondrial DNA in placenta: Associations with fetal growth and superoxide dismutase activity. Horm Res Paediatr. 2014;

93. Lefebvre T, Roche O, Seegers V, Cherif M, Khiati S, Gueguen N, et al. Study of mitochondrial function in placental insufficiency. Placenta. 2018;

94. El-Hattab AW, Scaglia F. Mitochondrial Cardiomyopathies. Front Cardiovasc Med. 2016;

95. Yu E, Mercer J, Bennett M. Mitochondria in vascular disease. Cardiovascular Research. 2012.

96. Bornstein B, Huertas R, Ochoa P, Campos Y, Guillen F, Garesse R, et al. Mitochondrial gene expression and respiratory enzyme activities in cardiac diseases. Biochim Biophys Acta. 1998;

97. Buchwald A, Till H, Unterberg C, Oberschmidt R, Figulla HR, Wiegand V. Alterations of the mitochondrial respiratory chain in human dilated cardiomyopathy. Eur Heart J. 1990;

98. Meyers DE, Basha HI, Koenig MK. Mitochondrial cardiomyopathy: pathophysiology, diagnosis, and management. Tex Heart Inst J. 2013;

99. Holmgren D, Wåhlander H, Eriksson BO, Oldfors A, Holme E, Tulinius M. Cardiomyopathy in children with mitochondrial disease: Clinical course and cardiological findings. Eur Heart J. 2003;

100. Yaplito-Lee J, Weintraub R, Jamsen K, Chow CW, Thorburn DR, Boneh a. Cardiac manifestations in oxidative phosphorylation disorders of childhood. J Pediatr. 2007;

101. Jauniaux E, Poston L, Burton GJ. Placental-related diseases of pregnancy: Involvement of oxidative stress and implications in human evolution. Human Reproduction Update. 2006.

102. Biri A, Bozkurt N, Turp A, Kavutcu M, Himmetoglu Ö, Durak I. Role of oxidative stress in intrauterine growth restriction. Gynecol Obstet Invest. 2007;

103. Bertero E, Maack C. Metabolic remodelling in heart failure. Nature Reviews Cardiology. 2018.

104. Dickinson H, Moss TJ, Gatford KL, Moritz KM, Akison L, Fullston T, et al. A review of fundamental principles for animal models of DOHaD research: An Australian perspective. Journal of Developmental Origins of Health and Disease. 2016.

105. Drummond GB, Paterson DJ, McGrath JC. ARRIVE: New guidelines for reporting animal research. Experimental Physiology. 2010;

106. Kilkenny C, Browne W, Cuthill IC, Emerson M, Altman DG. Editorial: Animal research: Reporting in vivo experiments-The ARRIVE Guidelines. Journal of Cerebral Blood Flow and Metabolism. 2011;

107. Savchev S, Figueras F, Gratacos E. Survey on the current trends in managing intrauterine growth restriction. Fetal Diagn Ther. 2014;

108. Statement P. The Apgar Score. Pediatrics. 2015;

109. Belenky A, Smith A, Zhang B, Lin S, Despres N, Wu AHB, et al. The effect of class-specific protease inhibitors on the stabilization of B-type natriuretic peptide in human plasma. Clin Chim Acta. 2004;

110. Prilutskiĭ AS, Khodakovskiĭ A V, Maĭlian EA. [A method of separating mononuclears on a density gradient]. Lab Delo. 1990;

111. Medja F, Allouche S, Frachon P, Jardel C, Malgat M, de Camaret BM, et al. Development and implementation of standardized respiratory chain spectrophotometric assays for clinical diagnosis. Mitochondrion. 2009;

112. Alvarez-Mora MI, Rodriguez-Revenga L, Madrigal I, Guitart-Mampel M, Garrabou G, Milà M. Impaired Mitochondrial Function and Dynamics in the Pathogenesis of FXTAS. Mol Neurobiol. 2016;

113. Casademont J, Garrabou G, Miró O, López S, Pons A, Bernardo M, et al. Neuroleptic treatment effect on mitochondrial electron transport chain: peripheral blood mononuclear cells analysis in psychotic patients. J Clin Psychopharmacol. 2007;

114. Yubero D, Montero R, Martín MA, Montoya J, Ribes A, Grazina M, et al. Secondary coenzyme Q10deficiencies in oxidative phosphorylation (OXPHOS) and non-OXPHOS disorders. Mitochondrion. 2016;

115. Morén C, González-Casacuberta I, Álvarez-Fernández C, Bañó M, Catalán-Garcia M, Guitart-Mampel M, et al. HIV-1 promonocytic and lymphoid cell lines: an in vitro model of in vivo mitochondrial and apoptotic lesion. J Cell Mol Med. 2017;

116. Neitzke U, Harder T, Plagemann A. Intrauterine Growth Restriction and Developmental Programming of the Metabolic Syndrome: A Critical Appraisal. Microcirculation. 2011.

117. Miller SL, Huppi PS, Mallard C. The consequences of fetal growth restriction on brain structure and neurodevelopmental outcome. J Physiol. 2016;

118. Barker DJ. Fetal origins of coronary heart disease. BMJ. 1995;

119. Hernandez S, Moren C, Catalán-García M, Lopez M, Guitart-Mampel M, Coll O, et al. Mitochondrial toxicity and caspase activation in HIV pregnant women. J Cell Mol Med. 2017;

120. Mayeur S, Lancel S, Theys N, Lukaszewski MA, Duban-Deweer S, Bastide B, et al. Maternal calorie restriction modulates placental mitochondrial biogenesis and bioenergetic efficiency: Putative involvement in fetoplacental growth defects in rats. World Review of Nutrition and Dietetics. 2014.

121. Torre I, González-Tendero A, García-Cañadilla P, Crispi F, García-GarciÁa F, Bijnens B, et al. Permanent cardiac sarcomere changes in a rabbit model of intrauterine growth restriction. PLoS One. 2014;

122. Batalle D, Muñoz-Moreno E, Arbat-Plana A, Illa M, Figueras F, Eixarch E, et al. Long-term reorganization of structural brain networks in a rabbit model of intrauterine growth restriction. Neuroimage. 2014;

123. Illa M, Eixarch E, Muñoz-Moreno E, Batalle D, Leal-Campanario R, Gruart A, et al. Neurodevelopmental Effects of Undernutrition and Placental Underperfusion in Fetal Growth Restriction Rabbit Models. Fetal Diagn Ther. 2017;

124. Illa M, Eixarch E, Batalle D, Arbat-Plana A, Muñoz-Moreno E, Figueras F, et al. Long-Term Functional Outcomes and Correlation with Regional Brain Connectivity by MRI Diffusion Tractography Metrics in a Near-Term Rabbit

Model of Intrauterine Growth Restriction. PLoS One. 2013;

125. Eixarch E, Batalle D, Illa M, Muñoz-Moreno E, Arbat-Plana A, Amat-Roldan I, et al. Neonatal neurobehavior and diffusion MRI changes in brain reorganization due to intrauterine growth restriction in a rabbit model. PLoS One. 2012;

126. Schipke J, Gonzalez-Tendero A, Cornejo L, Willführ A, Bijnens B, Crispi F, et al. Experimentally induced intrauterine growth restriction in rabbits leads to differential remodelling of left versus right ventricular myocardial microstructure. Histochem Cell Biol. 2017;

127. Holland O, Dekker Nitert M, Gallo LA, Vejzovic M, Fisher JJ, Perkins A V. Review: Placental mitochondrial function and structure in gestational disorders. Placenta. 2017.

128. Myatt L. Placental adaptive responses and fetal programming. In: Journal of Physiology. 2006.

129. Illsley NP, Caniggia I, Zamudio S. Placental metabolic reprogramming: Do changes in the mix of energy-generating substrates modulate fetal growth? Int J Dev Biol. 2010;

130. Schon EA, Dimauro S, Hirano M. Human mitochondrial DNA: Roles of inherited and somatic mutations. Nature Reviews Genetics. 2012.

131. Poidatz D, Dos Santos E, Duval F, Moindjie H, Serazin V, Vialard F, et al. Involvement of estrogen-related receptor-γ and mitochondrial content in intrauterine growth restriction and preeclampsia. Fertil Steril. 2015;

132. Lattuada D, Colleoni F, Martinelli A, Garretto A, Magni R, Radaelli T, et al. Higher Mitochondrial DNA Content in Human IUGR Placenta. Placenta. 2008;

133. Lee HC, Yin PH, Lu CY, Chi CW, Wei YH. Increase of mitochondria and mitochondrial DNA in response to oxidative stress in human cells. Biochem J. 2000;

134. Merz TM, Pichler Hefti J, Hefti U, Huber A, Jakob SM, Takala J, et al. Changes in mitochondrial enzymatic activities of monocytes during prolonged hypobaric hypoxia and influence of antioxidants: A randomized controlled study. Redox Rep. 2015;

135. Dodd MS, Atherton HJ, Carr CA, Stuckey DJ, West JA, Griffin JL, et al. Impaired in vivo mitochondrial krebs cycle activity after myocardial infarction assessed using hyperpolarized magnetic resonance spectroscopy. Circ Cardiovasc Imaging. 2014;

136. Sandoval-Acuña C, Ferreira J, Speisky H. Polyphenols and mitochondria: An update on their increasingly emerging ROS-scavenging independent actions. Archives of Biochemistry and Biophysics. 2014.

137. Cimen H, Han MJ, Yang Y, Tong Q, Koc H, Koc EC. Regulation of succinate dehydrogenase activity by SIRT3 in mammalian mitochondria. Biochemistry. 2010;

138. Giralt A, Villarroya F. SIRT3, a pivotal actor in mitochondrial functions: metabolism, cell death and aging. Biochem J. 2012;

139. Sun W, Liu C, Chen Q, Liu N, Yan Y, Liu B. SIRT3: A new regulator of

cardiovascular diseases. Oxidative Medicine and Cellular Longevity. 2018.

140. Koentges C, Bode C, Bugger H. SIRT3 in Cardiac Physiology and Disease. Front Cardiovasc Med. 2016;

141. Sack MN. The role of SIRT3 in mitochondrial homeostasis and cardiac adaptation to hypertrophy and aging. Journal of Molecular and Cellular Cardiology. 2012.

142. Lombard DB, Zwaans BMM. SIRT3: As simple as it seems? Gerontology. 2013.

143. Watson AL, Skepper JN, Jauniaux E, Burton GJ. Susceptibility of human placental syncytiotrophoblastic mitochondria to oxygen-mediated damage in relation to gestational age. J Clin Endocrinol Metab. 1998;

144. Ritchie HE, Oakes DJ, Kennedy D, Polson JW. Early Gestational Hypoxia and Adverse Developmental Outcomes. Birth Defects Research. 2017.

145. Yoshino J, Baur JA, Imai S ichiro. NAD+Intermediates: The Biology and Therapeutic Potential of NMN and NR. Cell Metabolism. 2018.

146. Zhang R, Shen Y, Zhou L, Sangwung P, Fujioka H, Zhang L, et al. Short-term administration of Nicotinamide Mononucleotide preserves cardiac mitochondrial homeostasis and prevents heart failure. J Mol Cell Cardiol. 2017;

147. Tanno M, Kuno A, Horio Y, Miura T. Emerging beneficial roles of sirtuins in heart failure. Basic Research in Cardiology. 2012.

148. Sehgal A, Skilton MR, Crispi F. Human fetal growth restriction: A cardiovascular journey through to adolescence. Journal of Developmental Origins of Health and Disease. 2016.

9. SUPPLEMENTARY DATA

Table S1. Raw data of absolute and relative enzymatic activities of complex I, II, IV, I+III and II+III of the mitochondrial respiratory chain, MRC subunits expression (SDHA, SDHB and COX5A), citrate synthase (CS) activity, Tom20 expression, Complex I-stimulated oxygen consumption (GM Oxidation), CoQ9 and CoQ10 levels, cellular ATP levels, lipid peroxidation, SOD2 expression and Sirtuin 3/β-actin levels in the experimental groups.

HEART	*Control*	*IUGR*	*% of increased (+) or decreased (-)*	*P value*
Complex I (nmol/minute·mg protein)	147.21±18.57	114.02±12.31	-22.55±8.36	NS
Complex I relative to CS activity (nmol/minute·mg protein)	0.33±0.04	0.28±0.03	-15.15±9.09	NS
Complex II (nmol/minute·mg protein)	272.68±11.45	240.08±8.63	-11.96±3.16	<0.05 [a]
Complex II relative to CS activity (nmol/minute·mg protein)	0.63±0.03	0.59±0.03	-6.35±4.76	NS
Complex IV (nmol/minute·mg protein)	576.95±23.93	487.06±30.71	-15.58±5.32	<0.05 [a]
Complex IV relative to CS activity (nmol/minute·mg protein)	1.34±0.08	1.17±0.07	-12.69±5.22	NS
Complex I+III (nmol/minute·mg protein)	111.62±4.99	100.71±4.99	-9.77±4.47	NS
Complex I+III relative to CS activity (nmol/minute·mg protein)	0.23±0.03	0.24±0.01	+4.35±4.35	NS
Complex II+III (nmol/minute·mg protein)	182.55±5.76	155.66±7.98	-14.73±4.37	<0.05 [a]
Complex II+III relative to CS activity (nmol/minute·mg protein)	0.43±0.02	0.37±0.01	-13.95±2.33	NS

SDHA/β-actin (AU)	2.60±0.19	2.85±0.27	+9.62±10.38	NS
SDHB/β-actin (AU)	1.02±0.11	1.37±0.13	+34.31±12.75	NS
COX5A/β-actin (AU)	2.50±0.61	2.29±0.64	-8.40±25.60	NS
Citrate Synthase (nmol/minute·mg protein)	436.96±21.72	419.33±20.56	-4.03±4.71	NS
Tom20/β-actin (AU)	4.09±0.18	6.60±1.30	+61.37±31.78	NS
GM Oxidation (pmol O_2/s·mg)	19.80±2.46	18.70±1.28	-5.56±6.46	NS
CoQ9 levels (µmol/L)	68.99±6.31	61.03±4.47	-11.54±6.48	NS
CoQ10 levels (µmol/L)	479.29±15.74	435.66±32.27	-9.10±6.73	NS
ATP levels (pmol ATP/mg protein)	0.57±0.03	0.54±0.01	-5.56±1.75	NS
Lipid peroxidation (µM MDA+HAE/mg protein)	14.02±0.89	8.55±0.61	-39.02±4.35	<0.001 [a]
SOD2/β-actin (AU)	6.05±1.02	4.41±0.76	-27.11±12.56	NS
SOD2 acetylation/β-actin (AU)	7.84±0.77	10.84±1.37	+38.27±17.47	NS
Ratio SOD2 acetylation/SOD2 expression (AU)	1.71±0.07	2.29±0.30	+33.92±17.54	NS
Sirtuin 3/β-actin (AU)	0.19±0.01	0.35±0.06	+84.21±31.58	<0.05 [a]
PLACENTA	***Control***	***IUGR***	***% of increased or decreased***	***P value***
Complex I (nmol/minute·mg protein)	10.28±1.37	8.33±0.52	-18.97±5.06	NS
Complex I relative to CS activity (nmol/minute·mg protein)	0.25±0.04	0.24±0.01	-4.00±4.00	NS
Complex II	17.94±0.99	14.85±0.62	-17.22±3.46	<0.005 [a]

(nmol/minute·mg protein)				
Complex II relative to CS activity (nmol/minute·mg protein)	0.41±0.02	0.42±0.02	+2.44±4.88	NS
Complex IV (nmol/minute·mg protein)	57.27±6.53	43.51±4.73	-24.03±8.26	NS
Complex IV relative to CS activity (nmol/minute·mg protein)	1.27±0.12	1.18±0.09	-7.09±7.09	NS
Complex I+III (nmol/minute·mg protein)	9.52±1.51	6.36±0.59	-33.19±6.20	NS
Complex I+III relative to CS activity (nmol/minute·mg protein)	0.21±0.02	0.18±0.02	-14.29±9.52	NS
Complex II+III (nmol/minute·mg protein)	28.44±2.24	20.01±1.26	-29.64±4.43	<0.001 [a]
Complex II+III relative to CS activity (nmol/minute·mg protein)	0.61±0.03	0.55±0.02	-9.84±3.28	NS
SDHA/β-actin (AU)	0.68±0.15	0.54±0.07	-20.59±10.29	NS
SDHB/β-actin (AU)	0.68±0.07	0.38±0.04	+44.12±5.88	<0.001 [a,] †
COX5A/β-actin (AU)	0.47±0.07	0.33±0.04	-29.79±8.51	NS
Citrate Synthase (nmol/minute·mg protein)	45.64±3.26	36.39±1.91	-20.27±4.18	NS
Tom20/β-actin (AU)	2.78±0.40	2.91±0.34	+4.68±12.23	NS
GM Oxidation (pmol O_2/s·mg)	1.95±0.47	1.45±0.37	-25.64±18.97	NS
CoQ9 levels (µmol/L)	33.19±0.00	34.63±1.44	+4.16±4.16	NS

CoQ10 levels (µmol/L)	55.99±6.14	54.89±8.61	-1.96±15.38	NS
ATP levels (pmol ATP/mg protein)	0.04±0.00	0.04±0.00	+5.71±8.57	NS
Lipid peroxidation (µM MDA+HAE/mg protein)	12.96±1.31	14.34±0.95	+10.65±7.33	NS
SOD2/β-actin (AU)	2.29±0.35	1.92±0.22	-16.16±9.61	NS
SOD2 acetylation/β-actin (AU)	5.21±0.60	5.64±0.48	+8.25±9.21	NS
Ratio SOD2 acetylation/SOD2 expression (AU)	3.03±0.46	3.94±0.53	+30.03±17.49	NS

Values are mean ± standard error of the mean. Case-control differences were sought by non-parametric statistical analysis and, in case of difference, significance was adjusted (^{a}) by maternal influence (†).

ATP: adenosine triphosphate; AU: arbitrary units; CoQ9 and 10: coenzyme Q9 and Q10; COX5A: cytochrome c oxidase subunit 5a; GM Oxidation: glutamate+malate oxidation; HAE: 4-hydroxyalkenal; IUGR: intrauterine growth restriction; MDA: malondialdehyde; NS: not significant; O_2: oxygen; SDHA: succinate dehydrogenase complex, subunit A; SDHB: succinate dehydrogenase complex, subunit B; SOD2: superoxid dismutase 2; Tom20: mitochondrial import receptor subunit TOM20.

Table S2. Associations between biometric data and experimental results in the IUGR and control offspring.

Parameter	With respect to	Correlation coefficient	P value	R^2
Birth weight (g)	Heart weight (g)	0.783	<0.001	0.610
	Left ventricle (g)	0.676	<0.001	0.446
	Right ventricle + septum (g)	0.735	<0.001	0.459
	Placental weight (g)	0.758	<0.001	0.557
	CI enzymatic activity[a] in heart	0.429	<0.05	0.157
	CII enzymatic activity[a] in heart	0.448	<0.05	0.117
	CII+III enzymatic activity[a] in heart	0.543	≤0.005	0.289
	Citrate synthase activity[a] in heart	0.517	<0.01	0.125
	Lipid peroxidation[b] in heart	0.591	<0.005	0.325
	Sirtuin 3/β-actin ratio (AU) in heart	-0.498	<0.05	0.153
	CI+III enzymatic activity[a] in placenta	0.380	<0.05	0.172
	CII+III enzymatic activity[a] in placenta	0.574	≤0.001	0.347
	Citrate synthase activity[a] in placenta	0.371	<0.05	0.217
	SDHB/β-actin ratio (AU) in placenta	0.570	≤0.001	0.304
Heart weight (g)	Left ventricle (g)	0.511	<0.005	0.322
	Right ventricle + Septum (g)	0.843	<0.001	0.658
	Heart/body weight x 100 (g)	0.469	≤0.005	0.106
	Placental weight (g)	0.575	<0.001	0.346
	Lipid peroxidation[b] in heart	0.710	<0.001	0.498
	Sirtuin 3/β-actin ratio (AU) in heart	-0.505	<0.05	0.266
	CII enzymatic activity[a] in placenta	0.450	<0.05	0.146
	CI+III enzymatic activity[a] in placenta	0.594	≤0.001	0.277
	CII+III enzymatic activity[a] in placenta	0.515	<0.005	0.234
	Citrate synthase activity[a] in placenta	0.402	<0.05	0.183
	SDHB/β-actin ratio (AU) in placenta	0.500	<0.01	0.349
Left ventricle (g)	Placental weight (g)	0.563	≤0.001	0.336
	CII enzymatic activity[a] in heart	0.480	<0.05	0.130
	CII+III enzymatic activity[a] in heart	0.512	<0.01	0.209
	Citrate synthase activity[a] in heart	0.594	<0.005	0.338
	CII enzymatic activity[a] in placenta	0.461	<0.05	0.230
	CIV enzymatic activity[a] in placenta	0.476	<0.05	0.412
	CII+III enzymatic activity[a] in placenta	0.507	<0.01	0.270
	Citrate synthase activity[a] in placenta	0.606	≤0.001	0.332
	SDHB/β-actin ratio (AU) in placenta	0.544	<0.005	0.251
Right ventricle + Septum (g)	Heart/body weight x 100 (g)	0.467	<0.05	0.048
	Sirtuin 3/β-actin ratio (AU) in heart	-0.593	<0.005	0.293
	CI+III enzymatic activity[a] in placenta	0.459	<0.05	0.228
	CII+III enzymatic activity[a] in placenta	0.442	<0.05	0.181
Heart/body weight x	CI+III enzymatic activity[a] in placenta	0.424	<0.05	0.018

100				
Placental weight (g)	Placenta/body weight x 100 (g)	0.436	<0.005	0.301
	CIV enzymatic activity[a] in placenta	0.436	<0.05	0.245
	CII+III enzymatic activity[a] in placenta	0.548	≤0.001	0.267
	SDHB/β-actin ratio (AU) in placenta	0.514	<0.005	0.364
Placenta/body weight x 100	Sirtuin 3/β-actin ratio (AU) in heart	0.732	<0.001	0.599
Lipid peroxidation in heart	CII enzymatic activity[a] in heart	0.436	<0.05	0.136
	CII+III enzymatic activity[a] in heart	0.432	<0.05	0.173
SDHB/β-actin ratio (AU) **in heart**	Total ATP levels[c] in heart	0.537	<0.01	0.226
SOD2/β-actin ratio (AU) **in heart**	Citrate synthase activity[a] in heart	-0.418	<0.05	0.112
SDHB/β-actin ratio (AU) **in placenta**	CII enzymatic activity[a] in placenta	0.497	<0.005	0.145
	CIV enzymatic activity[a] in placenta	0.617	<0.001	0.241
	CII+III enzymatic activity[a] in placenta	0.521	<0.005	0.192
	Citrate synthase activity[a] in placenta	0.613	<0.001	0.261
	SOD2/β-actin ratio (AU) in placenta	0.402	<0.05	0.314
COX5A/β-actin ratio (AU) **in placenta**	CIV enzymatic activity[a] in placenta	0.409	<0.05	0.149
	Citrate synthase activity[a] in placenta	0.406	<0.05	0.179
Tom20/β-actin ratio (AU) **in placenta**	CIV enzymatic activity[a] in placenta	0.429	<0.05	0.164
SOD2/β-actin ratio (AU) **in placenta**	CIV enzymatic activity[a] in placenta	0.513	<0.005	0.249
	CII+III enzymatic activity[a] in placenta	0.482	<0.01	0.216

Spearman correlations were used to seek for statistical associations. [a]: nmol/minute·mg protein; [b]: µM MDA+HAE/mg protein; [c]: pmol ATP/mg protein.

ATP: adenosine triphosphate; AU: arbitrary units; CI: complex I; CII: complex II; CI+III: complex I+III; CII+III: complex II+III; CIV: complex IV; COX5A: cytochrome c oxidase subunit 5a; g: grams; HAE: 4-hydroxyalkenal; IUGR: intrauterine growth restriction; MDA: malondialdehyde; R^2: coefficient of determination; SDHA: succinate dehydrogenase complex, subunit A; SDHB: succinate dehydrogenase complex, subunit B; SOD2: superoxid dismutase 2; Tom20: mitochondrial import receptor subunit TOM20.

Table S3. Experimental data in human placental tissue of study groups.

Mitochondrial parameters in PLACENTA	*Control*	*IUGR*	*% of increased (+) or decreased (-)*	*P value*
Complex I (nmol/minute·mg protein)	9.65±0.83	6.47±1.00	-32.95±10.36	<0.05
Complex I relative to CS activity (nmol/minute·mg protein)	0.21±0.03	0.20±0.04	-4.75±19.05	NS
Complex II (nmol/minute·mg protein)	30.06±1.06	31.22±1.56	+3.86±3.16	NS
Complex II relative to CS activity (nmol/minute·mg protein)	0.75±0.03	0.96±0.13	+28.00±17.33	NS
Complex IV (nmol/minute·mg protein)	19.52±1.04	23.93±3.07	+22.59±15.73	NS
Complex IV relative to CS activity (nmol/minute·mg protein)	0.50±0.03	0.69±0.09	+38.00±18.00	<0.05
Complex I+III (nmol/minute·mg protein)	7.25±0.88	7.99±1.62	+10.21±22.34	NS
Complex I+III relative to CS activity (nmol/minute·mg protein)	0.18±0.02	0.20±0.03	+11.11±16.67	NS
Complex II+III (nmol/minute·mg protein)	14.50±0.77	13.79±2.14	-4.90±14.76	NS
Complex II+III relative to CS activity (nmol/minute·mg protein)	0.35±0.01	0.41±0.04	+17.14±11.43	NS
Citrate Synthase (nmol/minute·mg protein)	41.58±1.74	37.75±5.88	-9.21±14.14	NS
PM oxidation (pmol O_2/s·mg)	9.15±1.59	4.93±0.53	-46.12±5.79	<0.05
GM oxidation (pmol O_2/s·mg)	8.75±1.71	4.40±1.71	-49.71±19.54	<0.05
ATP levels (pmol ATP/mg protein)	0.04±0.00	0.04±0.01	0.00±15.00	NS
Lipid peroxidation (μM MDA+HAE/mg protein)	15.67±1.32	13.82±1.34	-11.81±8.55	NS
Sirtuin 3/β-actin (AU)	0.45±0.10	0.98±0.23	+117.78±51.11	<0.05

Values are presented as mean ± standard error of the mean and as a percentage of increase or decrease ± standard error of the mean. Case-control differences were sought by non-parametric statistical analysis.

ATP: adenosine triphosphate; AU: arbitrary units; CS: citrate synthase; GM oxidation: glutamate+malate oxidation; HAE: 4-hydroxyalkenal; IUGR: intrauterine growth restriction; MDA: malondialdehyde; NS: not significant; O_2: oxygen; PM oxidation: pyruvate+malate oxidation;

Table S4. Experimental data in maternal peripheral blood mononuclear cells of study groups.

Mitochondrial parameters in Maternal PBMC	*Control*	*IUGR*	*% of increased (+) or decreased (-)*	*P value*
Complex II (nmol/minute·mg protein)	56.18±7.63	63.60±13.13	+13.21±23.37	NS
Complex II relative to CS activity (nmol/minute·mg protein)	0.38±0.03	0.39±0.02	+2.63±5.26	NS
Complex IV (nmol/minute·mg protein)	35.73±3.55	37.82±4.56	+5.85±12.76	NS
Complex IV relative to CS activity (nmol/minute·mg protein)	0.27±0.03	0.28±0.04	+3.70±14.81	NS
Citrate Synthase (nmol/minute·mg protein)	132.38±11.53	137.00±17.58	+3.49±13.28	NS
Cell oxidation (pmol O_2/s·mg)	5.50±0.63	5.90±1.53	+7.27±27.82	NS
PM oxidation (pmol O_2/s·mg)	6.34±1.11	4.34±0.72	-31.55±11.36	NS
GM oxidation (pmol O_2/s·mg)	4.88±0.68	3.66±0.51	-25.00±10.45	NS
ATP levels (pmol ATP/mg protein)	3.17±0.37	2.64±0.46	-16.72±14.51	NS
Lipid peroxidation (μM MDA+HAE/mg protein)	1.12±0.12	1.22±0.12	+8.93±16.96	NS

Values are presented as mean ± standard error of the mean and as a percentage of increase or decrease ± standard error of the mean. Case-control differences were sought by non-parametric statistical analysis.

ATP: adenosine triphosphate; Cell oxidation: cellular endogen oxidation (without substrates); CS: citrate synthase; GM oxidation: glutamate+malate oxidation; HAE: 4-hydroxyalkenal; IUGR: intrauterine growth restriction; MDA: malondialdehyde; NS: not significant; O_2: oxygen; PBMC: peripheral blood mononuclear cells; PM oxidation: pyruvate+malate oxidation.

Table S5. Experimental data in neonatal cord blood mononuclear cells of study groups.

Mitochondrial parameters in Neonatal CBMC	*Control*	*IUGR*	*% of increased (*) or decreased (-)*	*P value*
Complex II (nmol/minute·mg protein)	37.26±5.00	40.01±10.45	+7.38±28.05	NS
Complex II relative to CS activity (nmol/minute·mg protein)	0.43±0.04	0.73±0.17	+69.77±39.53	NS
Complex IV (nmol/minute·mg protein)	21.09±1.89	17.14±3.17	-18.73±15.03	NS
Complex IV relative to CS activity (nmol/minute·mg protein)	0.26±0.03	0.36±0.01	+38.46±37.31	NS
Citrate Synthase (nmol/minute·mg protein)	86.06±6.79	52.33±10.85	-39.19±12.61	<0.05
Cell oxidation (pmol O_2/s·mg)	4.58±0.74	2.49±0.65	-45.63±14.19	NS
PM oxidation (pmol O_2/s·mg)	4.83±1.22	2.42±0.55	-49.90±11.39	NS
GM oxidation (pmol O_2/s·mg)	3.93±1.02	1.74±0.45	-55.73±11.45	NS
ATP levels (pmol ATP/mg protein)	1.15±0.17	1.85±0.53	+60.87±46.09	NS
Lipid peroxidation (µM MDA+HAE/mg protein)	1.39±0.12	1.53±0.15	+10.07±10.79	NS
Mitochondrial DNA depletion (mt12SrRNA/nRNAseP ratio)	101.09±10.25	95.41±8.15	-5.62±8.06	NS

Values are presented as mean ± standard error of the mean and as a percentage of increase or decrease ± standard error of the mean. Case-control differences were sought by non-parametric statistical analysis.

ATP: adenosine triphosphate; CBMC: cord blood mononuclear cells; Cell oxidation: cellular endogen oxidation (without substrates); CS: citrate synthase; GM oxidation: glutamate+malate oxidation; HAE: 4-hydroxyalkenal; IUGR: intrauterine growth restriction; MDA: malondialdehyde; NS: not significant; O_2: oxygen; PM oxidation: pyruvate+malate oxidation.

Table S6 Significant associations between clinical data and experimental results in the cohort of IUGR and control pregnancies.

Parameter	With respect to	Correlation coefficient	P value	R^2
Birth weight (g)	Placental weight (g)	0.655	0.004	0.603
	BNP levels (pg/ml)	-0.600	0.000	0.526
	Oxygen consumption (PM oxidation)[a] in placenta	0.480	0.018	0.197
	Oxygen consumption (GM oxidation)[a] in placenta	0.505	0.008	0.279
	CI enzymatic activity[b] in placenta	0.412	0.026	0.195
	Sirtuin 3/β-actin ratio (AU) in placenta	-0.470	0.008	0.224
Placental weight (g)	Cord blood BNP levels (pg/ml)	-0.736	0.006	0.292
Cord blood BNP levels (pg/ml)	CI enzymatic activity[b] in placenta	-0.464	0.026	0.159
Oxygen consumption (GM oxidation)[a] in maternal PBMC	Oxygen consumption (GM oxidation)[a] in neonatal CBMC	0.544	0.007	0.115
CS activity in neonatal CBMC[b]	Oxygen consumption (Cell oxidation)[a] in neonatal CBMC	0.439	0.036	0.189
	Oxygen consumption (PM oxidation)[a] in placenta	0.507	0.014	0.159
	Oxygen consumption (GM oxidation)[a] in placenta	0.659	0.001	0.213
Sirtuin 3/β-actin ratio (AU) in placenta	CI enzymatic activity[b] in placenta	-0.416	0.034	0.095

Spearman correlations were used to seek for statistical associations. [a]: pmol O2/s·mg protein; [b]: nmol/minute·mg protein.

AU: arbitrary units; BNP: brain natriuretic peptide; CBMC: cord blood mononuclear cells; CI: MRC complex I; g: grams; GM oxidation: glutamate+malate oxidation; MRC: mitochondrial respiratory chain; PBMC: peripheral blood mononuclear cells; PM oxidation: pyruvate+malate oxidation; R^2: coefficient of determination.

10. ANNEX

Original articles related to this thesis

- **Study 1**

  Mariona Guitart-Mampel, Anna Gonzalez-Tendero, Sergio Niñerola, Constanza Morén, Marc Catalán-Garcia, Ingrid González-Casacuberta, Diana L. Juárez-Flores, Olatz Ugarteburu, Leslie Matalonga, Maria Victoria Cascajo, Frederic Tort, Ana Cortés, Ester Tobias, Jose C. Milisenda, Josep M. Grau, Fàtima Crispi, Eduard Gratacós, Glòria Garrabou, Francesc Cardellach. Cardiac and placental mitochondrial characterization in a rabbit model of intrauterine growth restriction. Biochim Biophys Acta. 2018 May; 1862(5): 1157-1167.

- **Study 2**

  Mariona Guitart-Mampel, Diana L. Juarez-Flores, Lina Youssef, Constanza Moren, Laura Garcia-Otero, Vicente Roca-Agujetas, Marc Catalan-Garcia, Ingrid Gonzalez-Casacuberta, Ester Tobias, José C. Milisenda, Josep M. Grau, Fàtima Crispi, Eduard Gratacos, Francesc Cardellach, Glòria Garrabou. Mitochondrial implication in human pregnancies with intrauterine growth restriction and associated foetal cardiovascular remodelling. Under review to Clinical Science.

Other original articles

- Pozdniakova S, **Guitart-Mampel M**, Garrabou G, Di Benedetto G, Ladilov Y, Regitz-Zagrosek V. 17β-estradiol reduces mitochondrial cAMP content and cytochrome oxidase activity in a phosphodiesterase 2-dependent manner. Br J Pharmacol. 2018 Jul 26.
- Juárez-Flores DL, González-Casacuberta I, Ezquerra M, Bañó M, Carmona-Pontaque F, Catalán-García M, **Guitart-Mampel M**, Rivero JJ, Tobias E, Milisenda JC, Tolosa E, Marti MJ, Fernández-Santiago R, Cardellach F, Morén C, Garrabou G. Exhaustion of mitochondrial and autophagic reserve may contribute to the development of LRRK2 G2019S -Parkinson's disease. J Transl Med. 2018.

- González-Casacuberta I, Morén C, Juárez-Flores DL, Esteve-Codina A, Sierra C, Catalán-García M, **Guitart-Mampel M**, Tobías E, Milisenda JC, Pont-Sunyer C, Martí MJ, Cardellach F, Tolosa E, Artuch R, Ezquerra M, Fernández-Santiago R, Garrabou G. Transcriptional alterations in skin fibroblasts from Parkinson's disease patients with parkin mutations. Neurobiol Aging. 2018.
- **Guitart-Mampel M**, Hernandez AS, Moren C, Catalan-Garcia M, Tobias E, Gonzalez-Casacuberta I, Juarez-Flores DL, Gatell JM, Cardellach F, Milisenda JC, Grau JM, Gratacos E, Figueras F, Garrabou G. Imbalance in mitochondrial dynamics and apoptosis in pregnancies among HIV-infected women on HAART with obstetric complications. J Antimicrob Chemother. 2017.
- Morén C, González-Casacuberta Í, Navarro-Otano J, Juárez-Flores D, Vilas D, Garrabou G, Milisenda JC, Pont-Sunyer C, Catalán-García M, **Guitart-Mampel M**, Tobías E, Cardellach F, Valldeoriola F, Iranzo A, Tolosa E. Colonic Oxidative and Mitochondrial Function in Parkinson's Disease and Idiopathic REM Sleep Behavior Disorder. Parkinsons Dis. 2017.
- Hernández S, Catalán-García M, Morén C, García-Otero L, López M, **Guitart-Mampel M**, Milisenda J, Coll O, Cardellach F, Gratacós E, Miró Ò, Garrabou G. Placental Mitochondrial Toxicity, Oxidative Stress, Apoptosis, and Adverse Perinatal Outcomes in HIV Pregnancies Under Antiretroviral Treatment Containing Zidovudine. J Acquir Immune Defic Syndr. 2017.
- Alvarez-Mora MI, Rodriguez-Revenga L, Madrigal I, **Guitart-Mampel M**, Garrabou G, Milà M. Impaired Mitochondrial Function and Dynamics in the Pathogenesis of FXTAS. Mol Neurobiol. 2017.
- Morén C, González-Casacuberta I, Álvarez-Fernández C, Bañó M, Catalán-Garcia M, **Guitart-Mampel M**, Juárez-Flores DL, Tobías E, Milisenda J, Cardellach F, Gatell JM, Sánchez-Palomino S, Garrabou G. HIV-1 promonocytic and lymphoid cell lines: an *in vitro* model of *in vivo* mitochondrial and apoptotic lesion. J Cell Mol Med. 2017.
- Hernandez S, Moren C, Catalán-García M, Lopez M, **Guitart-Mampel M**, Coll O, Garcia L, Milisenda J, Justamante A, Gatell JM, Cardellach F, Gratacos E, Miro Ò, Garrabou G. Mitochondrial toxicity and caspase activation in HIV pregnant women. J Cell Mol Med. 2017.
- Catalán-García M, Garrabou G, Morén C, **Guitart-Mampel M**, Hernando A, Díaz-Ramos À, González-Casacuberta I, Juárez DL, Bañó M, Enrich-Bengoa J, Emperador S, Milisenda JC, Moreno P, Tobías E, Zorzano A, Montoya J, Cardellach F, Grau JM. Mitochondrial DNA disturbances and deregulated

expression of oxidative phosphorylation and mitochondrial fusion proteins in sporadic inclusion body myositis. Clin Sci (Lond). 2016.

- Catalán-García M, Garrabou G, Morén C, **Guitart-Mampel M**, Gonzalez-Casacuberta I, Hernando A, Gallego-Escuredo J, Yubero D, Villaroya F, Montero R, O-Callaghan AS, Cardellach F, Grau J. BACE-1, PS-1 and sAPPβ levels are increased in plasma from sporadic inclusion body myositis patients: surrogate biomarkers among inflammatory myopathies. Mol Med. 2015.
- Morén C, Bañó M, González-Casacuberta I, Catalán-Garcia M, **Guitart-Mampel M**, Tobías E, Cardellach F, Pedrol E, Peraire J, Vidal F, Domingo P, Miró Ò, Gatell JM, Martínez E, Garrabou G. Mitochondrial and apoptotic *in vitro* modelling of differential HIV-1 progression and antiretroviral toxicity. J Antimicrob Chemother. 2015.
- Morén C, Noguera-Julián A, Garrabou G, Rovira N, Catalán M, Bañó M, **Guitart-Mampel M**, Tobías E, Hernández S, Cardellach F, Miró Ò, Fortuny C. Mitochondrial disturbances in HIV pregnancies. AIDS. 2015.

Reviews

- Morén C, Hernández S, **Guitart-Mampel M**, Garrabou G. Mitochondrial toxicity in human pregnancy: an update on clinical and experimental approaches in the last 10 years. Int J Environ Res Public Health. 2014